UNCLASSIFIED

AD NUMBER
AD850684
LIMITATION CHANGES
TO: **Approved for public release; distribution is unlimited.**
FROM: **Distribution: Further dissemination only as directed by Air Force Weapons Lab., Kirtland AFB, NM, MAY 1969, or higher DoD authority.**
AUTHORITY
AFWL ltr 30 Apr 1986

THIS PAGE IS UNCLASSIFIED

THIS REPORT HAS BEEN DELIMITED AND CLEARED FOR PUBLIC RELEASE UNDER DOD DIRECTIVE 5200.20 AND NO RESTRICTIONS ARE IMPOSED UPON ITS USE AND DISCLOSURE.

DISTRIBUTION STATEMENT A

APPROVED FOR PUBLIC RELEASE;
DISTRIBUTION UNLIMITED.

AD 850 684

AUTHORITY: AFWL

ltr 30 Apr 86

AD850684

AFWL-TR-68-123

AFWL-TR
68-123

EMP ENVIRONMENTAL CODES FOR LOW—ALTITUDE BURSTS AND GROUND SOURCES

Richard L. Knight
Robert E. Budwine
Ralph T. Day

The Dikewood Corporation
Albuquerque, New Mexico 87106

Contract F29601-68-C-0012

TECHNICAL REPORT NO. AFWL-TR-68-123

March 1969

AIR FORCE WEAPONS LABORATORY
Air Force Systems Command
Kirtland Air Force Base
New Mexico

This document may be further distributed by any holder only with specific prior approval of AFWL (WLRP), Kirtland AFB, NM, 87117.

AFWL-TR-68-123

AIR FORCE WEAPONS LABORATORY
Air Force Systems Command
Kirtland Air Force Base
New Mexico

AFWL-TR-68-123

EMP ENVIRONMENTAL CODES FOR LOW-ALTITUDE BURSTS AND GROUND SOURCES

Richard L. Knight   Robert E. Budwine
Ralph T. Day

The Dikewood Corporation
Albuquerque, New Mexico 87106
Contract F29601-68-C-0012

TECHNICAL REPORT NO. AFWL-TR-68-123

FOREWORD

This report was prepared by the Dikewood Corporation, Albuquerque, New Mexico, under Contract F29601-68-C-0012. The research was performed under Program Element 6.16.46.01.H, Project 5710. It was funded by the Defense Atomic Support Agency (DASA) under Subtask 04.091, and by the Space and Missiles Systems Organization (SAMSO) under PD 68-9.

Inclusive dates of research were October 1967 to October 1968. The report was submitted 27 January 1969 by the Air Force Weapons Laboratory Project Officer, Lt William A. Radasky (WLRP).

The Contractor's report number is DC-FR-2064.

This technical report has been reviewed and is approved.

William A. Radasky

WILLIAM A. RADASKY
Lieutenant, USAF
Project Officer

Harry F. Rizzo

HARRY F. RIZZO
Lt Colonel, USAF
Chief, Physics Branch

Claude K. Stambaugh

CLAUDE K. STAMBAUGH
Colonel, USAF
Chief, Research Division

ABSTRACT

(Distribution Limitation Statement No. 5)

Progress accomplished under Air Force Contract No. F29601-68-C-0012 toward predicting the electromagnetic pulse produced by a nuclear weapon is reported herein. This work consists of the following: (1) a real-time finite difference code, using prolate spheroidal coordinates, which will predict the electromagnetic fields produced by certain current distributions with azimuthal symmetry, (2) a retarded time code which in other respects is similar to the one listed above, (3) a one-dimensional finite difference code for predicting the fields of a current distribution with spherical symmetry, (4) a computer code which numerically evaluates the exact solution of Maxwell's equations for the case of spherical symmetry, (5) a numerical solution of the diffusion approximation of Maxwell's equations in a region which includes an infinitely conducting earth, (6) work toward obtaining a Green's function for Maxwell's equations with some restrictions on the time dependence of the conductivity, and (7) a numerical integration code that combines the results of two previously existing Monte Carlo neutron and gamma ray transport codes in order to obtain currents produced by gamma ray sources in the ground.

CONTENTS

I. EMP FINITE DIFFERENCE CODES

1. INTRODUCTION

Two digital computer codes, which calculate the electromagnetic pulse generated by a low-altitude nuclear burst in the presence of a finitely conducting earth, have been developed. It is assumed in the codes that the currents and conductivities are known functions of space and time, which have azimuthal symmetry. With this input, Maxwell's equations are solved in prolate spheroidal coordinates by a finite difference technique. The geometry for this coordinate system is described in Section I-4. The codes differ in that one is written in real time whereas the other employs the retarded time of the burst point. The primary advantages of the real time code are: (1) a definite physical boundary condition exists at the wave front in space (i.e., the fields are zero for $r > ct$), and (2) it is possible to have the mesh move along with the wave front and thus save computer storage if it is not necessary to calculate fields for great distances behind the wave front. Advantages of the retarded time code which at present are considered decisive are: (1) regridding both at the ground-air interface and at the wave front is much simpler than for the real-time code, and (2) the spatial derivatives at the wave front in the air are smaller than for the real time case. For these reasons a production version of the retarded-time code is presently being produced.

The current and conductivities which are now being used in the codes are calculated from the equations

$$\vec{J}(r, \tau) = \frac{J_o}{r^2} \frac{\exp\left[\alpha(\tau-\tau_p) - r/R_\gamma\right]}{1+\exp\left[(\alpha+\beta)(\tau-\tau_p)\right]} \hat{r} \qquad (1)$$

$$\sigma(r, \tau) = \frac{\sigma_o}{r^2} \frac{\exp\left[\alpha(\tau-\tau_p) - r/R_\rho\right]}{1+\exp\left[(\alpha+\beta)(\tau-\tau_p)\right]} \tag{2}$$

It is anticipated that future work will include writing codes to generate more realistic sources.

Identical problems have been run with these two codes. In regions where the fields have appreciable values the results compare quite favorably. Examples are depicted in the graphs in Appendix A. In addition, results of these codes have been compared to those of the one dimensional code described in Section I-5. In regions where the fields of the two dimensional codes are not affected by reflections from the ground, they give essentially the same output as the one dimensional code does.

The basic codes are described below. Versions are also written which contain regridding at the ground and also at the wave front for the retarded time code.

2. REAL-TIME EMP CODE FOR LOW ALTITUDE NUCLEAR BURSTS

a. Maxwell's Equations

In M.K.S. units Maxwell's equations are

$$\nabla \cdot \vec{D} = \rho \tag{3}$$

$$\nabla \cdot \vec{B} = 0 \tag{4}$$

$$\nabla \times \vec{E} = -\frac{\partial \vec{B}}{\partial t} \tag{5}$$

$$\nabla \times \vec{H} = \vec{j} + \frac{\partial \vec{D}}{\partial t} \tag{6}$$

The divergence equations may be treated as initial conditions since Maxwell's equations predict that if they are initially satisfied they will remain so. Our attention will thus be focused on the curl equations. In prolate spheroidal coordinates they are

$$
\begin{aligned}
&\frac{\hat{\xi}}{\sqrt{(\zeta^2-\xi^2a^2)(1-\xi^2)}}\Bigg[\frac{\partial}{\partial\zeta}\Bigg(\sqrt{(\zeta^2-a^2)(1-\xi^2)}\;E_\phi\Bigg)\\
&-\frac{\partial}{\partial\phi}\Bigg(\sqrt{\frac{\zeta^2-\xi^2a^2}{\zeta^2-a^2}}\;E_\zeta\Bigg)\Bigg]+\frac{\hat{\zeta}}{\sqrt{(\zeta^2-\xi^2a^2)(\zeta^2-a^2)}}\Bigg[\frac{\partial}{\partial\phi}\\
&\Bigg(\sqrt{\frac{\zeta^2-\xi^2a^2}{1-\xi^2}}\;E_\xi\Bigg)-\frac{\partial}{\partial\xi}\Bigg(\sqrt{(\zeta^2-a^2)(1-\xi^2)}\;E_\phi\Bigg)\Bigg]\\
&+\frac{\hat{\phi}\sqrt{(\zeta^2-a^2)(1-\xi^2)}}{\zeta^2-\xi^2a^2}\Bigg[\frac{\partial}{\partial\xi}\Bigg(\sqrt{\frac{\zeta^2-\xi^2a^2}{\zeta^2-a^2}}\;E_\zeta\Bigg)\\
&-\frac{\partial}{\partial\zeta}\Bigg(\sqrt{\frac{\zeta^2-\xi^2a^2}{1-\xi^2}}\;E_\xi\Bigg)\Bigg]=-\frac{\partial}{\partial t}\left(B_\xi\hat{\xi}+B_\zeta\hat{\zeta}+B_\phi\hat{\phi}\right) \qquad (7)
\end{aligned}
$$

and

$$
\begin{aligned}
&\frac{\hat{\xi}}{\sqrt{(\zeta^2-\xi^2a^2)(1-\xi^2)}}\Bigg[\frac{\partial}{\partial\zeta}\Bigg(\sqrt{(\zeta^2-a^2)(1-\xi^2)}\;H_\phi\Bigg)-\frac{\partial}{\partial\phi}\\
&\Bigg(\sqrt{\frac{\zeta^2-\xi^2a^2}{\zeta^2-a^2}}\;H_\zeta\Bigg)\Bigg]+\frac{\hat{\zeta}}{\sqrt{(\zeta^2-\xi^2a^2)(\zeta^2-a^2)}}\Bigg[\frac{\partial}{\partial\phi}\Bigg(\sqrt{\frac{\zeta^2-\xi^2a^2}{1-\xi^2}}\;H_\xi\Bigg)\\
&-\frac{\partial}{\partial\xi}\Bigg(\sqrt{(\zeta^2-a^2)(1-\xi^2)}\;H_\phi\Bigg)\Bigg]+\hat{\phi}\frac{\sqrt{(\zeta^2-a^2)(1-\xi^2)}}{\zeta^2-\xi^2a^2}\Bigg[\frac{\partial}{\partial\xi}\\
&\Bigg(\sqrt{\frac{\zeta^2-\xi^2a^2}{\zeta^2-a^2}}\;H_\zeta\Bigg)-\frac{\partial}{\partial\zeta}\Bigg(\sqrt{\frac{\zeta^2-\xi^2a^2}{1-\xi^2}}\;H_\xi\Bigg)\Bigg]=\left(j_\xi\hat{\xi}+j_\zeta\hat{\zeta}+j_\phi\hat{\phi}\right)\\
&\qquad+\frac{\partial}{\partial t}\left(D_\xi\hat{\xi}+D_\zeta\hat{\zeta}+D_\phi\hat{\phi}\right) \qquad (8)
\end{aligned}
$$

We assume the constitutive equations

$$\vec{D} = \epsilon\vec{E}, \quad \vec{B} = \mu\vec{H} \tag{9}$$

The problem considered has azimuthal symmetry. Thus no physical quantity is a function of ϕ. By using Eq. (9) and this symmetry condition, the curl equations are reduced to

$$\frac{\hat{\xi}}{\sqrt{(\zeta^2 - \xi^2 a^2)(1 - \xi^2)}} \frac{\partial}{\partial\zeta}\left(\sqrt{(\zeta^2 - a^2)(1 - \xi^2)}\; E_\phi\right)$$

$$- \frac{\hat{\zeta}}{\sqrt{(\zeta^2 - \xi^2 a^2)(\zeta^2 - a^2)}} \frac{\partial}{\partial\xi}\left(\sqrt{(\xi^2 - a^2)(1 - \xi^2)}\; E_\phi\right)$$

$$+ \hat{\phi}\frac{\sqrt{(\zeta^2 - a^2)(1 - \xi^2)}}{\zeta^2 - \xi^2 a^2}\left[\frac{\partial}{\partial\xi}\left(\sqrt{\frac{\zeta^2 - \xi^2 a^2}{\zeta^2 - a^2}}\; E_\zeta\right) - \frac{\partial}{\partial\zeta}\right.$$

$$\left.\left(\sqrt{\frac{\zeta^2 - \xi^2 a^2}{1 - \xi^2}}\; E_\xi\right)\right] = -\frac{\partial}{\partial t}\left(B_\xi\hat{\xi} + B_\zeta\hat{\zeta} + B_\phi\hat{\phi}\right) \tag{10}$$

$$\frac{c^2\hat{\xi}}{\sqrt{(\zeta^2 - \xi^2 a^2)(1 - \xi^2)}} \frac{\partial}{\partial\zeta}\left(\sqrt{(\zeta^2 - a^2)(1 - \xi^2)}\; B_\phi\right)$$

$$- \frac{c^2\hat{\zeta}}{\sqrt{(\zeta^2 - \xi^2 a^2)(\zeta^2 - a^2)}} \frac{\partial}{\partial\xi}\left(\sqrt{(\zeta^2 - a^2)(1 - \xi^2)}\; B_\phi\right)$$

$$+ c^2\hat{\phi}\frac{\sqrt{(\zeta^2 - a^2)(1 - \xi^2)}}{\zeta^2 - \xi^2 a^2}\left[\frac{\partial}{\partial\xi}\left(\sqrt{\frac{\zeta^2 - \xi^2 a^2}{\zeta^2 - a^2}}\; B_\zeta\right)\right.$$

$$- \frac{\partial}{\partial \zeta}\left(\sqrt{\frac{\zeta^2 - \xi^2 a^2}{1 - \xi^2}}\; B_\xi\right)\Bigg] = \frac{1}{\epsilon}\left(j_\xi \hat{\xi} + j_\zeta \hat{\zeta} + j_\phi \hat{\phi}\right) + \frac{\partial}{\partial t}$$

$$\left(E_\xi \hat{\xi} + E_\zeta \hat{\zeta} + E_\phi \hat{\phi}\right) \tag{11}$$

where

$$c = \frac{1}{\sqrt{\mu \epsilon}} \tag{12}$$

In scalar form, Eqs. (10) and (11) separate into two independent sets of coupled equations. One set involves the variables E_ξ, E_ζ, B_ϕ, j_ξ, and j_ζ. The other set relates E_ϕ, B_ξ, B_ζ, and j_ϕ. Maxwell's divergence equations behave similarly. We assume that for our problem $j_\phi = 0$. It then follows that if E_ϕ, B_ξ, and B_ζ are initially zero, they will remain so. Thus we set

$$E_\phi = B_\xi = B_\zeta = j_\phi = 0 \tag{13}$$

The curl equations become

$$\hat{\phi}\,\frac{\sqrt{(\zeta^2 - a^2)(1 - \xi^2)}}{\zeta^2 - \xi^2 a^2}\left[\frac{\partial}{\partial \xi}\left(\sqrt{\frac{\zeta^2 - \xi^2 a^2}{\zeta^2 - a^2}}\; E_\zeta\right)\right.$$

$$\left. - \frac{\partial}{\partial \zeta}\left(\sqrt{\frac{\zeta^2 - \xi^2 a^2}{1 - \xi^2}}\; E_\xi\right)\right] = - \frac{\partial B_\phi}{\partial t}\,\hat{\phi} \tag{14}$$

$$\frac{c^2\hat{\xi}}{\sqrt{(\zeta^2 - \xi^2 a^2)(1 - \xi^2)}} \frac{\partial}{\partial \zeta}\left(\sqrt{(\zeta^2 - a^2)(1 - \xi^2)}\, B_\phi\right)$$

$$\frac{c^2\hat{\zeta}}{\sqrt{(\zeta^2 - \xi^2 a^2)(\zeta^2 - a^2)}} \frac{\partial}{\partial \xi}\left(\sqrt{(\zeta^2 - a^2)(1 - \xi^2)}\, B_\phi\right)$$

$$= \frac{1}{\epsilon}(j_\xi \hat{\xi} + j_\zeta \hat{\zeta}) + \frac{\partial}{\partial t}(E_\xi \hat{\xi} + E_\zeta \hat{\zeta}) \tag{15}$$

In order to simplify these, the fields will be transformed according to

$$\begin{pmatrix} E_\xi \\ j_\xi \end{pmatrix} = \sqrt{(\zeta^2 - \xi^2 a^2)(1 - \xi^2)} \begin{pmatrix} E'_\xi \\ j'_\xi \end{pmatrix} \tag{16}$$

$$\begin{pmatrix} E_\zeta \\ j_\zeta \end{pmatrix} = \sqrt{(\zeta^2 - \xi^2 a^2)(\zeta^2 - a^2)} \begin{pmatrix} E'_\zeta \\ j'_\zeta \end{pmatrix} \tag{17}$$

$$B_\phi = \sqrt{(\zeta^2 - a^2)(1 - \xi^2)}\, B'_\phi \tag{18}$$

in which the primed quantities are those that have been used previously. In component form, the field equations then become

$$\frac{\partial E_\xi}{\partial t} = -\frac{j_\xi}{\epsilon} + c^2 \frac{\partial B_\phi}{\partial \zeta} \tag{19}$$

$$\frac{\partial E_\zeta}{\partial t} = -\frac{j_\zeta}{\epsilon} - c^2 \frac{\partial B_\phi}{\partial \xi} \tag{20}$$

$$\frac{\partial B_\phi}{\partial t} = \frac{\zeta^2 - a^2}{\zeta^2 - \xi^2 a^2} \frac{\partial E_\xi}{\partial \zeta} - \frac{1 - \xi^2}{\zeta^2 - \xi^2 a^2} \frac{\partial E_\zeta}{\partial \xi} \tag{21}$$

Make the substitution

$$j \longrightarrow j + \sigma E \tag{22}$$

Henceforth j will represent only that portion of the current resulting from Compton electrons.

Finally, we have

$$\frac{\partial E_\xi}{\partial t} = -\frac{\sigma}{\epsilon} E_\xi - \frac{j_\xi}{\epsilon} + c^2 \frac{\partial B_\phi}{\partial \zeta} \tag{23}$$

$$\frac{\partial E_\zeta}{\partial t} = -\frac{\sigma}{\epsilon} E_\zeta - \frac{j_\zeta}{\epsilon} - c^2 \frac{\partial B_\phi}{\partial \xi} \tag{24}$$

$$\frac{\partial B_\phi}{\partial t} = \frac{\zeta^2 - a^2}{\zeta^2 - \xi^2 a^2} \frac{\partial E_\xi}{\partial \zeta} - \frac{1 - \xi^2}{\zeta^2 - \xi^2 a^2} \frac{\partial E_\zeta}{\partial \xi} \tag{25}$$

This set of equations will be solved numerically below by a finite difference technique.

b. Difference Equations

Let

$$\xi = 1 + (1-i)\Delta\xi, \qquad \zeta = a + (j-1)\Delta\zeta, \qquad t = k\Delta t \tag{26}$$

so that at a mesh point a function of ξ, ζ, and t may be labeled f(i, j, k). Maxwell's curl equations (23) through (25) will be replaced by difference equations centered at (i, j, k-1/2). For mesh points in the air, we find

$$\frac{1}{\Delta t}\left[E_\xi(i,j,k)-E_\xi(i,j,k-1)\right]=\frac{c^2}{2\Delta\zeta}\left[B_\phi(i,j+1,k-1)\right.$$

$$\left.-B_\phi(i,j,k-1)+B_\phi(i,j,k)-B_\phi(i,j-1,k)\right]-\frac{\sigma(i,j,k-1/2)}{2\epsilon_0}$$

$$\left[E_\xi(i,j,k)+E_\xi(i,j,k-1)\right]-\frac{1}{\epsilon_0}j_\xi(i,j,k-1/2) \tag{27}$$

$$\frac{1}{\Delta t}\left[E_\zeta(i,j,k)-E_\zeta(i,j,k-1)\right]=-\frac{c^2}{2\Delta\xi}\left[B_\phi(i-1,j,k)\right.$$

$$\left.-B_\phi(i,j,k)+B_\phi(i,j,k-1)-B_\phi(i+1,j,k-1)\right]-\frac{\sigma(i,j,k-1/2)}{2\epsilon_0}$$

$$\left[E_\zeta(i,j,k)+E_\zeta(i,j,k-1)\right]-\frac{1}{\epsilon_0}j_\zeta(i,j,k-1/2) \tag{28}$$

$$\frac{1}{\Delta t}\left[B_\phi(i,j,k)-B_\phi(i,j,k-1)\right]=\frac{1}{\zeta^2-\xi^2a^2}\left\{\frac{\zeta^2-a^2}{2\Delta\zeta}\right.$$

$$\left[E_\xi(i,j+1,k-1)-E_\xi(i,j,k-1)+E_\xi(i,j,k)-E_\xi(i,j-1,k)\right]$$

$$-\frac{1-\xi^2}{2\Delta\xi}\left[E_\zeta(i-1,j,k)-E_\zeta(i,j,k)+E_\zeta(i,j,k-1)\right.$$

$$\left.\left.-E_\zeta(i+1,j,k-1)\right]\right\} \tag{29}$$

Provided the values of the fields are known on the z axis, on the line j-1, and for values of ξ greater than $1 + (1-i)\Delta\xi$ then the above are three equations that can be solved simultaneously for the three fields $E_\xi(i, j, k)$, $E_\zeta(i, j, k)$, and $B_\phi(i, j, k)$. From the symmetry of the problem it is easy to show that on the z axis for z>a,

$$\lim_{\xi \to 1} E_\xi(\xi, \zeta, t) = 0 \qquad \lim_{\xi \to 1} B_\phi(\xi, \zeta, t) = 0 \tag{30}$$

The value of E_ζ at $\xi = 1$ is obtained by leapfrogging the field forward in time, i.e.,

$$E_\zeta(1, j, k) = E_\zeta(1, j, k-1)\left[1 - \frac{\sigma(1, j, k-1)\Delta t}{\epsilon_0}\right]$$

$$+ \frac{c^2 \Delta t}{\Delta\xi} B_\phi(2, j, k-1) - \frac{j_\zeta(1, j, k-1)\Delta t}{\epsilon_0} \tag{31}$$

Similarly, for $\zeta = a$, $\xi > 0$, we have

$$E_\xi(i, 1, k) = E_\xi(i, 1, k-1)\left[1 - \frac{\sigma(i, 1, k-1)\Delta t}{\epsilon_0}\right]$$

$$+ \frac{c^2 \Delta t}{\Delta\zeta} B_\phi(i, 2, k-1) - \frac{j_\xi(i, 1, k-1)\Delta t}{\epsilon_0} \tag{32}$$

After these field values are found on the z axis, equations (27), (28), and (29) are used recursively to obtain the fields in the air mesh on a line of constant j.

The difference equations in the ground are

$$\frac{1}{\Delta t}\Big[E_\xi(i, j, k) - E_\xi(i, j, k-1)\Big] = \frac{u^2}{2\Delta\zeta}\Big[B_\phi(i, j, k) - B_\phi(i, j-1, k)$$

$$+ B_\phi(i, j+1, k-1) - B_\phi(i, j, k-1)\Big] - \frac{\sigma(i, j, k-1/2)}{2\epsilon}\Big[E_\xi(i, j, k)$$

$$+ E_\xi(i, j, k-1)\Big] - \frac{j_\xi(i, j, k-1/2)}{\epsilon} \tag{33}$$

$$\frac{1}{\Delta t}\Big[E_\zeta(i, j, k) - E_\zeta(i, j, k-1)\Big] = -\frac{u^2}{2\Delta\xi}\Big[B_\phi(i, j, k)$$

$$- B_\phi(i+1, j, k) + B_\phi(i-1, j, k-1) - B_\phi(i, j, k-1)\Big]$$

$$- \frac{\sigma(i, j, k-1/2)}{2\epsilon}\Big[E_\zeta(i, j, k) + E_\zeta(i, j, k-1)\Big] - \frac{1}{\epsilon} j_\zeta(i, j, k-1/2) \tag{34}$$

$$\frac{1}{\Delta t}\Big[(B_\phi(i, j, k) - B_\phi(i, j, k-1)\Big] = \frac{1}{\zeta^2 - \xi^2 a^2}\Bigg\{\frac{\zeta^2 - a^2}{2\Delta\zeta}$$

$$\Big[E_\xi(i, j, k) - E_\xi(i, j-1, k) + E_\xi(i, j+1, k-1) - E_\xi(i, j, k-1)\Big]$$

$$- \frac{1 - \xi^2}{2\Delta\xi}\Big[E_\zeta(i, j, k) - E_\zeta(i+1, j, k) + E_\zeta(i-1, j, k-1)$$

$$- E_\zeta(i, j, k-1)\Big]\Bigg\} \tag{35}$$

The nonzero electric fields on the z axis in the ground are obtained from

$$E_\zeta(i_m, j, k) = \left(1 - \frac{\sigma(i_m, j, k-1)\Delta t}{\epsilon}\right) E_\zeta(i_m, j, k-1)$$

$$- \frac{u^2 \Delta t}{\Delta \xi} B_\phi(i_m - 1, j, k-1) - \frac{j_\zeta(i_m, j, k-1)\Delta t}{\epsilon} \tag{36}$$

and from Eq. (32) by inserting parameters appropriate to the ground. In the above equation, i_m is the value of i corresponding to $\xi = -1$. Equations (33), (34), and (35) are then employed to obtain field values in the ground along a line of constant i in a manner analogous to that described above for the air mesh.

To treat the air-ground boundary, we define two lines of points labeled i_a and i_g for which $\xi = 0$. Even though these points have the same ξ coordinates, the first set is assumed to be in air and the other in the ground. The mesh points near the ground are labeled as shown in Figure 1.

The appropriate boundary conditions are that E_ζ and B_ϕ are continuous. This must hold for all time. Thus we infer that $\partial E_\zeta / \partial t$ and $\partial B_\phi / \partial t$ must be continuous. Whence

$$\frac{\partial E_\zeta(i_a, j, k-1/2)}{\partial t} = \frac{\partial E_\zeta(i_g, j, k-1/2)}{\partial t} \approx \frac{1}{2}\left[\frac{\partial E_\zeta(i_a - 1/2, j, k-1/2)}{\partial t}\right.$$

$$\left. + \frac{\partial E_\zeta(i_g + 1/2, j, k-1/2)}{\partial t}\right] \tag{37}$$

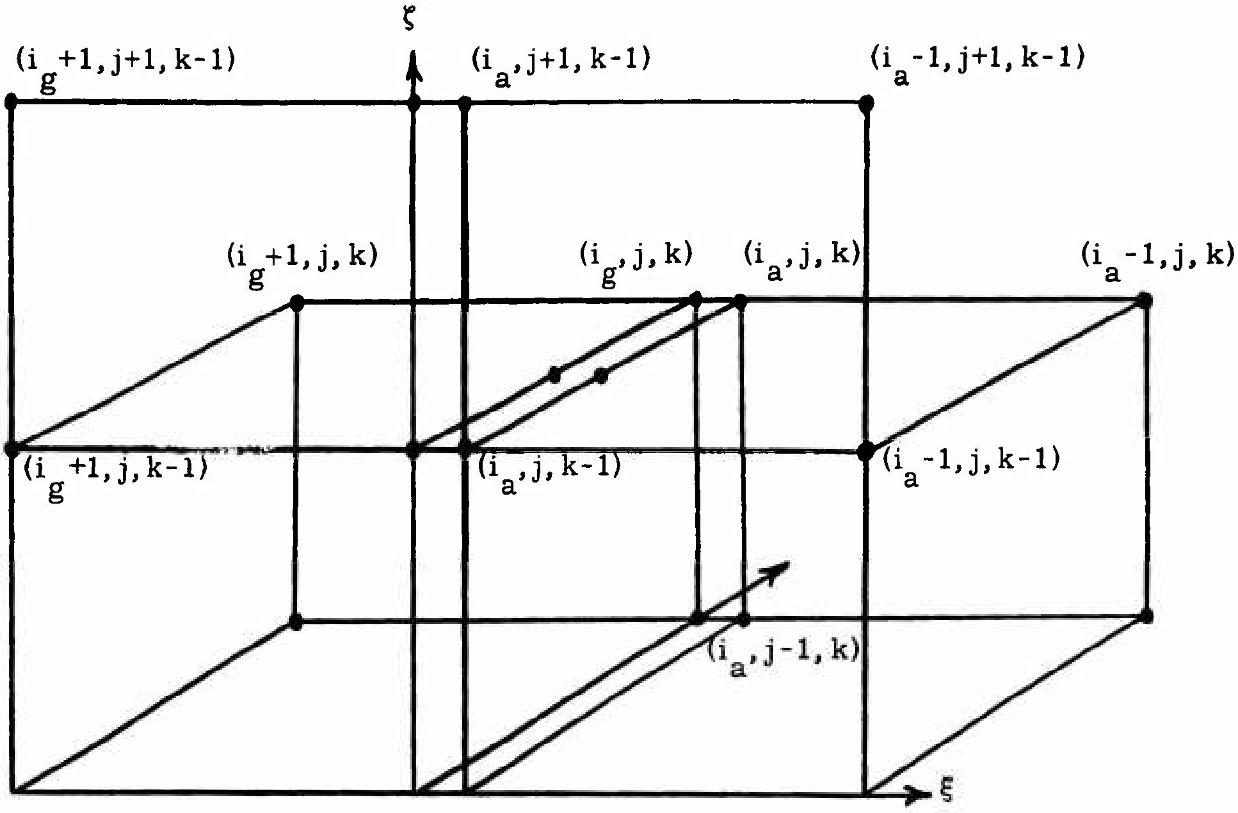

Figure 1

A Portion of the ξ-ζ Mesh Near the Ground

$$\frac{\partial B_\phi(i_a, j, k-1/2)}{\partial t} = \frac{\partial B_\phi(i_g, j, k-1/2)}{\partial t} \approx \frac{1}{2}\left[\frac{\partial B_\phi(i_a-1/2, j, k-1/2)}{\partial t}\right.$$

$$\left. + \frac{\partial B_\phi(i_g+1/2, j, k-1/2}{\partial t}\right] \tag{38}$$

Or

$$\frac{1}{\Delta\tau}\left[E_\zeta(i_a, j, k) - E_\zeta(i_a, j, k-1)\right] = -\frac{u^2}{8\Delta\xi}\left[B_\phi(i_g, j+1, k-1)\right.$$

$$- B_\phi(i_g+1, j+1, k-1) + B_\phi(i_g, j, k-1) - B_\phi(i_g+1, j, k-1)$$

$$\left. + B_\phi(i_g, j, k) - B_\phi(i_g+1, j, k) + B_\phi(i_g, j-1, k) - B_\phi(i_g+1, j-1, k)\right]$$

$$- \frac{c^2}{8\Delta\xi}\left[B_\phi(i_a-1, j+1, k-1) - B_\phi(i_a, j+1, k-1) + B_\phi(i_a-1, j, k-1)\right.$$

$$- B_\phi(i_a, j, k-1) + B_\phi(i_a-1, j, k) - B_\phi(i_a, j, k) + B_\phi(i_a+1, j-1, k)$$

$$\left. - B_\phi(i_a, j-1, k)\right] - \frac{\sigma(i_g+1/2, j, k-1/2)}{8\epsilon}\left[E_\zeta(i_g, j, k-1)\right.$$

$$\left. + E_\zeta(i_g, j, k) + E_\zeta(i_g+1, j, k) + E_\zeta(i_g+1, j, k-1)\right]$$

$$- \frac{\sigma(i_a-1/2, j, k-1/2)}{8\epsilon_0}\left[E_\zeta(i_a-1, j, k) + E_\zeta(i_a, j, k) + E_\zeta(i_a, j, k-1)\right.$$

$$\left. + E_\zeta(i_a-1, j, k-1)\right] - \frac{1}{2\epsilon} j_\zeta(i_g+1/2, j, k-1/2) - \frac{1}{2\epsilon_0}$$

$$j_\zeta(i_a-1/2, j, k-1/2) \tag{39}$$

$$\frac{1}{\Delta t}\left[B_\phi(i_a, j, k) - B_\phi(i_a, j, k-1)\right] = \frac{1}{8\Delta\zeta}\,\frac{\zeta^2 - a^2}{\zeta^2 - a^2\Delta\xi^2/4}$$

$$\Big[E_\xi(i_g+1, j+1, k-1) - E_\xi(i_g+1, j, k-1) + E_\xi(i_g+1, j, k)$$

$$- E_\xi(i_g+1, j-1, k) + E_\xi(i_g, j+1, k-1) - E_\xi(i_g, j, k-1)$$

$$+ E_\xi(i_g, j, k) - E_\xi(i_g, j-1, k) + E_\xi(i_a, j+1, k-1) - E_\xi(i_a, j, k-1)$$

$$+ E_\xi(i_a, j, k) - E_\xi(i_a, j-1, k) + E_\xi(i_a-1, j+1, k-1) - E_\xi(i_a-1, j, k-1)$$

$$+ E_\xi(i_a-1, j, k) - E_\xi(i_a-1, j-1, k)\Big] - \frac{1}{8\Delta\xi}\,\frac{1 - \Delta\xi^2/4}{\zeta^2 - a^2\Delta\xi^2/4}$$

$$\Big[E_\zeta(i_a-1, j, k) + E_\zeta(i_a-1, j, k-1) - E_\zeta(i_g+1, j, k-1)$$

$$- E_\zeta(i_g+1, j, k) + E_\zeta(i_a-1, j+1, k-1) + E_\zeta(i_a-1, j-1, k)$$

$$- E_\zeta(i_g+1, j+1, k-1) - E_\zeta(i_g+1, j-1, k)\Big] \tag{40}$$

Evaluate $\partial E_\xi/\partial t$ at $(i_a, j, k-1/2)$

$$\frac{1}{\Delta t}\left[E_\xi(i_a, j, k) - E_\xi(i_a, j, k-1)\right] = \frac{c^2}{2\Delta\zeta}\left[B_\phi(i_a, j+1, k-1)\right.$$

$$\left.- B_\phi(i_a, j, k-1) + B_\phi(i_a, j, k) - B_\phi(i_a, j-1, k)\right] - \frac{\sigma(i_a, j, k-1/2)}{2\epsilon_0}$$

$$\left[E_\xi(i_a, j, k) + E_\xi(i_a, j, k-1)\right] - \frac{1}{\epsilon_0} j_\xi(i_a, j, k-1/2) \tag{41}$$

Evaluate $\partial E_\xi / \partial t$ at $(i_g, j, k-1/2)$

$$\frac{1}{\Delta t}\left[E_\xi(i_g, j, k) - E_\xi(i_g, j, k-1)\right] = \frac{u^2}{2\Delta\zeta}\left[B_\phi(i_g, j+1, k-1)\right.$$

$$\left.- B_\phi(i_g, j, k-1) + B_\phi(i_g, j, k) - B_\phi(i_g, j-1, k)\right] - \frac{\sigma(i_g, j, k-1/2)}{2\epsilon}$$

$$\left[E_\xi(i_g, j, k) + E_\xi(i_g, j, k-1)\right] - \frac{1}{\epsilon} j_\xi(i_g, j, k-1/2) \tag{42}$$

After computing fields in the air and ground meshes for given i and k, Eqs. (39) through (42) can be solved simultaneously to give the four independent field components at the boundary.

3. RETARDED-TIME EMP CODE FOR LOW ALTITUDE NUCLEAR BURSTS

a. Maxwell's Equations

The time variable in this code will be taken as the retarded time of the burst point for waves that propagate in air. Thus put

$$\tau = t - \frac{r}{c} = t - \frac{\zeta - a\xi}{c} \tag{43}$$

where τ is the retarded time, t is the real time, c is the velocity of light in free space, and ξ and ζ are described in Section I-4. The corresponding transformations for the derivatives are

$$\left.\frac{\partial}{\partial\tau}\right|_{\xi,\zeta} = \left.\frac{\partial}{\partial t}\right|_{\xi,\zeta} \tag{44}$$

$$\nabla = \nabla_1 - \frac{\hat{r}}{c}\frac{\partial}{\partial\tau} \tag{45}$$

Here ∇_1 is the gradient operator at constant τ and $\hat{r}$ is the unit radial vector in a spherical polar coordinate system centered at the burst point of the weapon. After applying Eq. (43) through (45), Maxwell's equations in M.K.S. units become

$$\nabla_1 \cdot \vec{D} - \frac{1}{c}\,\hat{r}\cdot\frac{\partial\vec{D}}{\partial\tau} = \rho \tag{46}$$

$$\nabla_1 \cdot \vec{B} - \frac{1}{c}\,\hat{r}\cdot\frac{\partial\vec{B}}{\partial\tau} = 0 \tag{47}$$

$$\nabla_1 \times \vec{E} - \frac{1}{c}\,\hat{r}\times\frac{\partial\vec{E}}{\partial\tau} = -\frac{\partial\vec{B}}{\partial\tau} \tag{48}$$

$$\nabla_1 \times \vec{H} - \frac{1}{c}\,\hat{r}\times\frac{\partial\vec{H}}{\partial\tau} = \vec{j} + \frac{\partial\vec{D}}{\partial\tau} \tag{49}$$

In the section on geometry transformation coefficients, α_{ji} are determined such that

$$\hat{e}_i = \sum_j \alpha_{ji}\,\hat{u}_j \tag{50}$$

Where $\hat{e}_i$ are spherical polar unit vectors and $\hat{u}_j$ are prolate spheroidal unit vectors. In particular

$$\hat{r} = \alpha_{11}\hat{\xi} + \alpha_{21}\hat{\zeta} \tag{51}$$

Substitute this into Eq. (48) and (49) to obtain

$$\frac{\partial \vec{D}}{\partial \tau} = -\vec{j} + \nabla_1 \times \vec{H} - \frac{1}{c}(\alpha_{11}\hat{\xi} + \alpha_{21}\hat{\zeta}) \times \frac{\partial}{\partial \tau}(H_\xi \hat{\xi} + H_\zeta \hat{\zeta} + H_\phi \hat{\phi}) \tag{52}$$

$$\frac{\partial \vec{B}}{\partial \tau} = -\nabla_1 \times \vec{E} + \frac{1}{c}(\alpha_{11}\hat{\xi} + \alpha_{21}\hat{\zeta}) \times \frac{\partial}{\partial \tau}(E_\xi \hat{\xi} + E_\zeta \hat{\zeta} + E_\phi \hat{\phi}) \tag{53}$$

Recall that the prolate spheroidal unit vectors are cyclic in order $\xi - \zeta - \phi$, then these reduce to

$$\frac{\partial \vec{D}}{\partial \tau} = -\vec{j} + \nabla_1 \times \vec{H} - \frac{1}{c}\left[\alpha_{21}\frac{\partial H_\phi}{\partial \tau}\hat{\xi} - \alpha_{11}\frac{\partial H_\phi}{\partial \tau}\hat{\zeta} + \left(\alpha_{11}\frac{\partial H_\zeta}{\partial \tau} - \alpha_{21}\frac{\partial H_\xi}{\partial \tau}\right)\hat{\phi}\right] \tag{54}$$

$$\frac{\partial \vec{B}}{\partial \tau} = -\nabla_1 \times \vec{E} + \frac{1}{c}\left[\alpha_{21}\frac{\partial E_\phi}{\partial \tau}\hat{\xi} - \alpha_{11}\frac{\partial E_\phi}{\partial \tau}\hat{\zeta} + \left(\alpha_{11}\frac{\partial E_\zeta}{\partial \tau} - \alpha_{21}\frac{\partial E_\xi}{\partial \tau}\right)\hat{\phi}\right] \tag{55}$$

Assume azimuthal symmetry and write the remaining terms of the above equations as functions of ξ, ζ, ϕ. Also, set

$$\vec{D} = \epsilon\vec{E}, \qquad \vec{B} = \mu\vec{H} \tag{56}$$

Then

$$\frac{\partial}{\partial\tau}\left[E_\xi\hat{\xi} + E_\zeta\hat{\zeta} + E_\phi\hat{\phi}\right] = -\frac{1}{\epsilon}\left[j_\xi\hat{\xi} + j_\zeta\hat{\zeta} + j_\phi\hat{\phi}\right]$$

$$+ \frac{u^2\hat{\xi}}{\sqrt{(\zeta^2 - \xi^2 a^2)(1 - \xi^2)}}\frac{\partial}{\partial\zeta}\left(\sqrt{(\zeta^2 - a^2)(1 - \xi^2)}\, B_\phi\right)$$

$$- \frac{u^2\hat{\zeta}}{\sqrt{(\zeta^2 - \xi^2 a^2)(\zeta^2 - a^2)}}\frac{\partial}{\partial\xi}\left(\sqrt{(\zeta^2 - a^2)(1 - \xi^2)}\, B_\phi\right)$$

$$+ u^2\hat{\phi}\,\frac{\sqrt{(\zeta^2 - a^2)(1 - \xi^2)}}{\zeta^2 - \xi^2 a^2}\left[\frac{\partial}{\partial\xi}\left(\sqrt{\frac{\zeta^2 - \xi^2 a^2}{\zeta^2 - a^2}}\, B_\zeta\right) - \frac{\partial}{\partial\zeta}\right.$$

$$\left.\left(\sqrt{\frac{\zeta^2 - \xi^2 a^2}{1 - \xi^2}}\, B_\xi\right)\right] - \frac{u^2}{c}\left[\alpha_{21}\frac{\partial B_\phi}{\partial\tau}\hat{\xi} - \alpha_{11}\frac{\partial B_\phi}{\partial\tau}\hat{\zeta}\right.$$

$$\left. + \left(\alpha_{11}\frac{\partial B_\zeta}{\partial\tau} - \alpha_{21}\frac{\partial B_\xi}{\partial\tau}\right)\hat{\phi}\right] \tag{57}$$

$$\frac{\partial}{\partial\tau}(B_\xi\hat{\xi} + B_\zeta\hat{\zeta} + B_\phi\hat{\phi}) = -\frac{\hat{\xi}}{\sqrt{(\zeta^2 - \xi^2 a^2)(1 - \xi^2)}}\frac{\partial}{\partial\zeta}$$

$$\left(\sqrt{(\zeta^2 - a^2)(1 - \zeta^2)}\, E_\phi\right) + \frac{\hat{\zeta}}{\sqrt{(\zeta^2 - \xi^2 a^2)(\zeta^2 - a^2)}}\frac{\partial}{\partial\xi}$$

$$\sqrt{(\zeta^2 - a^2)(1 - \xi^2)}\, E_\phi \quad - \hat{\phi}\,\frac{\sqrt{(\zeta^2 - a^2)(1 - \xi^2)}}{\zeta^2 - \xi^2 a^2}\left[\frac{\partial}{\partial\xi}\right.$$

$$\left(\sqrt{\frac{\zeta^2 - \xi^2 a^2}{\zeta^2 - a^2}}\, E_\zeta\right) - \frac{\partial}{\partial \zeta}\left(\sqrt{\frac{\zeta^2 - \xi^2 a^2}{1 - \xi^2}}\, E_\xi\right)\Bigg] + \frac{1}{c}\Bigg[\alpha_{21} \frac{\partial E_\phi}{\partial \tau}\hat{\xi}$$

$$- \alpha_{11} \frac{\partial E_\phi}{\partial \tau}\hat{\zeta} + \left(\alpha_{11} \frac{\partial E_\zeta}{\partial \tau} - \alpha_{21} \frac{\partial E_\xi}{\partial \tau}\right)\hat{\phi}\Bigg] \tag{58}$$

The velocity of light, u, in the medium is determined by

$$u = \frac{1}{\sqrt{\mu\epsilon}} \tag{59}$$

Note that in component form, Eq. (57) and (58) separate into two uncoupled sets of equations involving E_ξ, E_ζ, j_ξ, j_ζ, B_ϕ, and E_ϕ, j_ϕ, B_ξ, and B_ζ. We assume that $j_\phi = 0$. Provided that the second set of fields is initially zero, Maxwell's equations predict they will remain so. Hence, we put

$$j_\phi = E_\phi = B_\xi = B_\zeta = 0 \tag{60}$$

The field equations then reduce to

$$\frac{\partial E_\xi}{\partial \tau} = -\frac{j_\xi}{\epsilon} + \frac{u^2}{\sqrt{(\zeta^2 - \xi^2 a^2)(1 - \xi^2)}} \frac{\partial}{\partial \zeta}\left(\sqrt{(\zeta^2 - a^2)(1 - \xi^2)}\, B_\phi\right)$$

$$- \frac{u^2 \alpha_{21}}{c} \frac{\partial B_\phi}{\partial \tau} \tag{61}$$

$$\frac{\partial E_\zeta}{\partial \tau} = -\frac{j_\zeta}{\epsilon} - \frac{u^2}{\sqrt{(\zeta^2 - \xi^2 a^2)(\zeta^2 - a^2)}} \frac{\partial}{\partial \xi} \sqrt{(\zeta^2 - a^2)(1 - \xi^2)}\, B_\phi$$

$$+ \frac{u^2 \alpha_{11}}{c} \frac{\partial B_\phi}{\partial \tau} \tag{62}$$

$$\frac{\partial B_\phi}{\partial \tau} = \frac{\sqrt{(\zeta^2 - a^2)(1 - \xi^2)}}{\zeta^2 - \xi^2 a^2} \left[\frac{\partial}{\partial \zeta} \left(\sqrt{\frac{\zeta^2 - \xi^2 a^2}{1 - \xi^2}}\, E_\xi \right) \right.$$

$$\left. - \frac{\partial}{\partial \xi} \left(\sqrt{\frac{\zeta^2 - \xi^2 a^2}{\zeta^2 - a^2}}\, E_\zeta \right) \right] + \frac{\alpha_{11}}{c} \frac{\partial E_\zeta}{\partial \tau} - \frac{\alpha_{21}}{c} \frac{\partial E_\xi}{\partial \tau} \tag{63}$$

Make the substitution

$$\vec{j} \longrightarrow \vec{j} + \sigma \vec{E} \tag{64}$$

Henceforth $\sigma\vec{E}$ will give the conduction portion of the current and $\vec{j}$ will denote only that part caused by Compton electrons. Also at this point, substitute the proper values of α_{ij} from Section I-4. Obtain

$$\frac{\partial E_\xi}{\partial \tau} = -\frac{\sigma}{\epsilon} E_\xi - \frac{j_\xi}{\epsilon} + \frac{u^2}{\sqrt{(\zeta^2 - \xi^2 a^2)(1 - \xi^2)}} \frac{\partial}{\partial \zeta} \left(\sqrt{(\zeta^2 - a^2)(1 - \xi^2)}\, B_\phi \right)$$

$$- \frac{u^2}{c} \sqrt{\frac{\zeta^2 - a^2}{\zeta^2 - \xi^2 a^2}} \frac{\partial B_\phi}{\partial \tau} \tag{65}$$

$$\frac{\partial E_\zeta}{\partial \tau} = -\frac{\sigma}{\epsilon} E_\zeta - \frac{j_\zeta}{\epsilon} - \frac{u^2}{\sqrt{(\zeta^2 - \xi^2 a^2)(\zeta^2 - a^2)}} \frac{\partial}{\partial \xi}\left(\sqrt{(\zeta^2 - a^2)(1 - \xi^2)}\; B_\phi\right)$$

$$- \frac{au^2}{c}\sqrt{\frac{1 - \xi^2}{\zeta^2 - \xi^2 a^2}}\; \frac{\partial B_\phi}{\partial \tau} \qquad (66)$$

$$\frac{\partial B_\phi}{\partial \tau} = \frac{\sqrt{(\zeta^2 - a^2)(1 - \xi^2)}}{\zeta^2 - \xi^2 a^2}\left[\frac{\partial}{\partial \zeta}\left(\sqrt{\frac{\zeta^2 - \xi^2 a^2}{1 - \xi^2}}\; E_\xi\right)\right.$$

$$\left. - \frac{\partial}{\partial \xi}\left(\sqrt{\frac{\zeta^2 - \xi^2 a^2}{\zeta^2 - a^2}}\; E_\zeta\right)\right] - \frac{a}{c}\sqrt{\frac{1 - \xi^2}{\zeta^2 - \xi^2 a^2}}\; \frac{\partial E_\zeta}{\partial \tau}$$

$$- \frac{1}{c}\sqrt{\frac{\zeta^2 - a^2}{\zeta^2 - \xi^2 a^2}}\; \frac{\partial E_\xi}{\partial \tau} \qquad (67)$$

Transform the fields according to

$$\begin{pmatrix} E_\xi \\ j_\xi \end{pmatrix} = \sqrt{(\zeta^2 - \xi^2 a^2)(1 - \xi^2)} \begin{pmatrix} E'_\xi \\ j'_\xi \end{pmatrix} \qquad (68)$$

$$\begin{pmatrix} E_\zeta \\ j_\zeta \end{pmatrix} = \sqrt{(\zeta^2 - \xi^2 a^2)(\zeta^2 - a^2)} \begin{pmatrix} E'_\zeta \\ j'_\zeta \end{pmatrix} \qquad (69)$$

$$B_\phi = \sqrt{(\zeta^2 - a^2)(1 - \xi^2)}\; B'_\phi \qquad (70)$$

in which the primed fields are those used previously. Maxwell's curl equations then become

$$\frac{\partial E_\xi}{\partial \tau} = -\frac{\sigma}{\epsilon} E_\xi - \frac{j_\xi}{\epsilon} + u^2 \frac{\partial B_\phi}{\partial \zeta} - \frac{u^2}{c} \frac{\partial B_\phi}{\partial \tau} \tag{71}$$

$$\frac{\partial E_\zeta}{\partial \tau} = -\frac{\sigma}{\epsilon} E_\zeta - \frac{j_\zeta}{\epsilon} - u^2 \frac{\partial B_\phi}{\partial \xi} - \frac{au^2}{c} \frac{\partial B_\phi}{\partial \tau} \tag{72}$$

$$\frac{\partial B_\phi}{\partial \tau} = \frac{\zeta^2 - a^2}{\zeta^2 - \xi^2 a^2} \frac{\partial E_\xi}{\partial \zeta} - \frac{1 - \xi^2}{\zeta^2 - \xi^2 a^2} \frac{\partial E_\zeta}{\partial \xi} - \frac{a}{c} \frac{1 - \xi^2}{\zeta^2 - \xi^2 a^2} \frac{\partial E_\zeta}{\partial \tau}$$

$$- \frac{1}{c} \frac{\zeta^2 - a^2}{\zeta^2 - \xi^2 a^2} \frac{\partial E_\xi}{\partial \tau} \tag{73}$$

b. Boundary Conditions in Retarded Time

In the limit as the distance between two points approaches zero, their associated retarded times become equal. Thus intuitively we expect that boundary conditions will remain the same in retarded time as they are in real time. This is demonstrated below in a more rigorous manner.

From Maxwell's differential equations (46) through (49), equivalent integral equations for retarded time may be derived. By integrating Eq. (46) over a three-dimensional space volume v, we obtain

$$\int_v \nabla \cdot \vec{D}\, dv = \int_v \rho dv + \frac{1}{c} \int_v \hat{r} \cdot \frac{\partial \vec{D}}{\partial \tau}\, dv \tag{74}$$

Apply Gauss's divergence theorem to the left side, obtain

$$\int_s \vec{D} \cdot d\vec{s} = q + \frac{1}{c} \frac{\partial}{\partial \tau} \int_v \hat{r} \cdot \vec{D}\, dv \tag{75}$$

where q is the charge in v. This is the equivalent of Gauss's law in retarded

time. From Eq. (47), a similar law may be found for $\vec{B}$

$$\int_s \vec{B} \cdot d\vec{s} = \frac{1}{c} \frac{\partial}{\partial \tau} \int_v \hat{r} \cdot \vec{B}\, dv \tag{76}$$

Thus in retarded time $\vec{B}$ is not necessarily solenoidal.

From Eq. (48)

$$\int_s \nabla \times \vec{E} \cdot d\vec{s} = -\int_s \frac{\partial \vec{B}}{\partial \tau} \cdot d\vec{s} + \frac{1}{c} \frac{\partial}{\partial \tau} \int_s \hat{r} \times \vec{E} \cdot d\vec{s} \tag{77}$$

Applying Stoke's theorem yields

$$\int_c \vec{E} \cdot d\vec{\ell} = -\frac{\partial}{\partial \tau} \int_s \vec{B} \cdot d\vec{s} + \frac{1}{c} \frac{\partial}{\partial \tau} \int_s \hat{r} \times \vec{E} \cdot d\vec{s} \tag{78}$$

in which c is the curve that bounds the surface s. This, of course, is the retarded time analog of Faraday's law of induction. Similarly from Eq. (49), one finds

$$\int_c \vec{H} \cdot d\vec{\ell} = \int_s \vec{j} \cdot d\vec{s} + \frac{\partial}{\partial \tau} \int_s \vec{D} \cdot d\vec{s} + \frac{1}{c} \frac{\partial}{\partial \tau} \int_s \hat{r} \times \vec{H} \cdot d\vec{s} \tag{79}$$

which is a generalization of Ampere's law in retarded time.

Now consider the boundary conditions in retarded time. From Causs' law Eq. (75) and the pillbox shown in Figure 2, one finds

$$\int_{s_\ell} \vec{D} \cdot d\vec{s} + (\vec{D}_1 - \vec{D}_2) \cdot \hat{n} = \frac{q}{\Delta s} + \frac{\delta}{2c} \frac{\partial}{\partial \tau} (\vec{D}_1 + \vec{D}_2) \cdot \hat{r} \tag{80}$$

Here it is assumed that $\vec{D}$ may be discontinuous on the boundary, but that it is continuous in regions 1 and 2 above and below the boundary. The lateral surface of the pillbox is labeled s_ℓ. Take the limit $\delta \longrightarrow 0$.

$$(\vec{D}_1 - \vec{D}_2) \cdot \hat{n} = \lambda \tag{81}$$

where λ is the surface charge density.

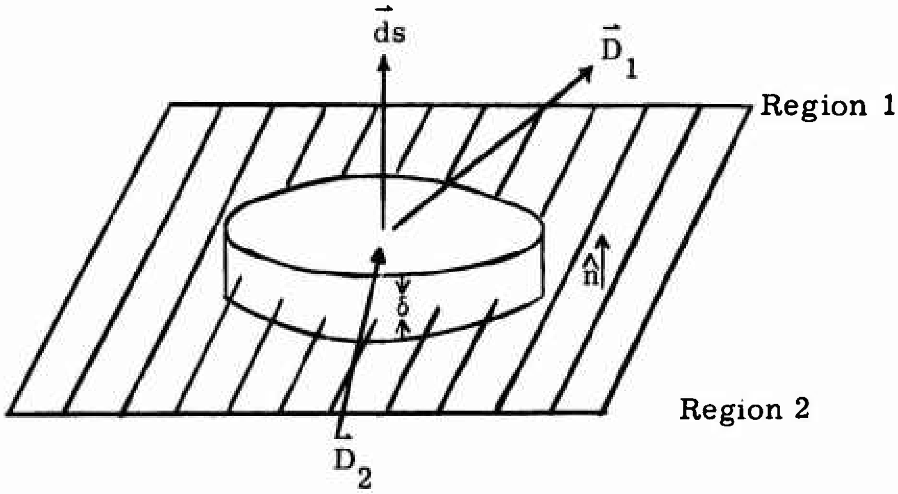

Figure 2

Gaussian Pillbox for the Determination of Boundary Conditions for Normal Field Components

Similarly, from Eq. (47), one finds

$$(\vec{B}_1 - \vec{B}_2) \cdot \hat{n} = 0 \tag{82}$$

From Eq. (76) and the contour shown in Figure 3, it follows that

$$(\vec{E}_1 - \vec{E}_2) \cdot \hat{t}\Delta \ell = -\frac{1}{2} \frac{\partial}{\partial t} (\vec{B}_1 + \vec{B}_2) \cdot \hat{n} \times \hat{t}\Delta \ell \delta + \frac{1}{2c} \frac{\partial}{\partial \tau} \hat{r}$$

$$\times (\vec{E}_1 + \vec{E}_2) \cdot \hat{n} \times \hat{t}\Delta \ell \delta \tag{83}$$

The contribution to the line integral from the sides δ has been omitted.

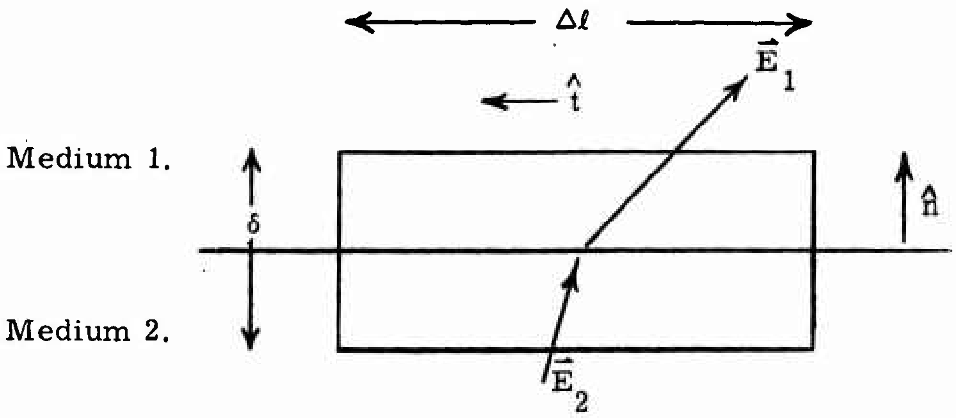

Figure 3

Contour Used in Determination of Boundary Conditions for Tangential Field Components

Cancel $\Delta \ell$ and take the limit $\delta \longrightarrow 0$, then

$$(\vec{E}_1 - \vec{E}_2) \cdot \hat{t} = 0 \tag{84}$$

From Eq. (77), a similar argument gives

$$(\vec{H}_1 - \vec{H}_2) \cdot \hat{t} = \vec{k} \cdot \hat{n} \times \hat{t} \tag{85}$$

where $\vec{k}$ is the surface current, $\hat{n}$ is the unit normal vector, and $\hat{t}$ is the unit tangent vector. Equations (81), (82), (84), and (85) will be recognized as the boundary conditions in real time.

For problems with azimuthal symmetry, it is a simple matter to show in real time that B_ϕ vanishes on the z axis. Let us look at the derivation in retarded time. Integrate Eq. (79) over the contour shown in Figure 4.

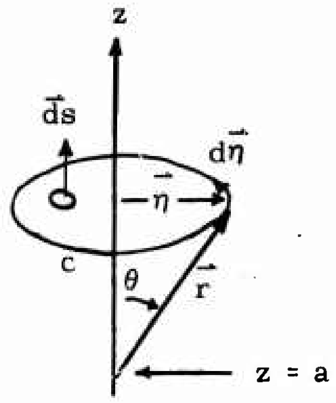

Figure 4

Contour for Evaluating $\vec{B}$ on the z Axis

For our problem, $\vec{B} = B_\phi \hat{\phi}$. The azimuthal symmetry ensures that the magnitude of $\vec{B}$ is constant on c. Therefore,

$$\int_c \vec{B} \cdot d\vec{\eta} = B_\phi \Big|_{\eta, z} (2\pi \eta) \tag{86}$$

Here η is a coordinate measured perpendicular to the z axis. Provided η is small enough that $\vec{B}$ does not change appreciably over the surface s, we can, for points on the z axis other than the burst point, set

$$\frac{\partial}{\partial \tau} \int_s \hat{r} \times \vec{B} \cdot \vec{ds} \simeq \frac{\partial B_\phi}{\partial \tau}\Big|_{\eta=0, z} \int_s \sin\theta ds \tag{87}$$

Use the approximation

$$\sin\theta \simeq \frac{\eta}{z - a} \tag{88}$$

which is valid for $\eta \ll z - a$. Then Eq. (87) becomes

$$\frac{\partial}{\partial\tau}\int_s \hat{r} \times \vec{B} \cdot d\vec{s} \simeq \frac{2\pi\eta^3}{3(z-a)} \left.\frac{\partial B_\phi}{\partial\tau}\right|_{\eta=0,\,z} \tag{89}$$

Assume that j_z, $\partial E_z/\partial\tau$, and $\partial B_\phi/\partial\tau$ are finite on the z axis and that the constitutive equations (56) hold. Then in the limit $\eta \longrightarrow 0$, Eq. (79), (86), and (89) yield

$$\lim_{\eta\to 0}(2\pi\eta)\, B_\phi(\eta, z, \tau) = \lim_{\eta\to 0}\left[\mu\pi\eta^2 j_z(\eta, z, \tau) + \frac{\pi\eta^2}{c^2}\frac{\partial E_z(\eta, z, \tau)}{\partial\tau} + \frac{2\pi\eta^3}{3c(z-a)}\frac{\partial B_\phi(\eta, z, \tau)}{\partial\tau}\right] \tag{90}$$

or

$$\lim_{\eta\to 0} B_\phi(\eta, z, \tau) = 0 \tag{91}$$

Another obvious symmetry condition is that

$$\lim_{\eta\to 0} E_\eta(\eta, z, \tau) = 0 \tag{92}$$

c. Difference Equations

At a mesh point the independent variables may be written

$$\xi = 1 + (1 - i)\Delta\xi, \qquad \zeta = a + (j - 1)\Delta\zeta, \qquad t = k\Delta t \tag{93}$$

With this notation, Maxwell's curl equations (71), (72), and (73) may be replaced by difference equations centered at (i, j, k-1/2). We find

$$\frac{1}{\Delta\tau}\left[E_\xi(i,\ j,\ k) - E_\xi(i,\ j,\ k-1)\right] = -\frac{\sigma(i,\ j,\ k-1/2)}{2\epsilon}$$

$$\left[E_\xi(i,\ j,\ k) + E_\xi(i,\ j,\ k-1)\right] - \frac{j_\xi(i,\ j,\ k-1/2)}{\epsilon} + \frac{u^2}{2\Delta\zeta}$$

$$\left[B_\phi(i,\ j+1,\ k-1) - B_\phi(i,\ j,\ k-1) + B_\phi(i,\ j,\ k) - B_\phi(i,\ j-1,\ k)\right]$$

$$-\frac{u^2}{c\Delta t}\left[B_\phi(i,\ j,\ k) - B_\phi(i,\ j,\ k-1)\right] \tag{94}$$

$$\frac{1}{\Delta\tau}\left[E_\zeta(i,\ j,\ k) - E_\zeta(i,\ j,\ k-1)\right] = -\frac{\sigma(i,\ j,\ k-1/2)}{2\epsilon}$$

$$\left[E_\zeta(i,\ j,\ k) + E_\zeta(i,\ j,\ k-1)\right] - \frac{j_\zeta(i,\ j,\ k-1/2)}{\epsilon} - \frac{u^2}{2\Delta\xi}$$

$$\left[B_\phi(i-1,\ j,\ k) - B_\phi(i,\ j,\ k) + B_\phi(i,\ j,\ k-1) - B_\phi(i+1,\ j,\ k-1)\right]$$

$$-\frac{au^2}{c\Delta\tau}\left[B_\phi(i,\ j,\ k) - B_\phi(i,\ j,\ k-1)\right] \tag{95}$$

$$\frac{1}{\Delta\tau}\left[B_\phi(i,\ j,\ k) - B_\phi(i,\ j,\ k-1)\right] = \frac{1}{2\Delta\zeta}\left(\frac{\zeta^2 - a^2}{\zeta^2 - \xi^2 a^2}\right)\Bigg|_{i,\,j}$$

$$\left[E_\xi(i,\ j+1,\ k-1) - E_\xi(i,\ j,\ k-1) + E_\xi(i,\ j,\ k) - E_\xi(i,\ j-1,\ k)\right]$$

$$+\frac{1}{2\Delta\xi}\left(\frac{1-\xi^2}{\zeta^2-\xi^2a^2}\right)\Bigg|_{i,j}\Big[E_\zeta(i+1,\ j,\ k-1)-E_\zeta(i,\ j,\ k-1)$$

$$+E_\zeta(i,\ j,\ k)-E_\zeta(i-1,\ j,\ k)\Big]-\frac{a}{c\Delta\tau}\left(\frac{1-\xi^2}{\zeta^2-\xi^2a^2}\right)\Bigg|_{i,j}\Big[E_\zeta(i,\ j,\ k)$$

$$-E_\zeta(i,\ j,\ k-1)\Big]-\frac{1}{c\Delta\tau}\left(\frac{\zeta^2-a^2}{\zeta^2-\xi^2a^2}\right)\Bigg|_{i,j}\Big[E_\xi(i,\ j,\ k)$$

$$-E_\xi(i,\ j,\ k-1)\Big] \qquad (96)$$

These equations may be used both in the air and the ground meshes provided appropriate values of u, σ, and ϵ are inserted. The nonzero field components on the z axis can be obtained from equations (31), (32), and (36). Equations (94), (95), and (96) are then solved by a method analogous to that used in the real-time code. The one difference in the methods is that in the retarded time code the fields are determined in the air mesh along a line of constant j, the boundary conditions at the ground are applied, then the fields are obtained in the ground mesh along this same line in the direction of decreasing ξ; whereas in the real-time code, the boundary conditions are applied last.

To facilitate handling the boundary conditions at the ground, two lines of points are defined which have $\xi = 0$. One set of these is assumed to be in air and the other to be in the ground. The mesh near the boundary is labeled as shown in Figure 1.

The boundary conditions at this interface are that E_ζ and B_ϕ are continuous. This implies that $\partial E_\zeta/\partial\tau$ and $\partial B_\phi/\partial\tau$ are continuous. Thus we set

$$\frac{\partial E_\zeta(i_a, j, k-1/2)}{\partial \tau} = \frac{\partial E_\zeta(i_g, j, k-1/2)}{\partial \tau} \approx \frac{1}{2}\left[\frac{\partial E_\zeta(i_a-1/2, j, k-1/2)}{\partial \tau}\right.$$

$$\left. + \frac{\partial E_\zeta(i_g+1/2, j, k-1/2)}{\partial \tau}\right] \tag{97}$$

$$\frac{\partial B_\phi(i_a, j, k-1/2)}{\partial \tau} = \frac{\partial B_\phi(i_g, j, k-1/2)}{\partial \tau} \approx \frac{1}{2}\left[\frac{\partial B_\phi(i_a-1/2, j, k-1/2)}{\partial \tau}\right.$$

$$\left. + \frac{\partial B_\phi(i_g+1/2, j, k-1/2)}{\partial \tau}\right] \tag{98}$$

By writing Eq. (97) and (98) in difference form, we obtain

$$\frac{1}{\Delta\tau}\left[E_\zeta(i_a, j, k) - E_\zeta(i_a, j, k-1)\right] = -\frac{\sigma(i_g+1/2, j, k-1/2)}{8\epsilon}$$

$$\left[E_\zeta(i_g, j, k) + E_\zeta(i_g+1, j, k) + E_\zeta(i_g+1, j, k-1) + E_\zeta(i_g, j, k-1)\right]$$

$$-\frac{j_\zeta(i_g+1/2, j, k-1/2)}{2\epsilon} - \frac{u^2}{4\Delta\xi}\left[B_\phi(i_a, j, k) - B_\phi(i_g+1, j, k)\right.$$

$$\left. + B_\phi(i_a, j, k-1) - B_\phi(i_g+1, j, k-1)\right] - \frac{au^2}{4c\Delta\tau}\left[B_\phi(i_g+1, j, k)\right.$$

$$\left. - B_\phi(i_g+1, j, k-1) + B_\phi(i_a, j, k) - B_\phi(i_a, j, k-1)\right]$$

$$-\frac{\sigma(i_a-1/2, j, k-1/2)}{8\epsilon_0}\left[E_\zeta(i_a-1, j, k) + E_\zeta(i_a, j, k)\right.$$

$$+ E_\zeta(i_a, j, k-1) + E_\zeta(i_a-1, j, k-1)\Big] - \frac{j_\zeta(i_a-1/2, j, k-1/2)}{2\epsilon_0}$$

$$- \frac{c^2}{4\Delta\xi}\Big[B_\phi(i_a-1, j, k) - B_\phi(i_a, j, k) + B_\phi(i_a-1, j, k-1)$$

$$- B_\phi(i_a, j, k-1)\Big] - \frac{ac}{4\Delta\tau}\Big[B_\phi(i_a-1, j, k) - B_\phi(i_a-1, j, k-1)$$

$$+ B_\phi(i_a, j, k) - B_\phi(i_a, j, k-1)\Big] \qquad (99)$$

and

$$\frac{1}{\Delta\tau}\Big[B_\phi(i_a, j, k) - B_\phi(i_a, j, k-1)\Big] = \frac{1}{8\Delta\zeta}\,\frac{\zeta^2 - a^2}{\zeta^2 - a^2\Delta\xi^2/4}$$

$$\Big[E_\xi(i_a, j+1, k-1) - E_\xi(i_a, j, k-1) + E_\xi(i_a, j, k) - E_\xi(i_a, j-1, k)$$

$$+ E_\xi(i_a-1, j+1, k-1) - E_\xi(i_a-1, j, k-1) + E_\xi(i_a-1, j, k)$$

$$- E_\xi(i_a-1, j-1, k) + E_\xi(i_g+1, j+1, k-1) - E_\xi(i_g+1, j, k-1)$$

$$+ E_\xi(i_g+1, j, k) - E_\xi(i_g+1, j-1, k) + E_\xi(i_g, j+1, k-1)$$

$$- E_\xi(i_g, j, k-1) + E_\xi(i_g, j, k) - E_\xi(i_g, j-1, k)\Big] - \frac{1}{4\Delta\xi}$$

$$\frac{1 - \Delta\xi^2/4}{\zeta^2 - a^2\Delta\xi^2/4}\Big[E_\zeta(i_a-1, j, k) + E_\zeta(i_a-1, j, k-1) - E_\zeta(i_g+1, j, k)$$

$$- E_\zeta(i_g+1, j, k-1)\Big] - \frac{1}{4c\Delta\tau}\,\frac{\zeta^2 - a^2}{\zeta^2 - a^2\Delta\xi^2/4}\Big[E_\xi(i_a, j, k)$$

$$- E_\xi(i_a, j, k-1) + E_\xi(i_a-1, j, k) - E_\xi(i_a-1, j, k-1)$$

$$+ E_\xi(i_g, j, k) - E_\xi(i_g, j, k-1) + E_\xi(i_g+1, j, k) - E_\xi(i_g+1, j, k-1)\Big]$$

$$- \frac{a}{4c\Delta\tau}\,\frac{1 - \Delta\xi^2/4}{\zeta^2 - a^2\Delta\xi^2/4}\Big[2E_\zeta(i_a, j, k) - 2E_\zeta(i_a, j, k-1) + E_\zeta(i_a-1, j, k)$$

$$- E_\zeta(i_a-1, j, k-1) + E_\zeta(i_g+1, j, k) - E_\zeta(i_g+1, j, k-1)\Big] \qquad (100)$$

Evaluate $\partial E_\xi/\partial\tau$ at $(i_a, j, k-1/2)$

$$\frac{1}{\Delta\tau}\Big[E_\xi(i_a, j, k) - E_\xi(i_a, j, k-1)\Big] = -\frac{\sigma(i_a, j, k-1/2)}{2\epsilon_0}$$

$$\Big[E_\xi(i_a, j, k) + E_\xi(i_a, j, k-1)\Big] - \frac{j_\xi(i_g, j, k-1/2)}{\epsilon_0} + \frac{c^2}{2\Delta\zeta}$$

$$\Big[B_\phi(i_a, j+1, k-1) - B_\phi(i_a, j, k-1) + B_\phi(i_a, j, k)$$

$$- B_\phi(i_a, j-1, k)\Big] - \frac{c}{\Delta\tau}\Big[B_\phi(i_a, j, k) - B_\phi(i_a, j, k-1)\Big] \qquad (101)$$

Evaluate $\partial E_\xi/\partial\tau$ at $(i_g, j, k-1/2)$

$$\frac{1}{\Delta\tau}\left[E_\xi(i_g, j, k) - E_\xi(i_g, j, k-1)\right] = -\frac{\sigma(i_g, j, k-1/2)}{2\epsilon}$$

$$\left[E_\xi(i_g, j, k) + E_\xi(i_g, j, k-1)\right] - \frac{j_\xi(i_g, j, k-1/2)}{\epsilon} + \frac{u^2}{2\Delta\zeta}$$

$$\left[B_\phi(i_g, j+1, k-1) - B_\phi(i_g, j, k-1) + B_\phi(i_g, j, k) - B_\phi(i_g, j-1, k)\right]$$

$$-\frac{u^2}{c\Delta\tau}\left[B_\phi(i_g, j, k) - B_\phi(i_g, j, k-1)\right] \qquad (102)$$

Evaluate Maxwell's curl equations at $(i_g+1, j, k-1/2)$

$$\frac{1}{\Delta\tau}\left[E_\xi(i_g+1, j, k) - E_\xi(i_g+1, j, k-1)\right] = \frac{\sigma(i_g+1, j, k-1/2)}{2\epsilon}$$

$$\left[E_\xi(i_g+1, j, k) + E_\xi(i_g+1, j, k-1)\right] - \frac{j_\xi(i_g+1, j, k-1/2)}{\epsilon}$$

$$+\frac{u^2}{2\Delta\zeta}\left[B_\phi(i_g+1, j+1, k-1) - B_\phi(i_g+1, j, k-1) + B_\phi(i_g+1, j, k)\right.$$

$$\left.- B_\phi(i_g+1, j-1, k)\right] - \frac{u^2}{c\Delta\tau}\left[B_\phi(i_g+1, j, k) - B_\phi(i_g+1, j, k-1)\right] \qquad (103)$$

$$\frac{1}{\Delta\tau}\left[E_\zeta(i_g+1, j, k) - E_\zeta(i_g+1, j, k-1)\right] = -\frac{\sigma(i_g+1, j, k-1/2)}{2\epsilon}$$

$$\left[E_\zeta(i_g+1, j, k) + E_\zeta(i_g+1, j, k-1)\right] - \frac{j_\zeta(i_g+1, j, k-1/2)}{\epsilon}$$

$$- \frac{u^2}{2\Delta\xi}\Big[B_\phi(i_g, j, k) - B_\phi(i_g+1, j, k) + B_\phi(i_g+1, j, k-1)$$

$$- B_\phi(i_g+2, j, k-1)\Big] - \frac{au^2}{c\Delta\tau}\Big[B_\phi(i_g+1, j, k) - B_\phi(i_g+1, j, k-1)\Big] \quad (104)$$

$$\frac{1}{\Delta\tau}\Big[B_\phi(i_g+1, j, k) - B_\phi(i_g+1, j, k-1)\Big] = \frac{1}{2\Delta\zeta}\,\frac{\zeta^2 - a^2}{\zeta^2 - a^2\Delta\xi^2}$$

$$\Big[E_\xi(i_g+1, j+1, k-1) - E_\xi(i_g+1, j, k-1) + E_\xi(i_g+1, j, k)$$

$$- E_\xi(i_g+1, j-1, k)\Big] - \frac{1}{2\Delta\xi}\,\frac{1 - \Delta\xi^2}{\zeta^2 - a^2\Delta\xi^2}\Big[E_\zeta(i_g, j, k) - E_\zeta(i_g+1, j, k)$$

$$+ E_\zeta(i_g+1, j, k-1) - E_\zeta(i_g+2, j, k-1)\Big] - \frac{1}{c\Delta\tau}\,\frac{\zeta^2 - a^2}{\zeta^2 - a^2\Delta\xi^2}$$

$$\Big[E_\xi(i_g+1, j, k) - E_\xi(i_g+1, j, k-1)\Big] - \frac{a}{c\Delta\tau}\,\frac{1 - \Delta\xi^2}{\zeta^2 - a^2\Delta\xi^2}$$

$$\Big[E_\zeta(i_g+1, j, k) - E_\zeta(i_g+1, j, k-1)\Big] \quad (105)$$

For given j and k, Equations (99) through (105) are solved simultaneously for the four independent field quantities at the air-ground boundary and for the three field quantities at the point (i_g+1, j, k).

4. GEOMETRY FOR THE LOW-ALTITUDE EMP CODES

By referring to Figure 5, define prolate spheroidal coordinates as

$$\xi = \frac{1}{2a}(r_1 - r), \qquad \zeta = \frac{1}{2}(r_1 + r), \qquad \phi = \tan^{-1}\frac{y}{x} \qquad (106)$$

Note that surfaces of constant ξ are hyperboloids of revolution and those of constant ζ are prolate spheroids (i.e., prolate ellipsoids of revolution). Also observe that all real space lies within the range of coordinates

$$\zeta \geq a, \qquad -1 \leq \xi \leq 1 \qquad (107)$$

The z axis is separated into three segments determined by

$$x = y = 0 \text{ or } \begin{cases} \xi = 1 & \text{for } z < a & (108) \\ \zeta = a & \text{for } -a < z < a & (109) \\ \xi = -1 & \text{for } z < -a & (110) \end{cases}$$

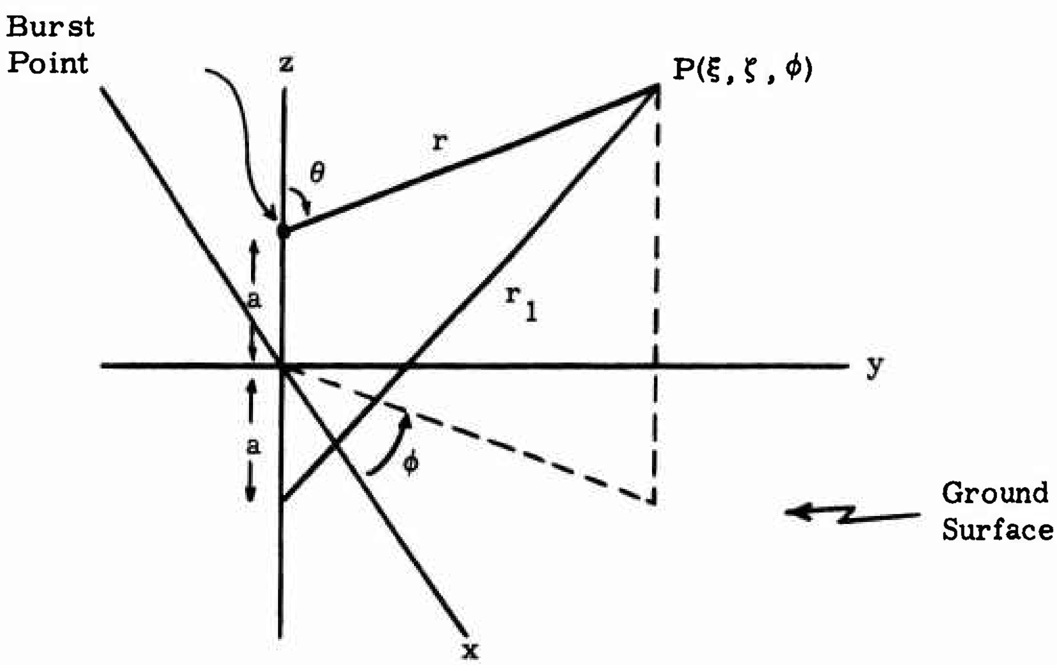

Figure 5

Geometry for the Prolate Spheroidal Coordinate System

The x-y plane is taken as the ground-air interface and according to Eq. (106) is the degenerate hyperboloid determined by $\xi = 0$. The burst point of the weapon is on the z axis at the point $z = a$ which is also described by $\zeta = a$, $\xi = 1$. The wave front of the electromagnetic pulse generated by the weapon spreads out in air from the burst point with velocity c and is determined by $r = ct$, or by

$$\zeta - a\xi = ct \tag{111}$$

Thus for fixed t the wave front describes a straight line in the prolate spheroidal coordinate system.

From Eq. (106) we find

$$r_1 = \zeta + a\xi \tag{112}$$

$$r = \zeta - a\xi \tag{113}$$

Now

$$r_1^2 = (\zeta + a\xi)^2 = x^2 + y^2 + (z + a)^2 \tag{114}$$

$$r^2 = (\zeta - a\xi)^2 = x^2 + y^2 + (z - a)^2 \tag{115}$$

From these it follows that the transformation equations from cartesian coordinates to prolate spheroidal coordinates are

$$\xi = \frac{1}{2a}\sqrt{x^2 + y^2 + (z + a)^2} - \frac{1}{2a}\sqrt{x^2 + y^2 + (z - a)^2} \tag{116}$$

$$\zeta = \frac{1}{2}\sqrt{x^2 + y^2 + (z + a)^2} + \frac{1}{2}\sqrt{x^2 + y^2 + (z - a)^2} \tag{117}$$

$$\phi = \tan^{-1}\frac{y}{x} \tag{118}$$

where principal square roots are intended. The inverse transformations are

$$x = \sqrt{(\zeta^2 - a^2)(1 - \xi^2)}\ \cos\phi \tag{119}$$

$$y = \sqrt{(\zeta^2 - a^2)(1 - \xi^2)}\ \sin\phi \tag{120}$$

$$z = \xi\,\zeta \tag{121}$$

Transformation equations from a spherical polar coordinate system centered at the burst point to prolate spheroidal coordinates may be obtained in a similar manner, we find

$$\xi = \frac{2(a/r + \cos\theta)}{1 + \sqrt{1 + (4a/r)(a/r + \cos\theta)}} \tag{122}$$

$$\zeta = \frac{r}{2}\left[1 + \sqrt{1 + (4a/r)(a/r + \cos\theta)}\right] \tag{123}$$

The azimuthal angle is the same in both coordinate systems. The inverse transformations are

$$r = \zeta - a\xi \tag{124}$$

$$\theta = \cos^{-1}\left(\frac{\xi\,\zeta - a}{\zeta - a\xi}\right) \tag{125}$$

We now seek the scale factors h_ξ, h_ζ, and h_ϕ such that

$$ds^2 = h_\xi^2\, d\xi^2 + h_\zeta^2\, d\zeta^2 + h_\phi^2\, d\phi^2 \tag{126}$$

where ds is an element of length. To find these, differentiate Equations (119) through (121) and substitute into

$$ds^2 = dx^2 + dy^2 + dz^2 \tag{127}$$

Obtain

$$ds^2 = \frac{\zeta^2 - \xi^2 a^2}{1 - \xi^2} d\xi^2 + \frac{\zeta^2 - \xi^2 a^2}{\zeta^2 - a^2} d\zeta^2 + (\zeta^2 - a^2)(1 - \xi^2)\, d\phi^2 \tag{128}$$

comparing Equations (126) and (128) gives

$$h_\xi = \sqrt{\frac{\zeta^2 - \xi^2 a^2}{1 - \xi^2}} \tag{129}$$

$$h_\zeta = \sqrt{\frac{\zeta^2 - \xi^2 a^2}{\zeta^2 - a^2}} \tag{130}$$

$$h_\phi = \sqrt{(\zeta^2 - a^2)(1 - \xi^2)} \tag{131}$$

Because Eq. (128) does not contain cross terms in $d\xi$, $d\zeta$, and $d\phi$ it follows that we are dealing with an orthogonal coordinate system. Incidentally, the coordinates are cyclic in the order ξ -ζ -ϕ.

By using Eqs. (129) through (131) one easily finds expressions for the various vector operations in prolate spheroidal coordinates.

$$\nabla f = \sqrt{\frac{1 - \xi^2}{\zeta^2 - \xi^2 a^2}} \frac{\partial f}{\partial \xi} \hat{\xi} + \sqrt{\frac{\zeta^2 - a^2}{\zeta^2 - \xi^2 a^2}} \frac{\partial f}{\partial \zeta} \hat{\zeta} + \sqrt{(\zeta^2 - a^2)(1 - \xi^2)} \frac{\partial f}{\partial \phi} \hat{\phi} \tag{132}$$

$$\nabla \cdot \vec{f} = \frac{1}{\zeta^2 - \xi^2 a^2} \left\{ \frac{\partial}{\partial \xi} \left(\sqrt{(\zeta^2 - \xi^2 a^2)(1 - \xi^2)}\, f_\xi \right) + \frac{\partial}{\partial \zeta} \right.$$

$$\left. \left(\sqrt{(\zeta^2 - \xi^2 a^2)(\zeta^2 - a^2)}\, f_\zeta \right) + \frac{\partial}{\partial \phi} \left(\frac{\zeta^2 - \xi^2 a^2}{\sqrt{(\zeta^2 - a^2)(1 - \xi^2)}}\, f_\phi \right) \right\} \tag{133}$$

$$\nabla \mathrm{x}\, \vec{f} = \frac{\hat{\xi}}{\sqrt{(\zeta^2 - \xi^2 a^2)(1 - \xi^2)}} \left[\frac{\partial}{\partial \zeta} \left(\sqrt{(\zeta^2 - a^2)(1 - \xi^2)}\, f_\phi \right) \right.$$

$$\left. - \frac{\partial}{\partial \phi} \left(\sqrt{\frac{\zeta^2 - \xi^2 a^2}{\zeta^2 - a^2}} \right) f_\zeta \right] + \frac{\hat{\zeta}}{\sqrt{(\zeta^2 - \xi^2 a^2)(\zeta^2 - a^2)}} \left[\frac{\partial}{\partial \phi} \right.$$

$$\left. \left(\sqrt{\frac{\zeta^2 - \xi^2 a^2}{1^2 - \xi^2}}\, f_\xi \right) - \frac{\partial}{\partial \xi} \left(\sqrt{(\zeta^2 - a^2)(1 - \xi^2)}\, f_\phi \right) \right]$$

$$+ \hat{\phi} \frac{\sqrt{(\zeta^2 - a^2)(1 - \xi^2)}}{\zeta^2 - \xi^2 a^2} \left[\frac{\partial}{\partial \xi} \left(\sqrt{\frac{\zeta^2 - \xi^2 a^2}{\zeta^2 - a^2}}\, f_\zeta \right) \right.$$

$$\left. - \frac{\partial}{\partial \zeta} \left(\sqrt{\frac{\zeta^2 - \xi^2 a^2}{1 - \xi^2}}\, f_\xi \right) \right] \tag{134}$$

$$\nabla^2 f = \frac{1}{\zeta^2 - \xi^2 a^2} \left\{ \frac{\partial}{\partial \xi} \left[(1 - \xi^2) \frac{\partial f}{\partial \zeta} \right] + \frac{\partial}{\partial \xi} \left[(\zeta^2 - a^2) \frac{\partial f}{\partial \zeta} \right] \right.$$

$$\left. + \frac{\partial}{\partial \phi} \left[\frac{\zeta^2 - \xi^2 a^2}{(\zeta^2 - a^2)(1 - \xi^2)} \frac{\partial f}{\partial \phi} \right] \right\} \tag{135}$$

Let us now consider the vector transformation equations between prolate spheroidal coordinates and other orthogonal systems. For convenience denote the base vectors in the prolate spheroidal system by $\hat{u}_i$ and those of the other system by $\hat{e}_i$. We may expand $\hat{e}_i$ in terms of the $\hat{u}_i$.

$$\hat{e}_i = \sum_j \alpha_{ji} \hat{u}_j \tag{136}$$

But

$$\hat{e}_i \cdot \hat{e}_j = \delta_{ij} = \sum_{k,\ell} (\alpha_{ki} \hat{u}_k) \cdot (\alpha_{\ell j} \hat{u}_\ell) = \sum_{k,\ell} \alpha_{ki} \alpha_{\ell j} (\hat{u}_k \cdot \hat{u}_\ell)$$

$$= \sum_{k,\ell} \alpha_{ki} \alpha_{\ell j} \delta_{k\ell} = \sum_k \alpha_{ki} \alpha_{kj} \tag{137}$$

i.e.,

$$\sum_k \alpha_{ki} \alpha_{kj} = \delta_{ij} \tag{138}$$

similarly it can be shown that

$$\sum_i \alpha_{ki} \alpha_{\ell i} = \delta_{k\ell} \tag{139}$$

Equations (138) and (139) are the orthogonality relations for the transformation coefficients α_{ij}. Multiply (136) by α_{ki} and sum over i.

$$\sum_i \alpha_{ki} \hat{e}_i = \sum_{i,j} \alpha_{ki} \alpha_{ji} \hat{u}_j = \sum_j \delta_{kj} \hat{u}_j = \hat{u}_k \tag{140}$$

Equation (139) has been used. Thus

$$\hat{u}_i = \sum_j \alpha_{ij} \hat{e}_j \tag{141}$$

Any vector may be expanded in terms of either set of base vectors.

$$\vec{f} = \sum_i f_i \hat{e}_i = \sum_{i,j} f_i \alpha_{ji} \hat{u}_j = \sum_j f'_j \hat{u}_j \tag{142}$$

Here f'_j are the components of f in prolate spheroidal coordinates and f_i are those in the system with base vectors $\hat{e}_i$. Observe that

$$f'_i = \sum_j \alpha_{ij} f_j \tag{143}$$

Multiply this by α_{ik}, sum over i, and use the orthogonality relation. Obtain

$$f_i = \sum_j \alpha_{ji} f'_j \tag{144}$$

An easy way to determine the transformation matrix is to find an expression for the prolate spheroidal unit vectors in terms of those of the other coordinate system and compare to Eq. (141). Now,

$$\hat{\xi} = h_\xi \nabla\xi , \qquad \hat{\zeta} = h_\zeta \nabla\zeta , \qquad \hat{\phi} = h_\phi \nabla\phi \tag{145}$$

we wish to find the transformation to spherical polar coordinates centered at the burst point. By taking the gradients of Equations (122) and (123) and employing Equations (129), (130), and (145) we find

$$\hat{\xi} = -\frac{a}{h_\xi} \hat{r} - \frac{1}{h_\zeta} \hat{\theta} \tag{146}$$

$$\hat{\zeta} = \frac{1}{h_\zeta} \hat{r} - \frac{a}{h_\xi} \hat{\theta} \tag{147}$$

Of course $\hat{\phi}$ is identical to the corresponding spherical polar unit vector. By comparing Eq. (141) with Eqs. (146) and (147) the desired transformation matrix is obtained

$$(\alpha_{ij}) = \begin{pmatrix} -\frac{a}{h_\xi} & -\frac{1}{h_\zeta} \\ \frac{1}{h_\zeta} & -\frac{a}{h_\xi} \end{pmatrix} \qquad (148)$$

The inverse matrix is

$$(\alpha_{ij})^{-1} = (\alpha_{ji}) = \begin{pmatrix} -\frac{a}{h_\xi} & \frac{1}{h_\zeta} \\ -\frac{1}{h_\zeta} & -\frac{a}{h_\xi} \end{pmatrix} \qquad (149)$$

5. ELECTROMAGNETIC FIELDS WITH SPHERICAL SYMMETRY

a. Finite Difference Code

A finite difference code is described below for calculating electromagnetic fields for problems with spherical symmetry. The assumption is made that the conductivity and Compton current terms are functions only of the radial distance between the source and field points and time. It is well known that source distributions of this symmetry produce no radiating fields. Here this occurs because the symmetry reduces Maxwell's equations to a particularly simple form involving the radial component of the electric field and time. Because of this simplicity, the code runs very rapidly, which is a primary advantage of the method. This code has been used as a test case for the two-dimensional codes described above.

In M.K.S. units and spherical polar coordinates Maxwell's curl equations are

$$\frac{\hat{r}}{r^2 \sin\theta}\left[\frac{\partial}{\partial\theta}(r \sin\theta E_\phi) - \frac{\partial}{\partial\phi}(r E_\theta)\right] + \frac{\hat{\theta}}{r \sin\theta}\left[\frac{\partial E_r}{\partial\phi}\right.$$

$$\left.- \frac{\partial}{\partial r}(r \sin\theta E_\phi)\right] + \frac{\hat{\phi}}{r}\left[\frac{\partial}{\partial r}(r E_\theta) - \frac{\partial E_r}{\partial\theta}\right] = -\frac{\partial}{\partial t}$$

$$\left[B_r \hat{r} + B_\theta \hat{\theta} + B_\phi \hat{\phi}\right] \tag{150}$$

$$\frac{\hat{r}}{r^2 \sin\theta}\left[\frac{\partial}{\partial\theta}(r \sin\theta H_\phi) - \frac{\partial}{\partial\phi}(r H_\theta)\right] + \frac{\hat{\theta}}{r \sin\theta}\left[\frac{\partial H_r}{\partial\phi}\right.$$

$$\left.- \frac{\partial}{\partial r}(r \sin\theta H_\phi)\right] + \frac{\hat{\phi}}{r}\left[\frac{\partial}{\partial r}(r H_\theta) - \frac{\partial H_r}{\partial\theta}\right] = (j_r \hat{r} + j_\theta \hat{\theta} + j_\phi \hat{\phi})$$

$$+ \frac{\partial}{\partial t}(D_r \hat{r} + D_\theta \hat{\theta} + D_\phi \hat{\phi}) \tag{151}$$

Assume the constitutive equations

$$\vec{B} = \mu \vec{H}, \qquad \vec{D} = \epsilon \vec{E} \tag{152}$$

with μ and ϵ constant. Also, because of the assumed azimuthal symmetry no physical quantity depends on ϕ. With this, Eq. (151) and (152) yield

$$\frac{\hat{r}}{r^2 \sin\theta}\left[\frac{\partial}{\partial\theta}(r \sin\theta\, E_\phi)\right] - \frac{\hat{\theta}}{r \sin\theta}\left[\frac{\partial}{\partial r}(r \sin\theta\, E_\phi)\right]$$

$$+ \frac{\hat{\phi}}{r}\left[\frac{\partial}{\partial r}(r E_\theta) - \frac{\partial E_r}{\partial\theta}\right] = - \frac{\partial}{\partial t}(B_r \hat{r} + B_\theta \hat{\theta} + B_\phi \hat{\phi}) \tag{153}$$

$$\frac{\hat{r}c^2}{r^2 \sin\theta}\frac{\partial}{\partial\theta}(r \sin\theta\, B_\phi) - \frac{\hat{\theta}c^2}{r \sin\theta}\frac{\partial}{\partial r}(r \sin\theta\, B_\phi)$$

$$+ \frac{\hat{\phi}c^2}{r}\left[\frac{\partial}{\partial r}(r\, B_\theta) - \frac{\partial B_r}{\partial\theta}\right] = \frac{j_r}{\epsilon}\hat{r} + \frac{j_\theta}{\epsilon}\hat{\theta} + \frac{j_\phi}{\epsilon}\hat{\phi}$$

$$+ \frac{\partial}{\partial t}(E_r \hat{r} + E_\theta \hat{\theta} + E_\phi \hat{\phi}) \tag{154}$$

where

$$c = \frac{1}{\sqrt{\mu\epsilon}} \tag{155}$$

Note that in scalar form, these reduce to two sets of coupled equations. One set involves E_ϕ, B_r, B_θ, and j_ϕ. The other relates E_r, E_θ, B_ϕ, j_r, and j_θ. We assume that the current distribution is such that $j_\phi = 0$. Then if E_ϕ, B_r, and B_θ are initially zero, Maxwell's equations predict that they will remain so. Thus we set

$$E_\phi = B_r = B_\theta = j_\phi = 0 \tag{156}$$

Equations (153) and (154) then become

$$\frac{\partial E_r}{\partial t} = -\frac{j_r}{\epsilon} + \frac{c^2}{r^2 \sin\theta} \frac{\partial}{\partial \theta} (r \sin\theta \, B_\phi) \tag{157}$$

$$\frac{\partial E_\theta}{\partial t} = -\frac{j_\theta}{\epsilon} - \frac{c^2}{r \sin\theta} \frac{\partial}{\partial r} (r \sin\theta \, B_\phi) \tag{158}$$

$$\frac{\partial B_\phi}{\partial t} = \frac{1}{r} \frac{\partial E_r}{\partial \theta} - \frac{1}{r} \frac{\partial}{\partial r} (r E_\theta) \tag{159}$$

When transformed to retarded time, Equations (157) through (159) provide the basis for several EMP calculations involving azimuthal symmetry. If also one demands that no quantity depends on θ so that spherical symmetry obtains, it follows that

$$\frac{\partial E_r}{\partial t} = -\frac{j_r}{\epsilon} \tag{160}$$

$$\frac{\partial E_\theta}{\partial t} = -\frac{j_\theta}{\epsilon} - \frac{c^2}{r} \frac{\partial}{\partial r} (r B_\phi) \tag{161}$$

$$\frac{\partial B_\phi}{\partial t} = -\frac{1}{r} \frac{\partial}{\partial r} (r E_\theta) \tag{162}$$

Observe that these equations are decoupled into two sets, one involving E_r, j_r and the other involving E_θ, j_θ, and B_ϕ. Now, because of the azimuthal symmetry j_θ and E_θ are zero on the z axis. The spherical symmetry demands that they cannot depend on θ. They are thus zero everywhere. From Eq. (162) it is evident that B_ϕ is constant. Thus, if B_ϕ is initially zero the above reduces to

$$\frac{\partial E_r}{\partial t} = -\frac{j_r}{\epsilon} \tag{163}$$

Put

$$j_r \longrightarrow j_r + \sigma E_r \tag{164}$$

where j_r is now the Compton current and E_r is the conduction current. Then Eq. (163) becomes

$$\frac{\partial E_r}{\partial t} = -\frac{j_r}{\epsilon} - \frac{\sigma E_r}{\epsilon} \tag{165}$$

This is the differential equation that determines the radial component of the electric field for problems with spherical symmetry.

This equation may be put in difference form as follows. Let

$$r = j\Delta r, \qquad t = k\Delta t \tag{166}$$

then Eq. (165) may be expanded about the point (j, k-1/2).

$$\frac{1}{\Delta t}\left[E_r(j,\ k) - E_r(j,\ k-1)\right] = -\frac{1}{\epsilon}\Big[j_r(j,\ k-1/2) + \sigma(j,\ k-1/2)\, E_r(j,\ k-1/2)\Big] \tag{167}$$

Or

$$E_r(j,\ k) = \frac{-\dfrac{j_r(j,\ k-1/2)\Delta t}{\epsilon} + \left(1 - \dfrac{\sigma(j,\ k-1/2)\Delta t}{2\epsilon}\right) E_r(j,\ k-1)}{1 + \dfrac{\sigma(j,\ k-1/2)\Delta t}{2\epsilon}} \tag{168}$$

Provided the current and conductivity are known functions of time and the initial field $E_r(j, 0)$ is given, the field $E_r(r, t)$ for a given distance $r = j\Delta r$ and for times $t = k\Delta t > 0$ may be determined recursively from the above equation. Because E(j, k) depends only on the field E(j, k-1) are not at the fields at other values, we conclude that it is not a propagating field.

b. Exact Solution

In addition to the finite difference code for calculating fields with spherical symmetry, a computer code for evaluating the exact solution to these spherically symmetric fields has been developed. For this special physical situtation Maxwell's equations become

$$\nabla \times \vec{H} = \vec{j}(\vec{r}, t) + \sigma(\vec{r}, t)\, \vec{E}(\vec{r}, t) + \epsilon_0 \frac{\partial \vec{E}}{\partial t} = 0 \tag{169}$$

which has as an exact solution*

$$E(r, t) = -\int^{t} j(t') \exp\left\{-\int_{t'}^{t} \sigma(t'')dt''\right\} dt' \tag{170}$$

The code, the listing for which is in Appendix B, is for numerically evaluating the above integrals for arbitrary currents and conductivities of the form of Eqs. (1) and (2). This technique might be of value for obtaining the fields inside of 300 meters to be used as boundary conditions for a finite-difference code.

---

* See Longmire, C. L., Close-In E.M. Effects, LAMS-3072, E-3, May 1964.

II. DIFFUSION EQUATION

1. PROGRAM AND CALCULATIONS

A code for the CDC-6600 at the Air Force Weapons Laboratory, Kirtland Air Force Base, has been written and used to calculate EMP above an infinitely conducting ground in the diffusion approximation. In the general case of Maxwell's equations, one obtains

$$\nabla^2 \vec{B} = -\mu \nabla \times \vec{J} + \frac{1}{c^2} \frac{\partial^2 \vec{B}}{\partial t^2} + \mu \left[-\vec{\nabla}\sigma \times \vec{E} + \sigma \frac{\partial \vec{B}}{\partial t} \right] \tag{171}$$

and if the conductivity σ is a slowly varying function of space and if

$$\mu\sigma \left| \frac{\partial \vec{B}}{\partial t} \right| \gg \frac{1}{c^2} \left| \frac{\partial^2 \vec{B}}{\partial t^2} \right| \tag{172}$$

as may be the case in a highly conducting medium, then Eq. (171) reduces to

$$\nabla^2 \vec{B} - \mu\sigma \frac{\partial \vec{B}}{\partial t} = -\mu \nabla \times \vec{J} \tag{173}$$

the inhomogeneous diffusion equation. In the particular case of azimuthal symmetry cylindrical coordinates are useful and the diffusion equation becomes

$$\frac{\partial^2 B_\phi}{\partial z^2} - \mu\,\sigma(t) \frac{\partial B_\phi}{\partial t} = -\mu \frac{\partial J_r}{\partial z} \tag{174}$$

which can be solved by using Green's functions*. A complete description of

* Graham, W. R., Babb, D. D., RM-4905-PR, January 1966.

the code and its listing will be described in a forthcoming EMP Theoretical Note. Numerous calculations have been made for various weapons at various distances. Some illustrative cases are included in Appendix III.

2. EARLY TIME FIELDS AND LIMITS OF VALIDITY

When the conductivity is low, at early times, the condition Eq. (172) is not satisfied and one knows that the diffusion equation approach is not valid. Also in the solution by Green's functions there is a homogeneous term (see footnote on page 48) that involves the initial B_ϕ field. This field from the earliest times (as calculated by the diffusion equation) is clearly incorrect, but its influence was felt to be negligible on the peak values of the magnetic field because, it was argued, the homogeneous part caused by the Compton currents was so extremely large. Numerous runs on the computer gave evidence that this was not always the case. Hence, analytical examples that showed that for some weapons the early time fields were unimportant to the peak value were found, but for other cases they contributed as much as half the peak field. That is not to say that even in the most unfavorable cases were the peak answers in error by 50 percent, but rather that half the contribution was in error by some undetermined amount. A reasonable estimate is that the undetermined amount would surely be less than the value calculated. The net consequence of this result is that in some cases one should attempt to do better on the early time fields.

3. CRITIQUE AND SUGGESTIONS FOR THE FUTURE

From these studies, one may say that the diffusion equation approach to calculating the EMP from a nuclear burst is a simple and rather accurate method provided that the early time fields are small, or are handled in a proper manner, and that the ground approximates a perfect conductor. The method is considerably simpler than a finite difference scheme in that it takes far less computer time and is not plagued by such questions as stability

or convergence. One problem that has occurred in this approach is the question of the size of the time cuts. The time dependence of the current and conductivities has been approximated* by a series of exponentials of the form

$$J(r, t) = J(r, T_0)\, e^{\beta_0(t - t_0)}, \quad T_0 < t < T_1 \tag{175}$$

$$J(r, t) = J(r, T_1)\, e^{\beta_1(t - T_1)}, \quad T_1 < t < T_2 \tag{176}$$

$$J(r, t) = J(r, T_2)\, e^{\beta_2(t - T_2)}, \quad T_2 < t < T_3 \tag{177}$$

. . . .

. . . .

and so on for as many time cuts as one feels are needed to approximate the given current curve; and similarly for the conductivity. It was found empirically on the computer that the values of the calculated fields were somewhat sensitive to the size of the time cuts, i.e., if more smaller time cuts, $T_1 - T_0$, $T_2 - T_1$, ..., etc., were used to approximate a given current or conductivity curve (say 20 instead of seven or eight), the values of the fields calculated changed by perhaps 10 percent at peak value. This problem was reduced to negligible status by simply increasing the number of time cuts to such an extent that the field values were not changed by further increases in the number of time cuts. Thus it was thought that the variations observed were due to increasing accuracy in the representation of the current and conductivity curves. More recently, analytical studies of the question have shown that it is not a matter of numerics, but rather a basic feature of the

* Graham, W. R., Babb, D. D., RM-4905-PR, January 1966.

method of solution. That the matter is not a very serious one is indicated by the convergence of the numerical values with the increasing number of time cuts and by the agreement of the field values obtained with fields calculated by other approaches*.

A further extension of this general method to nondiffusion fields and to a finitely conducting earth has been found. It is based on the use of a Green's function not for the diffusion equation, but rather for the complete equation

$$\nabla^2 \vec{B} - \mu\sigma \frac{\partial \vec{B}}{\partial t} - \mu\epsilon \frac{\partial^2 \vec{B}}{\partial t^2} = -\mu \nabla \times \vec{J} \tag{178}$$

The Green's function for this equation is well known if σ is a constant**. The present effort has been toward extending the Green's function to cases for which σ is a function of time. This has been accomplished for a linear time dependency. In the future it is hoped that this work can be extended to more useful time dependencies such as an exponential. If this is done, one will have an analytic method for calculating the propagation of wave fields in conducting media. The results could easily be checked by taking the limiting cases of very large σ (diffusion equation) and $\sigma = 0$ (wave equation). This type of calculation might be especially useful for calculation of close in fields, or for a layered conducting earth.

---

* As for instance by the method of Graham, The Electromagnetic Fields Produced by a General Current Distribution in a Conductive Environment Under Certain Symmetry Conditions, Technical Report No. WL-TR-64-153, January, 1965.

** See Morse, P. M., Feshback, H., Methods of Theoretical Physics, Vol. I.

III. GROUND SOURCES

1. INTRODUCTION TO GROUND SOURCES

The earth under a nuclear explosion slightly above the surface is bombarded by neutrons, causing it to become a source of gamma radiation. This radiation in turn produces Compton current and ionizes the air. Because these effects--Compton current and ionization of the air--are sources of EMP phenomena, they are called "ground sources."

The intensity of the radiation sources created by monoenergetic sources of neutrons has been calculated by a Monte Carlo computer code run at the Los Alamos Scientific Laboratory. The results of this run have been analyzed to separate out the manner in which gamma sources vary with time, range, depth, and gamma energy. They have also been separated into two components that can be ascribed to different kinds of neutron interaction with dirt, namely inelastic collisions and capture collisions. The results of this analysis are the six S functions described in Section 2-b below. In order to make the ground sources continuous with respect to space and time, four of the S functions, those with a spatial or temporal dependence, have been approximated by functions that are continuous with respect to space and time.

Gamma radiation from the earth interacts with the air to produce ground sources. The ground sources caused by a monoenergetic gamma source at a specified point in the ground were computed by the Monte Carlo computer code called TIGRE. The results, called "TIGRE quantities," are described in Section 2-c.

We have worked toward combining the results of these two Monte Carlo codes in such a way that they are usable as inputs to an EMP ground burst code.

The task is not complete; this report describes the current state of the project. Portions of the task reported previously are not redocumented here. Final results, including graphs of ground sources, will be reported in a memorandum to WLRPE.

2. CALCULATING GROUND SOURCES

a. Introduction

INT is a computer code that calculates ground sources produced at some point (in the air) and time (since the burst) per neutron of some energy. The point is described by its range, distance from the origin--the point on the ground directly below the burst--and its angle from the vertical. Currents are described by the components J_r, which is positive for a current going away from the origin, and J_θ, which is perpendicular to J_r and positive for a downward current. Thus an upward current at the surface would be represented by a negative $J_\theta\ (90^\circ)$ and a zero $J_r\ (90^\circ)$.

INT always calculates ground sources for a standard set of 11 neutron energies and 10 angles and always computes the average ionization rate, Q, for each neutron energy. For an input range and time, INT's standard output is 21 numbers--Q, J_r at 10 angles, and J_θ at 10 angles--for each of the 11 neutron energies.

Q has the units ion pairs/meter^3 · second · neutron; the Js have the units amperes/meter^2 · neutron.

The calculation of ground sources can be thought of as having three parts. The first is the calculation of gamma sources. The second is the accounting for the attenuation of these sources as they travel through the air. The third is a mechanism for combining the first two, i.e., for obtaining the effect at some point in the air caused by sources distributed through the ground.

The sources of gammas are represented by the function $S(E_N, E_\gamma, r, z, t)$, which has been expressed in the form $S = S_{ei} \cdot S_{ri} \cdot S_{zi} + S_{ec} \cdot S_{rc} \cdot S_{zc}$. The latter six functions are called "S functions." They are described in Section 2-b.

The effects in the air at point p of sources in the ground at point g vary with the location of the source with respect to the burst, its γ energy, and the location of p with respect to the source. In general, an

effect F is of the form $F(E_N, E_\gamma, g, p, t) = T(E_\gamma, g, p, t) \cdot S(E_N, E_\gamma, g, t')$. The quantity T is called a TIGRE quantity and is described in Section 2-c.

An effect $F = T \cdot S$ is the result of a point source in the ground. It is necessary to take into account all of the ground in order to have a ground source $F(E_N, p, t)$ as described in the first three paragraphs of Section 2-a. To calculate

$$F(E_N, p, t) = \int_{\text{ground}} \left(\int_{E_\gamma} \left[T \cdot S \right] \right)$$

the ground is divided into range, depth, and angle bins by using a cylindrical coordinate system centered on the burst axis, and the E_γ spectrum is represented by six discrete energies. The coding which accomplishes the indicated integration is described in Section 2-d.

b. Sources of Gammas

Basic Definitions: The distribution of the secondary source of gammas induced in the ground by a near-surface, monoenergetic neutron impulse has been expressed in the following form:

$$S(E_N, E_\gamma, r, z, t) = S_{ei}(E_N, E_\gamma) \cdot S_{ri}(E_N, r, t) \cdot S_{zi}(E_N, z, t) \cdot 10^{10}$$

$$+ S_{ec}(E_\gamma) \cdot S_{rc}(E_N, r, t) \cdot S_{zc}(E_N, z, t) = \frac{\text{photon energy produced}}{\text{(volume)(time)(neutron)}} \qquad (179)$$

Here E_N is the energy per neutron of the monoenergetic neutron source, E_γ is the energy per photon of the secondary gammas, r, z are cylindrical coordinates with the origin at the surface directly below the point of burst, and t is the time after source impulse.

Energies are in MeV. The units of S are MeV/meter^3 · sec · neutron. The units of the six functions are:

S_{ei}, S_{ec}	dimensionless
S_{zi}	cm^{-1}
S_{zc}	meters^{-1}
S_{ri}	MeV · meters^{-2} · shake^{-1}
S_{rc}	MeV · meters^{-2} · second^{-1}

The "i" terms arise from inelastic collisions; the "c" terms arise from capture.

The four functions S_{ri}, S_{zi}, S_{rc}, and S_{zc} have been curve fit as functions of the spatial and time variables. E_N and E_γ have been left as discrete variables. E_N is a discrete source neutron energy designated by the "file number" or "file."

Four of the functions have been normalized. Specifically:

$$\sum_{E_\gamma} S_{ei} = 1, \qquad \sum_{E_\gamma} S_{ec} = 1, \qquad \int_0^{-\infty} S_{zi} dZ = 1, \qquad \int_0^{-\infty} S_{zc} dZ = 1 \qquad (180)$$

LASL Bin Definitions: The six functions, before any curve fitting, were derived from the output of a Monte Carlo code run at the Los Alamos Scientific Laboratory. The range of each variable was divided into bins as follows:

Time bins in microseconds

0 - 3 - 10 - 30 - 300 - 3000 - 30000 - 300000

Radial bins in meters

0 - 50 - 100 - 150 - 200 - 300 - 400 - 500

Depth bins in meters

0 - 0.1 - 0.3 - 0.5 - 1.

γ energy bins in MeV

0 - 1 - 2 - 3 - 5 - 8 - 12

Files 2 through 12, representing 11 monoenergetic neutron sources, were used. The correspondence between file number and neutron energy in MeV is as follows:

File	2	3	4	5	6	7	8	9	10	11	12
MeV	14	10	8	6	4.5	3	2	1	.3	.1	.01

All files assume dry ground. The pre-fit values of the six functions derived from LASL Monte Carlo data are listed in the computer output hereafter referred to as SOURCE.

<u>Functions of Gamma Energy (S_{ei} and S_{ec}):</u> The total gamma energy, E_γ, spectrum has been divided into six energy bins with boundaries at 0 - 1 - 2 - 3 - 5 - 8 - 12 MeV. S_{ec} and S_{ei} give the fraction of the total energy produced in each energy bin.

$$\left.\begin{matrix} S_{ei}(i) \\ S_{ec}(i) \end{matrix}\right\} = \frac{1}{\text{total gamma energy produced by} \left\{\begin{matrix}\text{inelastic collision} \\ \text{capture}\end{matrix}\right\}} \cdot \int_{E_{\gamma_i}}^{E_{\gamma_{i+1}}} E_\gamma \, dN(E_\gamma) \tag{181}$$

where $dN(E_\gamma)$ = number of $\left\{\begin{matrix}\text{inelastic}\\ \text{capture}\end{matrix}\right\}$ produced photons having an energy between E_γ and $E_\gamma + dE_\gamma$. The values of S_{ei} and S_{ec} used by program INT can be read directly from SOURCE, as no curve fitting was done for these functions. Note that S_{ec} is the same for all files since it is independent of neutron energy.

$\underline{S_{zc}}$: S_{zc} has been curve fit, first as a function of z, then as a function of time. The functional form assumed is

$$S_{zc}(z,t) = \frac{1-\beta_3(t)}{\sqrt{\pi\beta_1(t)}} \; \frac{\exp\left[-\dfrac{z^2}{4\beta_1(t)}\right] - \exp\left\{\dfrac{\left[z-2\beta_2(t)\right]^2}{4\beta_1(t)}\right\}}{\operatorname{erf}\left(\dfrac{\beta_2(t)}{\sqrt{\beta_1(t)}}\right)}$$

$$+ \frac{\beta_3(t)}{\beta_4(t)} \exp\left[\frac{z}{\beta_4(t)}\right] \qquad (182)$$

where $z > 0$ above ground and $z < 0$ below ground. Here β_1 has the dimensions meters^2, β_2 and β_4 are in meters, and β_3 is dimensionless.

$$\operatorname{erf}(x) = \frac{2}{\sqrt{\pi}} \int_0^x e^{-y^2}\, dy \qquad (183)$$

The computer code that fit S_{zc} was called the SZC code. For each time bin the first section of this code produced betas. The bin boundaries, z_n, were greater than 0 for the running of this code. A corresponding change was made in the assumed form of S_{zc}. After this fit, the following substitutions were made: $\beta_1 = 1/\sqrt{\beta_1}$ and $\beta_4 = 1/\beta_4$. Then subroutine TIMFIT fit each set of β_i (i fixed, file fixed, time bin varying) to the form $\lambda + \alpha \ln(t)$, t in shakes,

with the following time segmentation:

$$\beta_\eta(t) = \begin{cases} \lambda_{Mn} + \alpha_{Mn}\ln(t) \; 3\mu < t < 3\text{mseconds} \\ \lambda_{Fn} + \alpha_{Fn}\ln(t) \quad 3\text{m} < t < 300\text{mseconds} \end{cases} \tag{184}$$

for n = 1, 2, 3, 4.

The coefficients, lambdas and alphas, are listed in the document "Ground Source Terms*."

$\underline{S_{zi}}$: S_{zi} has been curve fit, first as a function of depth, then as a function of time. The functional form assumed was

$$S_{zi}(z,t) = \frac{1}{\lambda(t)} \exp\left[\frac{z}{\lambda(t)}\right] \tag{185}$$

$\lambda(t)$ was fit to the form $\lambda + \alpha\ln(t)$ with the segmentation:

$$\lambda(t) = \begin{cases} \lambda_{01} + \alpha_1\ln(t) \;\; .06\mu < t < 3\mu \text{ seconds} \\ \lambda_0 + \alpha\ln(t) \qquad 3\mu < t < 300\mu \text{ seconds} \end{cases} \tag{186}$$

The dimension of lambda are cm. The argument of ln(t) is in shakes, and z is less than 0 below the ground.

The values of the lambdas and alphas are listed in the document "Ground Source Terms."

$\underline{S_{rc}}$: The radial dependence of the capture term is assumed to have the form

* Unpublished

$$S_{rc}(r,t) = \frac{1}{2\pi r}\left\{Z(t) \cdot \delta(r) + \left[A(t) + B(t) \cdot r\right] \exp\left[-r \cdot C(t)\right]\right\} \tag{187}$$

The following assumes that S_{zc} is slowly varying and hence can be taken outside the integral of the total source function and fit as described above.

The LASL data has a table of values, $S_{rc0}(n,j)$, for each file. The n indicates a radial bin, the j a time bin. The problem was to find a function $S_{rc}(r,t)$ such that

$$S_{rc0}(n,j) = \int_{r_n}^{r_{n+1}} \int_{T_j}^{T_{j+1}} S_{rc}(r,t) dt 2\pi r dr \tag{188}$$

Range Fit: The function

$$S_{rc1}(r,j) = \frac{1}{2\pi r}\left\{B_0(j) \cdot \delta(r) + \frac{B_1(j) + B_2(j) \cdot r}{B_3(j)} \exp\left[-\frac{r}{B_3(j)}\right]\right\} \tag{189}$$

was fit to the $S_{rc0}(n,j)$s by a range fit program so that

$$S_{rc0}(n,j) \approx \int_{r_n}^{r_{n+1}} S_{rc1}(r,j) 2\pi r dr \tag{190}$$

for each j. The output was a set of values for B_0, B_1, B_2, and B_3. A few of these values were then improved by hand calculations.

Time Fit: From Eq. (188) and (190) it can be seen that the desired $S_{rc}(r,t)$ must have the property

$$S_{rc1}(r, j) = \int_{T_j}^{T_{j+1}} S_{rc}(r, t)dt \tag{191}$$

$S_{rc2}(r, t)$ was taken to be $S_{rc1}(r, j)/\left(T_{j+1} - T_j\right)$. To simplify the form of the result the following substitutions were made:

$$Z(j) = \frac{B_0(j)}{T_{j+1} - T_j}, \qquad A(j) = \frac{B_1(j)}{B_3(j)(T_{j+1} - T_j)} \tag{192}$$

$$B(j) = \frac{B_2(j)}{B_3(j)(T_{j+1} - T_j)}, \qquad C(j) = \frac{1}{B_3(j)} \tag{193}$$

Thus

$$S_{rc2}(r, t) = \frac{1}{2\pi r} \left\{Z(j) \cdot \delta(r) + \left[A(j) + B(j) \cdot r\right] \exp\left[- C(j) \cdot r\right]\right\} \tag{194}$$

for t in time bin j, and Eq. (190) is satisfied.

For programming purposes S_{rc} was separated into two parts, the first corresponding to the $\delta(r)$ term and the second corresponding to those terms multiplied by the exponential. Neither of these functions of time was continuous. Because continuity with respect to time is highly desirable, continuous functions were constructed in the following manner: Let F(J) be either of these functions for some fixed r. The continuous function to be constructed shall be called G(t). Let $t_{m, J}$ be the geometric midpoint of time bin J and t_J the upper boundary of time bin J. $T_0 = 0$, the lower boundary of the first time bin. G is to be constructed for time bins i through j.

i	j	F
1	7	$\frac{1}{2\pi} Z$
2	7	$\frac{1}{2\pi r} (A + B \cdot r) \exp\left[- C \cdot r\right]$

For

$$t_{i-1} \leq t < t_{m,i}, \quad G(t) = F(i)(\text{"front step"}) \tag{195}$$

$$t_{m,j} \leq t \leq t_j, \quad G(t) = F(j)(\text{"back step"}) \tag{196}$$

At all midpoints $t_{m,J}$, $G(t_{m,J}) = F(J)$.

$G(t_J)$ shall now be defined so that a linear interpolation among these points and the $G(t_{m,J})$s will satisfy

$$\sum_{J=i}^{j} F(J) = \int_{t_{i-1}}^{t_j} G(t)dt \tag{197}$$

This requirement is slightly less strict than its antecedent Eq. (191).

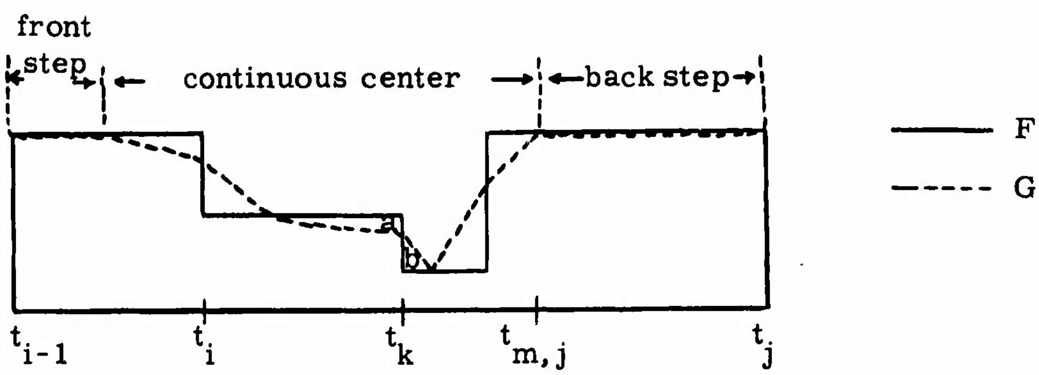

Figure 6

Creating a Continuous Function

To satisfy Eq. (197) we define $G(t_k)$, see illustration above, to be such that (the area of triangle a) = (the area of triangle b). That is

$$G(t_k) = \frac{(t_{m,k+1} - t_k)\, G(t_{m,k+1}) + (t_k - t_{m,k})\, G(t_k)}{(t_{m,k+1} - t_k) + (t_k - t_{m,k})} \tag{198}$$

for all k from i to j-1, inclusive. Equivalently,

$$G(t_k) = \frac{(t_{m,k+1} - t_k)\, F(k+1) + (t_k - t_{m,k})\, F(k)}{t_{m,k+1} - t_{m,k}} \tag{199}$$

for all k from i to j-1, inclusive.

If we now set

$$T(0) = t_{i-1} \qquad T(2) = t_i \qquad \ldots \qquad T(N) = t_j \tag{200}$$

$$T(1) = t_{m,i} \qquad T(3) = t_{m,i\ 1} \qquad \ldots \tag{201}$$

then we may write the interpolation to be used between $t_{m,i}$ and $t_{m,j-1}$ as

$$G(t) = G\left[T(M-1)\right] + \left\{G\left[T(M)\right] - G\left[T(M-1)\right]\right\} \frac{t - T(M-1)}{T(M) - T(M-1)} \tag{202}$$

for $T(M-1) \leq t \leq T(M)$. ("continuous center")

To compute this continuous center when $F = 1/2\pi Z$ one needs a table of $G\left[T(M)\right]$ s. These were computed by program CFITC and are found in Program INT in the array AZ.

When $F = \left[1/(2\pi r)\right]\ (A + B \cdot r) \exp\left[- C \cdot r\right]$ the $G\left[T(M)\right]$ s depend continuously on r. They are computed for program INT by subroutine SRC3.

A listing of the parameters A, B, C, and Z is given in "Ground Source Terms" where they are called AA, AB, AC, and AZ, respectively.

$\underline{S_{ri}}$: The functional form assumed for the radial distribution of the inelastic term is

$$S_{ri}(r, t) = \frac{1}{2\pi r}\left[b_1(t) + b_2(t) \cdot r + b_3(t) \cdot r^2\right] \exp\left[-\frac{r}{b_4(t)}\right] \tag{203}$$

Dimensions:

$b_1 \quad \frac{\text{MeV}}{\text{meter shake}}$

$b_2 \quad \frac{\text{MeV}}{\text{meter}^2\ \text{shake}}$

$b_3 \quad \frac{\text{MeV}}{\text{meter}^3\ \text{shake}}$

$b_4 \quad \text{meter}$

$S_{ri} \quad \frac{\text{MeV}}{\text{meter}^2\ \text{shake}}$

Most range fits were made by program SRI, third edition. For a description of the range fit, see "SRI CODE as revised by Ralph Day, October 1967*." The result of this range fit is a function continuous with respect to r but a step function with respect to t,

---

* Unpublished

$$S_{ri3}(r, J) = S_{ri}(r, t) = \frac{1}{2\pi r}\left[A(J) + B(J) \cdot r + C(J) \cdot r^2\right] \exp\left[- r \cdot R(J)\right] \quad (204)$$

for t in time bin J, which has the units MeV/meter^2 shake. A continuous function of time is created in exactly the same way as for S_{rc}. Let F(J) = $S_{ri3}(r, J) \times 10^8$ for some fixed r. The description of the creation of G(t) from F(J) on pages is now applicable with but three exceptions: When $F = S_{ri3} \cdot 10^8$ then i = 1, j = 4, and the $G\left[T(M)\right]$s are computed by subroutine SRI3. The units of G(t) are MeV/meter^2 second. A listing of the parameters A, B, C, and R is given in "Ground Source Terms" where they are called BA, BB, BC, and BR, respectively.

LASL data for times greater than 0.003 seconds was ignored in computing S_{ri}.

c. Gamma Transport--TIGRE Quantities

A source of gammas in the ground has the functional dependence $S(E_N, E_\gamma, r, z, t)$. An effect F caused by that source, be it a J_r, a J_θ, or a Q, depends on the strength of the source and on the position of the source with respect to the point p at which the effect occurs. TIGRE quantities give this latter dependence.

The point p is described by spherical coordinates with the origin at the surface directly below the burst center. The point g in the ground at which S is evaluated is described by a cylindrical coordinate system (r, z, α) centered on the burst axis with z = 0 being the surface of the ground. Let ϕ' be the angle from the vertical of a line directed from g to p, and r' be the length of that line. Further, let z be the vertical coordinate of point g. The appropriate TIGRE quantity is $T_a(E_\gamma, z, r', \phi')$, a = q, r, or θ. Thus

$$Q(E_N, E_\gamma, p, g, t) = T_q(E_\gamma, z, r', \phi') \cdot S \quad (205)$$

$$J_r(E_N, E_\gamma, p, g, t) = T_r(E_\gamma, z, r', \phi') \cdot S \quad (206)$$

$$J_\theta(E_N, E_\gamma, p, g, t) = T_\theta(E_\gamma, z, r', \phi') \cdot S \qquad (207)$$

The functional dependence of S is not specified in the above equations. An effect F at p at time t is the result of gammas that left g r'/c seconds earlier, c being the speed of light. Thus we wish to calculate S at time $t' = t - r'/c$. Now we have

$$Q(E_N, E_\gamma, p, g, t) = T_q(E_\gamma, z, r', \phi') \cdot S(E_N, r, E_\gamma, z, t') \qquad (208)$$

$$J_r(E_N, E_\gamma, p, g, t) = T_r(E_\gamma, z, r', \phi') \cdot S(E_N, r, E_\gamma, z, t') \qquad (209)$$

$$J_\theta(E_N, E_\gamma, p, g, t) = T_\theta(E_\gamma, z, r', \phi') \cdot S(E_N, r, E_\gamma, z, t') \qquad (210)$$

d. Integration

So far, a ground source at point p, caused by a gamma source at point g, has been calculated. To find a ground source F at p accounting for all the ground, one must integrate through the ground. To this end, the ground is divided into bins in an obvious manner by the (r, z, α) cylindrical coordinate system. F is computed by a summation over these bins of the effect caused by a source at the center of each bin times the volume of that bin.

To find a ground source, one must also take into account all gamma energies. Because of the way S_{ei} and S_{ec} have been constructed, a summation suffices. Thus

$$F(E_N, p, t) = \int_g \sum (T \cdot S)\, d(\text{vol})$$

$$= \sum_r \sum_\alpha \sum_{E_\gamma} \sum_z T \cdot S \cdot (\text{bin volume}) \qquad (211)$$

For each of the six E_γ, a standard set of seven zs is used. These represent midpoints of depth bins and are

E_γ	z_1	z_2	z_3	z_4	z_5	z_6	z_7
0.5	0.01	0.03	0.05	0.08	0.1	0.15	0.25
1.5	0.015	0.05	0.08	0.1	0.15	0.2	0.3
2.5	0.015	0.05	0.08	0.13	0.2	0.3	0.4
4.	0.02	0.06	0.1	0.15	0.2	0.3	0.4
6.5	0.02	0.06	0.1	0.15	0.2	0.35	0.6
10.	0.025	0.08	0.14	0.2	0.3	0.4	0.6

Thirty-six bins represent the variation of α over half its range. Because of the symmetry with respect to the plane defined by the burst axis and point p, the remainder of the variation of α can be (and is) represented by doubling the volume of the bin.

Range bins were 10 meters wide and extended to 500 meters or to the greatest distance a neutron of the energy under consideration could have traveled since the burst, whichever was shorter. A term for r = 0, which arose from the curve fitting of S_{rc}, was included.

INT, the coding described in Section 2-d, has the number and size of depth, alpha, and range bins fixed as described above. This has the limitation of giving rough approximations to ground sources at points near the ground. When the point at which ground sources are being computed is close to the ground, then all of the ground bins appear to be out at a side and none of them are directly below. For "low" ground sources a different grid should be used.

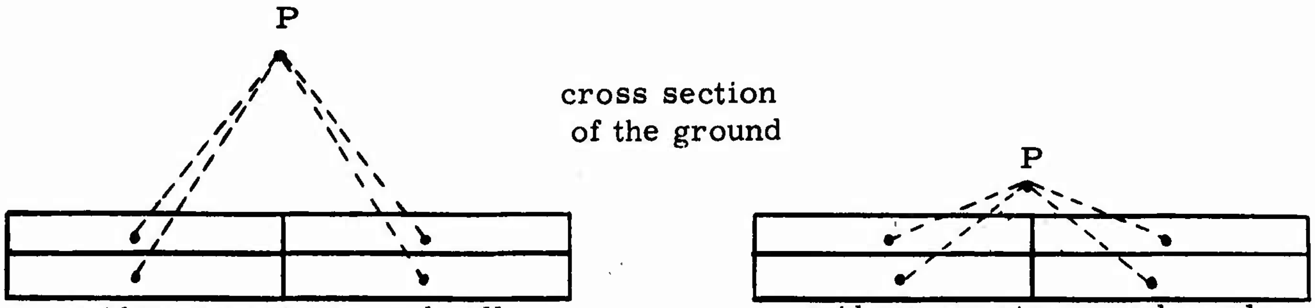

Figure 7

A Limitation of Rigid Ground Gridding

The TIGRE quantities giving the radial and theta components of current assume that the center of the coordinate system is directly above the point gamma source. That is, they assume the U, V coordinate system is Figure 8. To calculate J_r and J_θ in the Y, Z plane the following transformations must be used.

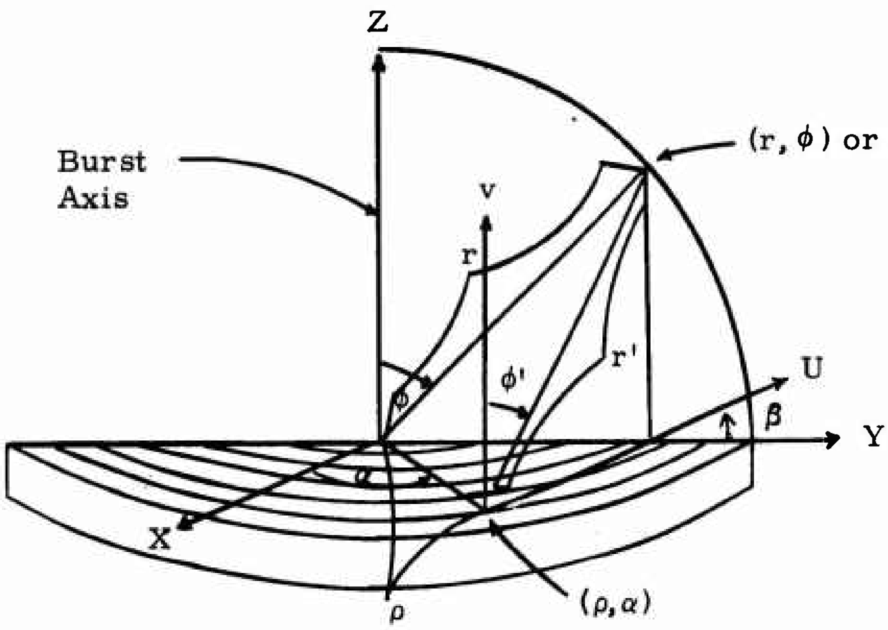

Figure 8

Coordinate Systems and Variables

Assume all gamma source points lie in the X, Y plane. Let a typical such point have polar coordinates (ρ, α). The range for α is $\left[-\pi/2, \pi/2\right]$. The X, Y, Z coordinates of this point are $(\rho \cos\alpha, \rho \sin\alpha, 0)$.

Because of azimuthal symmetry, it is sufficient to assume that all points at which current and energy information is required lie in the upper right-hand quadrant of the Y, Z plane. Let a typical such point have polar coordinates (r, ϕ). The X, Y, Z coordinates of this point are $(0, r \sin\phi, r \cos\phi)$.

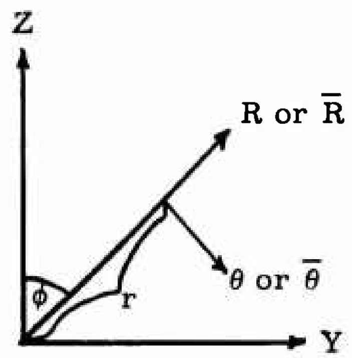

Figure 9
The Y, Z Plane

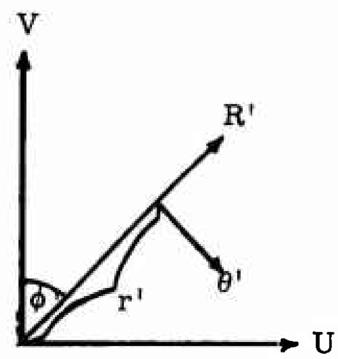

Figure 10
The U, V Plane

Let U, V be the axis of a coordinate system having its origin at (ρ, α), its V axis parallel to and with the same sense as the Z axis, and its U axis positively directed through the foot of the normal through (r, ϕ) to the X, Y plane. Let (r', ϕ') be the polar coordinates of the point (r, ϕ) relative to the U, V axes. Then

$$r' = \sqrt{(\rho \cos\alpha)^2 + (\rho \sin\alpha - r \sin\phi)^2 + (r \cos\phi)^2}$$

$$= \sqrt{\rho^2 - 2r\rho \sin\alpha \sin\phi + r^2} \tag{212}$$

and $\phi' = \text{Arccos}\left(r \cos\phi / r'\right)$.

Let $\overline{R}$ and $\overline{\theta}$ be unit vectors of a polar coordinate system in the Y, Z plane as shown in Figure 9. Similarly let $\overline{R}'$ and $\overline{\theta}'$ be unit vectors of a polar coordinate system in the U, V plane.

The U, V components of a unit vector directed from the U, V origin toward (r', ϕ') are $(\sin\phi', \cos\phi')$. A unit vector in the corresponding θ direction has the U, V components $(\cos\phi', -\sin\phi')$.

Let

$$\overline{J} = J_{r'}\overline{R}' + J_{\theta'}\overline{\theta}' \tag{213}$$

be a current vector at (r', ϕ') caused by a gamma source at (ρ, α). From the above considerations we see that the current in terms of U, V components is

$$\begin{pmatrix} J_u \\ J_v \end{pmatrix} = \begin{pmatrix} \sin\phi' & \cos\phi' \\ \cos\phi' & -\sin\phi' \end{pmatrix} \begin{pmatrix} J_{r'} \\ J_{\theta'} \end{pmatrix} = C \begin{pmatrix} J_{r'} \\ J_{\theta'} \end{pmatrix} \tag{214}$$

Let J_y and J_z be components of the projection of $\overline{J}$ onto the Y, Z plane. We see that

$$\begin{pmatrix} J_y \\ J_z \end{pmatrix} = \begin{pmatrix} A_{1,1} & 0 \\ 0 & 1 \end{pmatrix} \begin{pmatrix} J_u \\ J_v \end{pmatrix} = A \cdot \begin{pmatrix} J_u \\ J_v \end{pmatrix} \tag{215}$$

$$A_{1,1} = \frac{r \sin\phi - \rho\sin\alpha}{\rho^2 - 2r\rho \sin\phi \sin\alpha + r^2 \sin^2\phi} \tag{216}$$

$A_{1,1}$ is $\cos\beta$ where β is, as shown in Figure 8, the angle between U and Y.

The transformation matrix from the Y, Z system to the R, θ system is

$$B = \begin{pmatrix} \sin\phi & \cos\phi \\ \cos\phi & -\sin\phi \end{pmatrix} \tag{217}$$

Thus

$$\begin{pmatrix} J_r \\ J_\theta \end{pmatrix} = B \cdot A \cdot C \cdot \begin{pmatrix} J_{r'} \\ J_{\theta'} \end{pmatrix}$$

$$= \begin{pmatrix} A_{1,1} \sin\phi \sin\phi' + \cos\phi \cos\phi' & A_{1,1} \sin\phi \cos\phi' - \cos\phi \sin\phi' \\ A_{1,1} \cos\phi \sin\phi' - \sin\phi \cos\phi' & A_{1,1} \cos\phi \cos\phi' + \sin\phi \sin\phi' \end{pmatrix}$$

$$\cdot \begin{pmatrix} J_{r'} \\ J_{\theta'} \end{pmatrix} \tag{218}$$

The current components $J_{r'}$ and $J_{\theta'}$ are computed by taking the product of: a TIGRE quantity, T; a gamma source strength per unit volume, S; and the volume of the bin under consideration. See Eq. (211).

INT integrates through the gamma spectrum and through the ground. For a given range and time the code computes for each of 11 neutron energies: J_r and J_θ at a set of 10 angles, and Q averaged over these angles. The angles are the midpoints of bins 9° wide, i.e., 4.5°, 13.5°, 22.5°, ..., 85.5°. It has been run for ranges 2, 3, 5, 7, 10, 15, 20, 22, 24, 26, 30, 40, 70, 100, 200, 400, 600, 800, 1000, 1400, and 1500 meters and times from 0.3μseconds to 2275.1μseconds.

3. USING GROUND SOURCES

Ground sources are desired as inputs to computer codes that calculate the EMP effects of a near-surface nuclear detonation. More specifically, they are required for the code G, which requires ground sources at a sequence of (range, time) points. The ionization rate is required to be a single number representing Q at all θ and all ϕ, for the specified (range, time) point. Current density is required to be broken into two perpendicular components, J_r and J_θ, of the spherical coordinate system. J_r is required to be analyzed into a finite series of ordinary Legendre polynomials; J_θ is required to be analyzed into a similar series of associated Legendre polynomials. In both series only odd-numbered polynomials are allowed. Thus G requires J_r be represented by the first n odd coefficients of a series of ordinary Legendre polynomials and that J_θ be represented by the first n odd coefficients of a series of associated Legendre polynomials. As Q, the current is assumed to be the same for all ϕ.

Ground sources are computed by INT on a "per-neutron" basis for each of several discrete neutron energies. Before G can use these sources, they must be converted by means of the neutron spectrum to numbers representing all neutron energies.

The coding that integrates over neutron energies and calculates coefficients of Legendre polynomial expansions of functions of θ, is called GROUSE.

INT (RR, TSEC)

Computes ground sources at RR meters and TSEC seconds. Programmed for use as a subroutine in a restartable program. Prints inputs; stores results on TAPE 5.

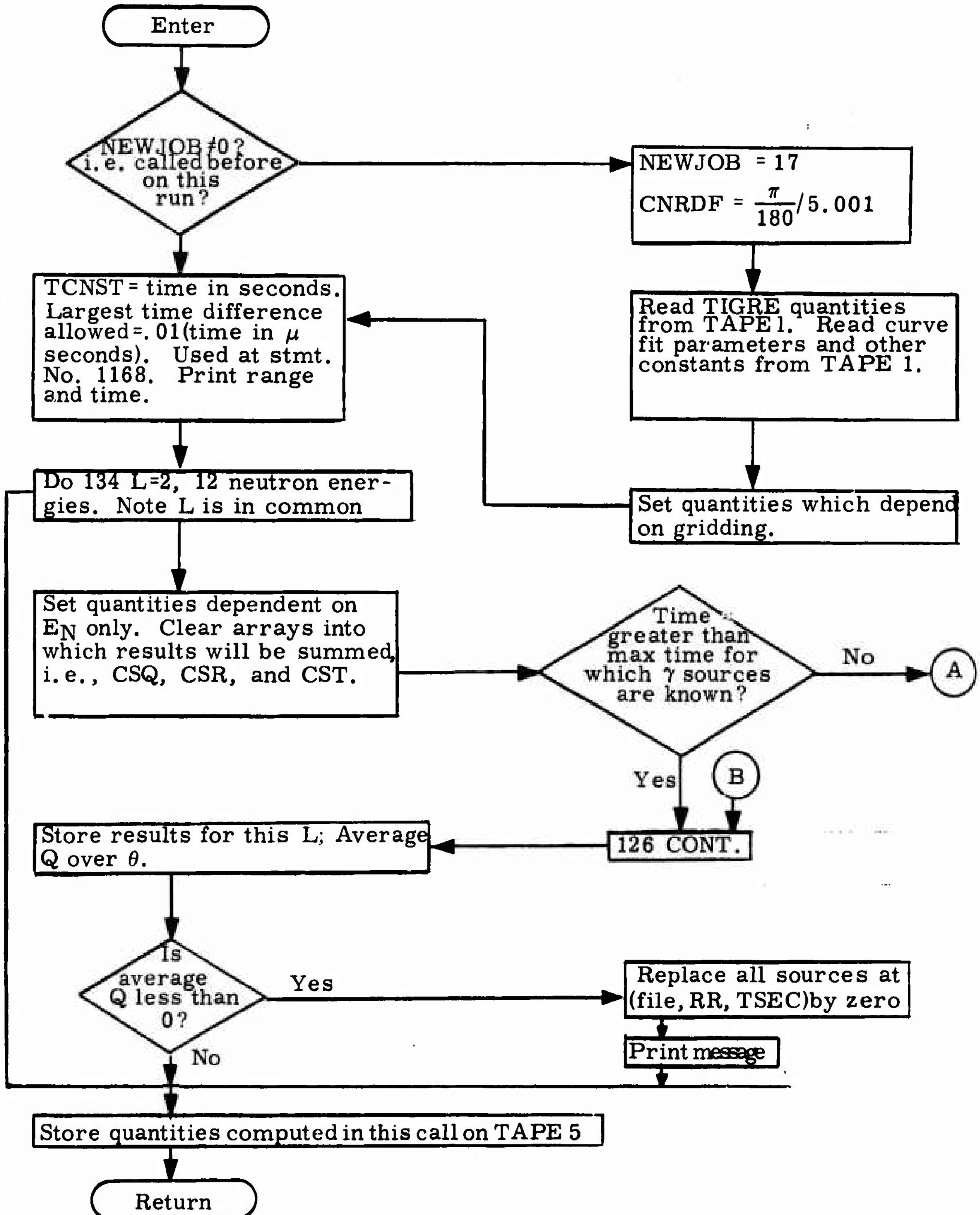

Integrate Over Ground

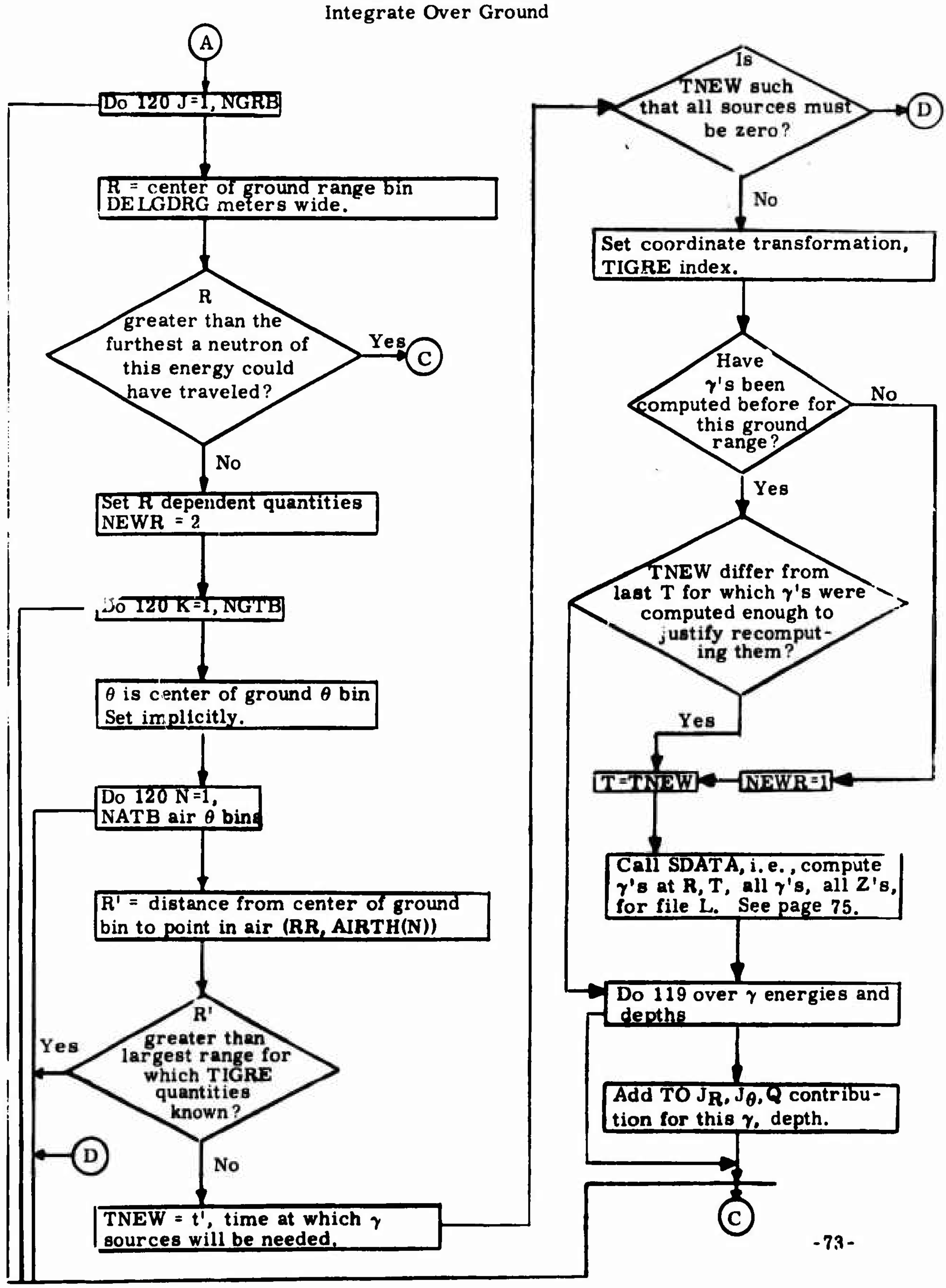

Ground Zero Component

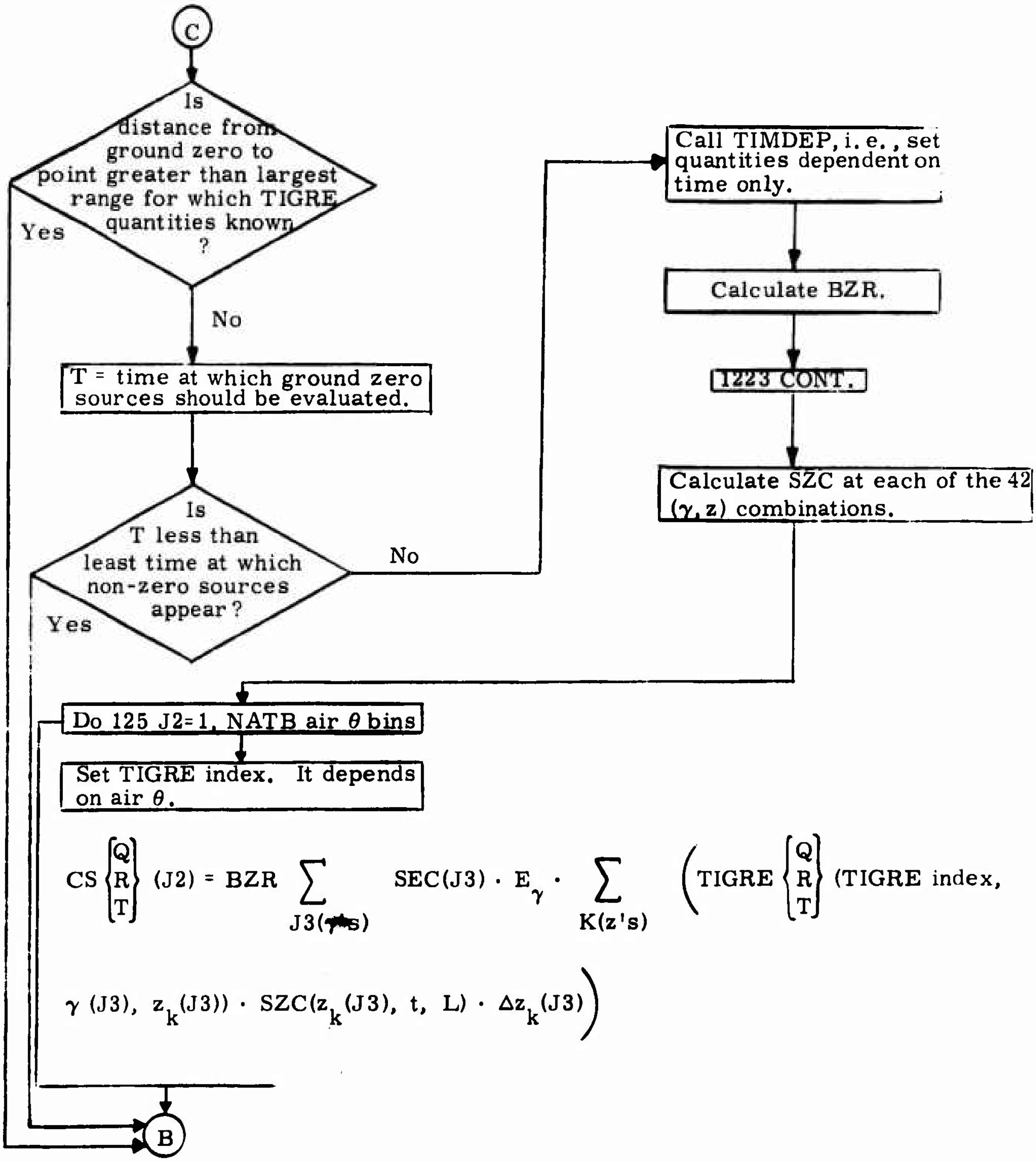

Subroutine SDATA

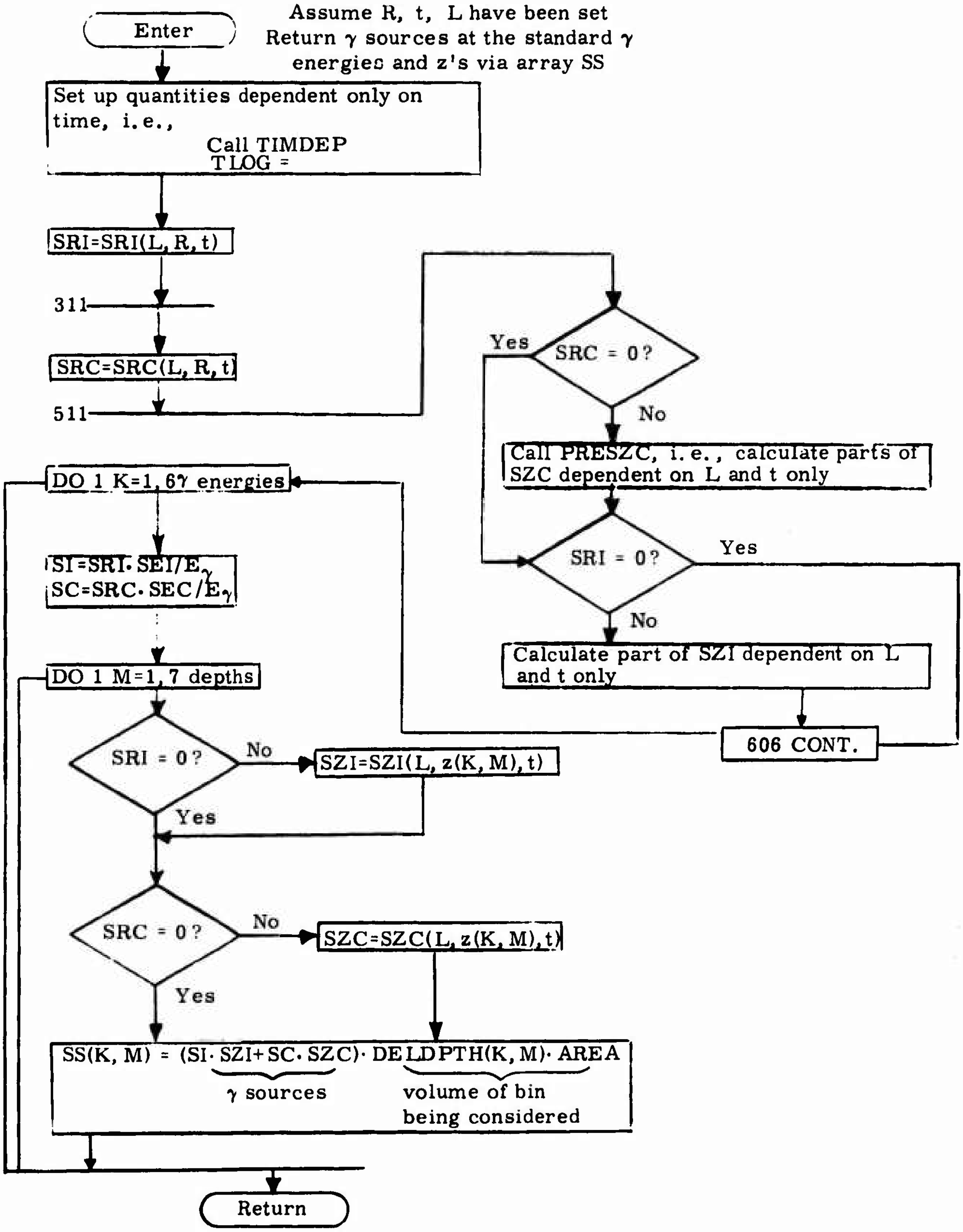

APPENDIX I. EXAMPLE PROBLEMS FOR THE FINITE-DIFFERENCE CODES

The field plots shown in this appendix were obtained by putting the current and conductivity pulses of equations similar to Eq. (1) and (2) into the real-time prolate spheroidal code, the retarded-time prolate spheroidal code, and the one-dimensional code. The intent is to compare the codes, thus the shape of the current and conductivity pulses were not chosen to be representative of any weapon. The burst height used is 300 meters and the spatial grid size is five meters. The plots labeled "3" are for a field point 35 meters above the ground, whereas those labeled "4" are for a field point 15 meters above the ground.

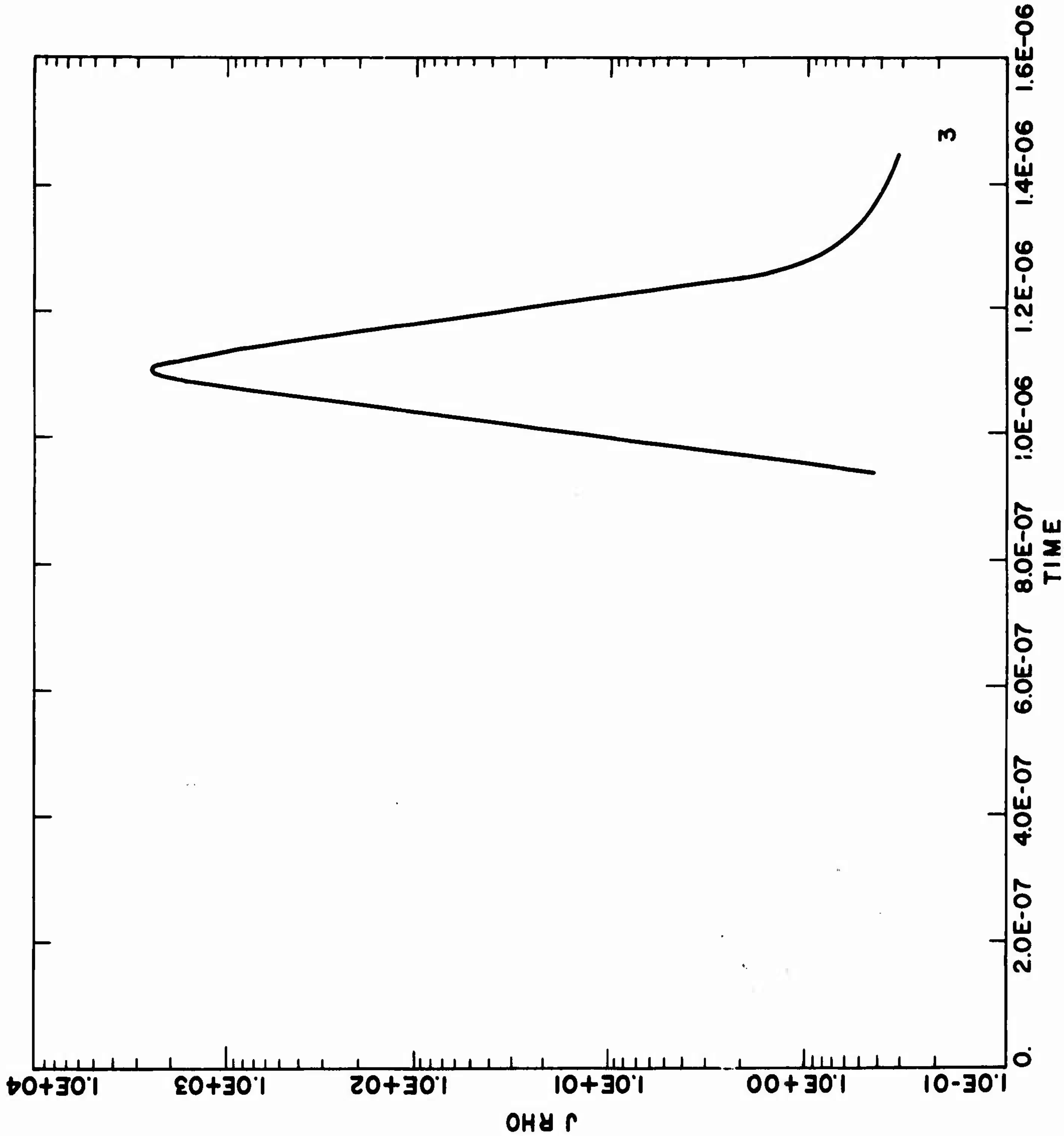

J RHO
1.0E+04
1.0E+03
1.0E+02
1.0E+01
1.0E+00
1.0E-01
TIME
0.
2.0E-07
4.0E-07
6.0E-07
8.0E-07
1.0E-06
1.2E-06
1.4E-06
1.6E-06
3

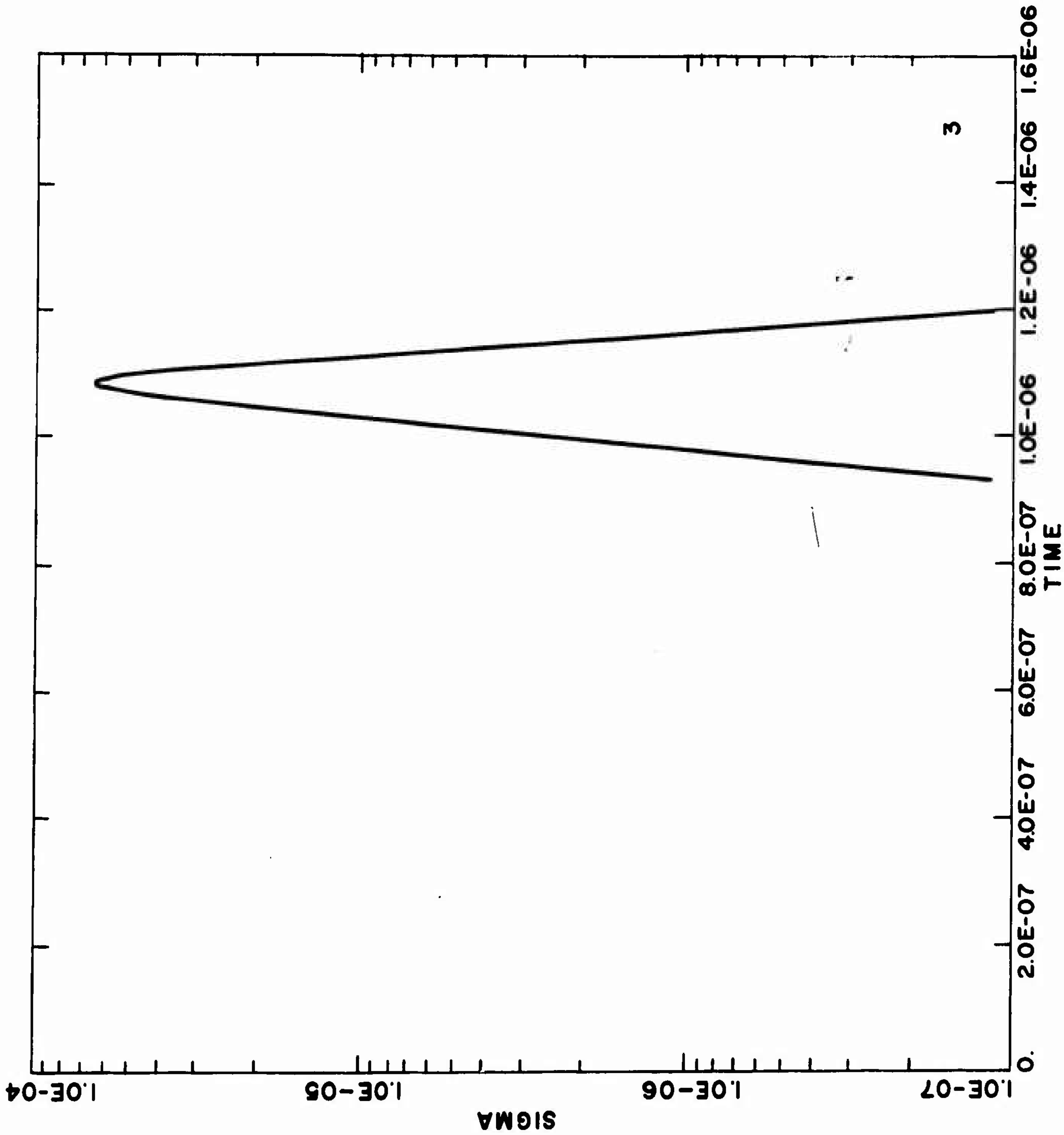

SIGMA
1.0E-04
1.0E-05
1.0E-06
1.0E-07
TIME
0.
2.0E-07
4.0E-07
6.0E-07
8.0E-07
1.0E-06
1.2E-06
1.4E-06
1.6E-06
3

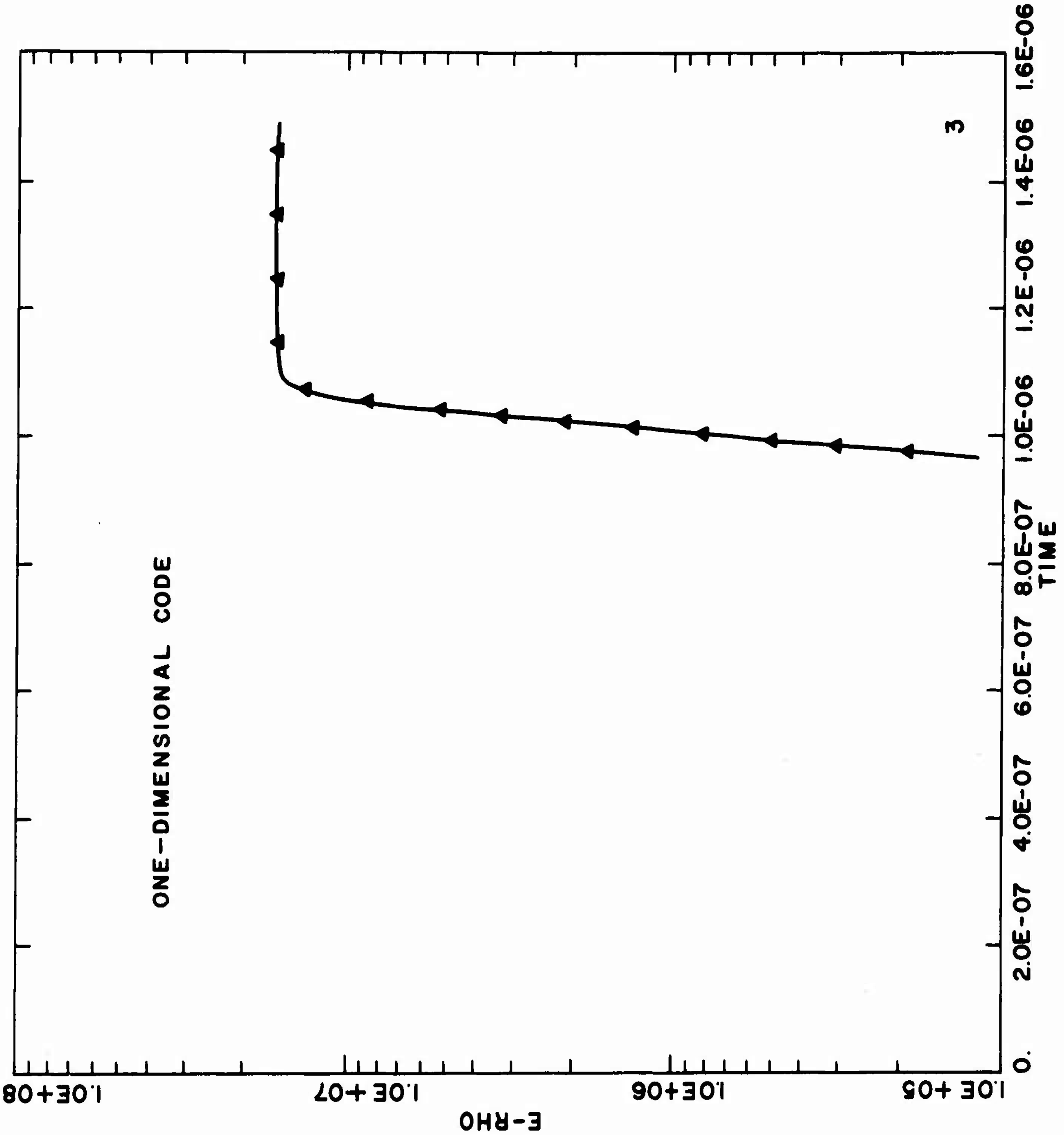
ONE-DIMENSIONAL CODE
3
TIME
E-RHO
0.
2.0E-07
4.0E-07
6.0E-07
8.0E-07
1.0E-06
1.2E-06
1.4E-06
1.6E-06
1.0E+05
1.0E+06
1.0E+07
1.0E+08

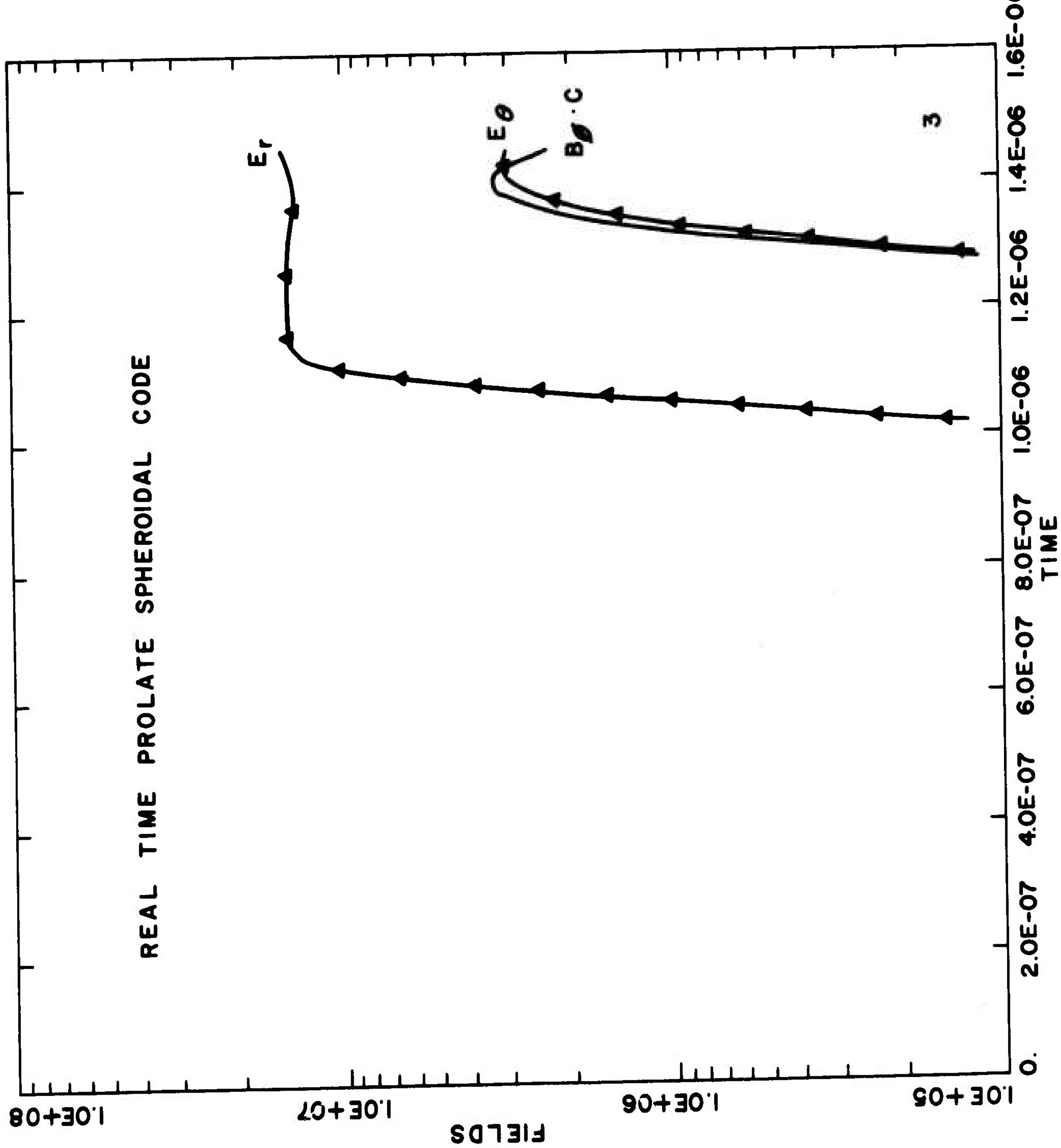

REAL TIME PROLATE SPHEROIDAL CODE
FIELDS
TIME
1.0E+05
1.0E+06
1.0E+07
1.0E+08
0.
2.0E-07
4.0E-07
6.0E-07
8.0E-07
1.0E-06
1.2E-06
1.4E-06
1.6E-06
E_r
E_θ
$B_\phi \cdot C$
3

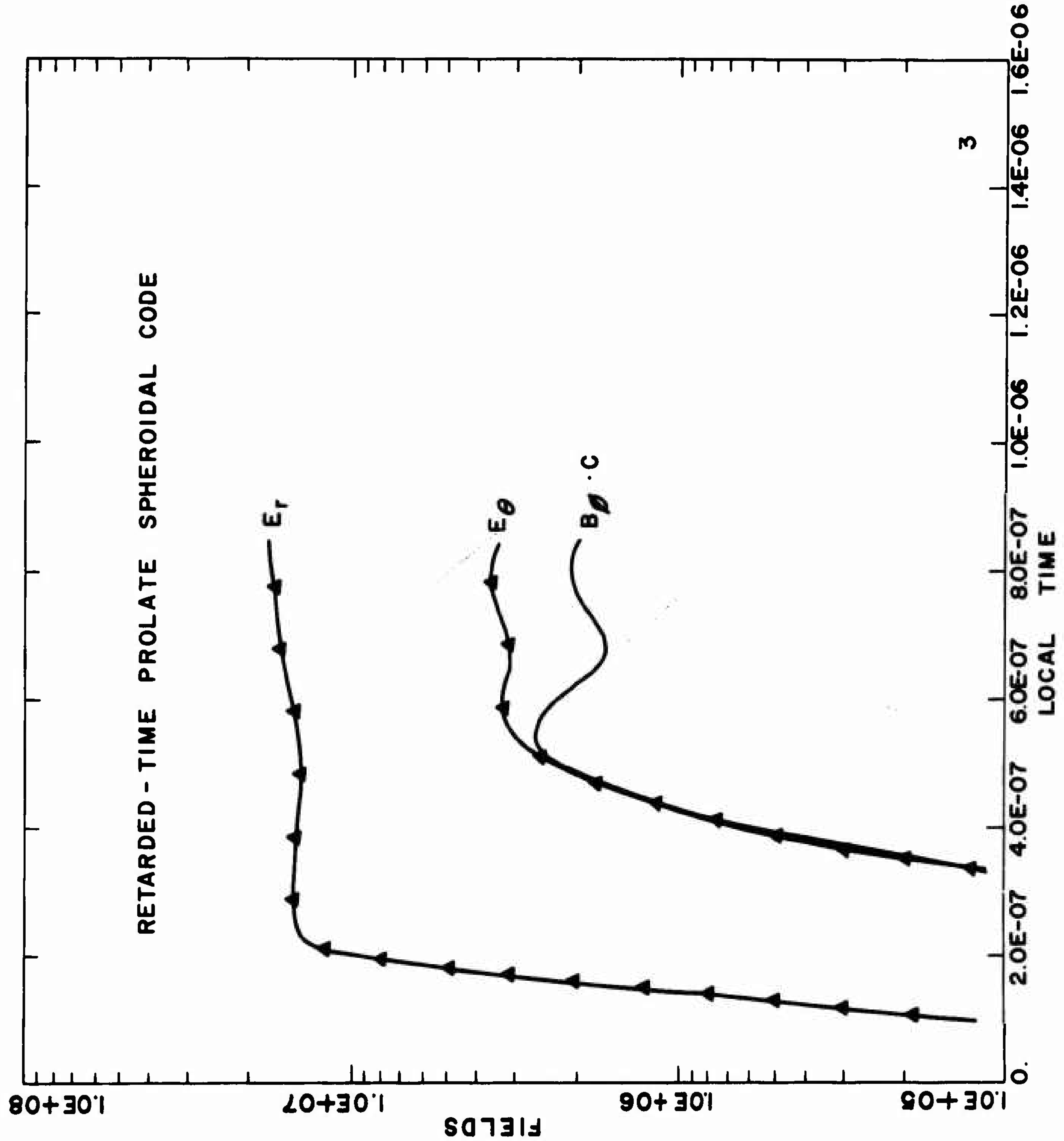
RETARDED - TIME PROLATE SPHEROIDAL CODE
E_r
E_θ
$B_\phi \cdot C$
3
FIELDS
1.0E+05
1.0E+06
1.0E+07
1.0E+08
LOCAL TIME
0.
2.0E-07
4.0E-07
6.0E-07
8.0E-07
1.0E-06
1.2E-06
1.4E-06
1.6E-06

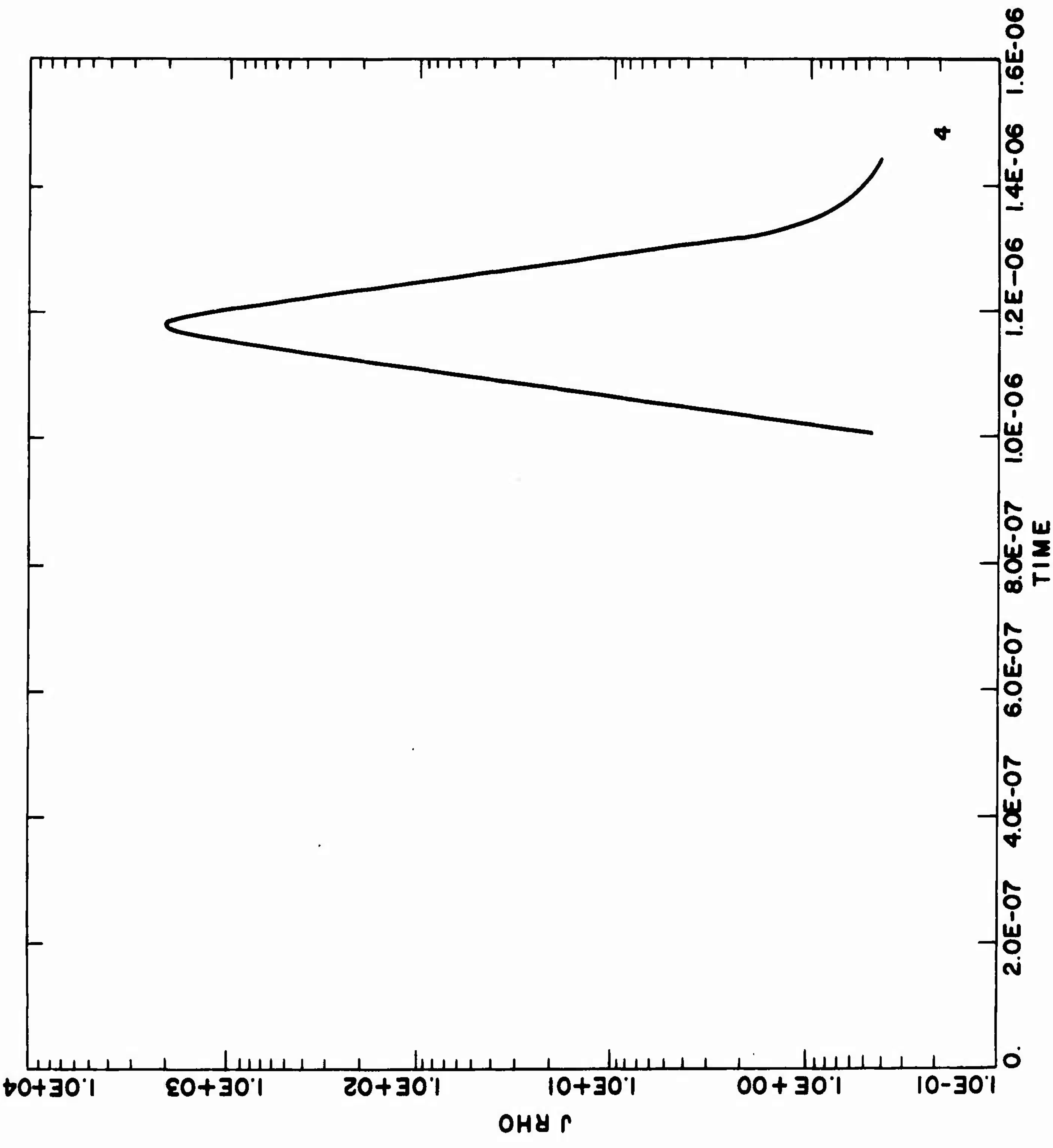
4
TIME
0.
2.0E-07
4.0E-07
6.0E-07
8.0E-07
1.0E-06
1.2E-06
1.4E-06
1.6E-06
J RHO
1.0E-01
1.0E+00
1.0E+01
1.0E+02
1.0E+03
1.0E+04

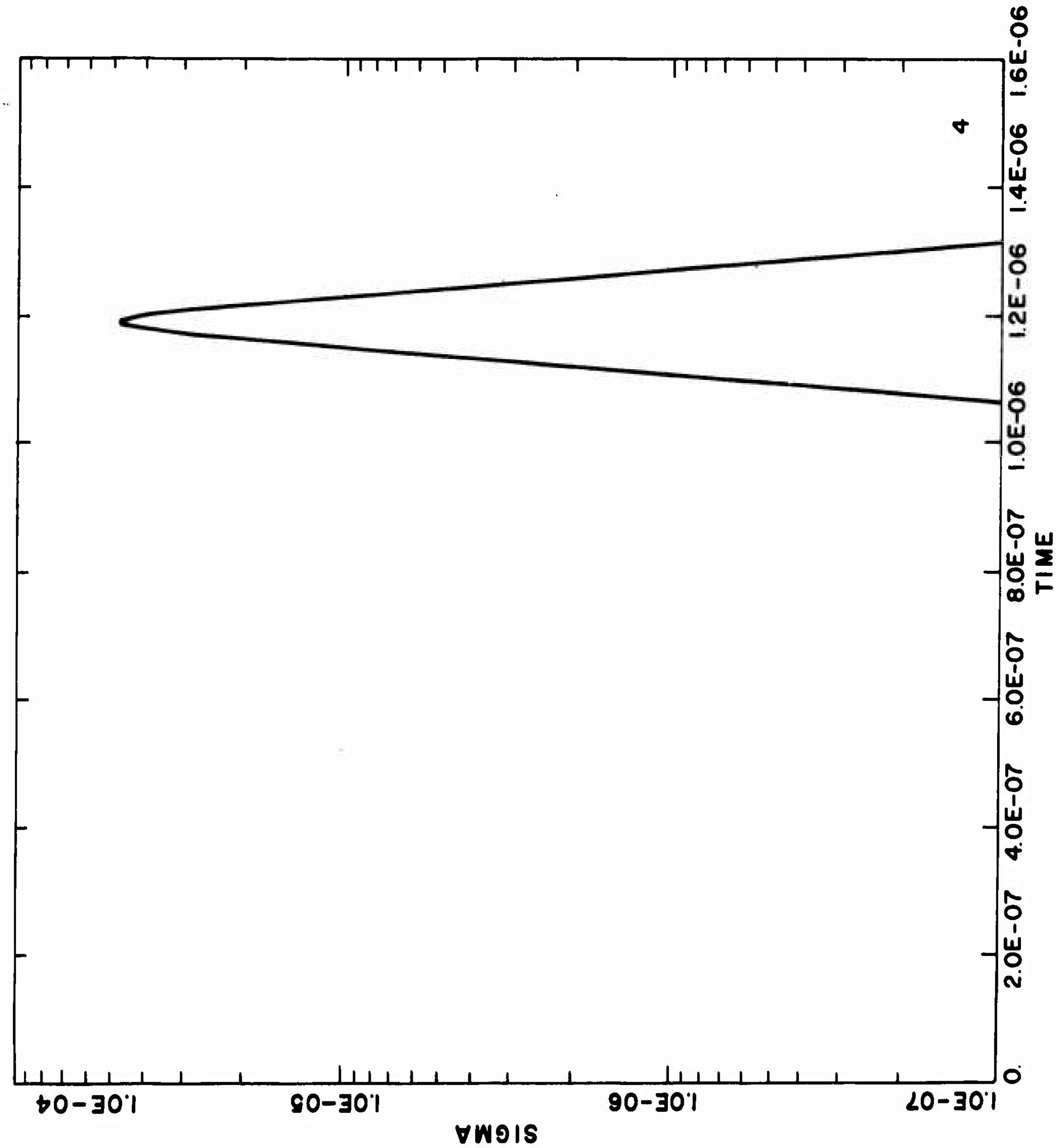
SIGMA
1.0E-04
1.0E-05
1.0E-06
1.0E-07
TIME
0.
2.0E-07
4.0E-07
6.0E-07
8.0E-07
1.0E-06
1.2E-06
1.4E-06
1.6E-06
4

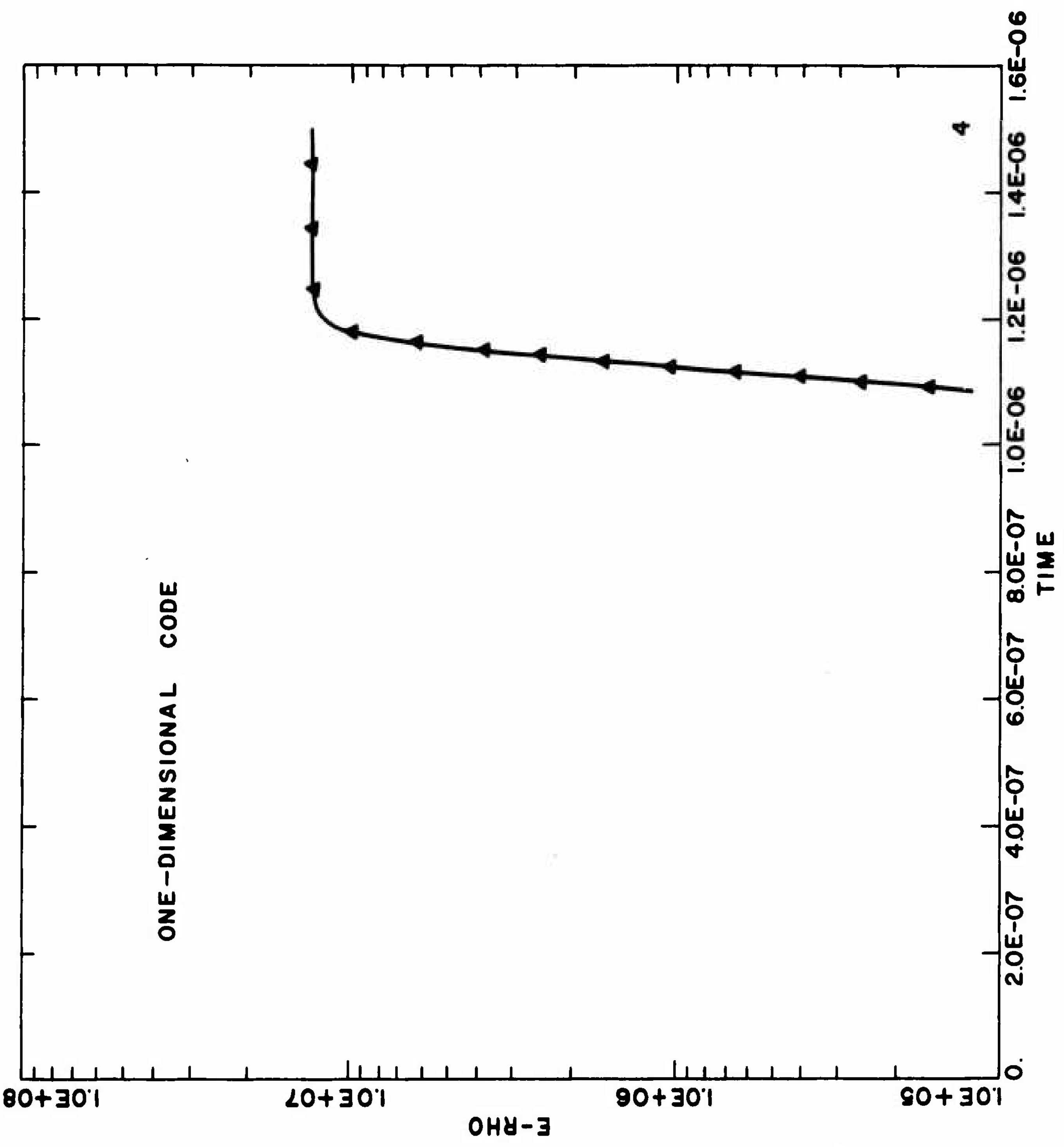
ONE-DIMENSIONAL CODE
4
E-RHO
1.0E+05
1.0E+06
1.0E+07
1.0E+08
TIME
0.
2.0E-07
4.0E-07
6.0E-07
8.0E-07
1.0E-06
1.2E-06
1.4E-06
1.6E-06

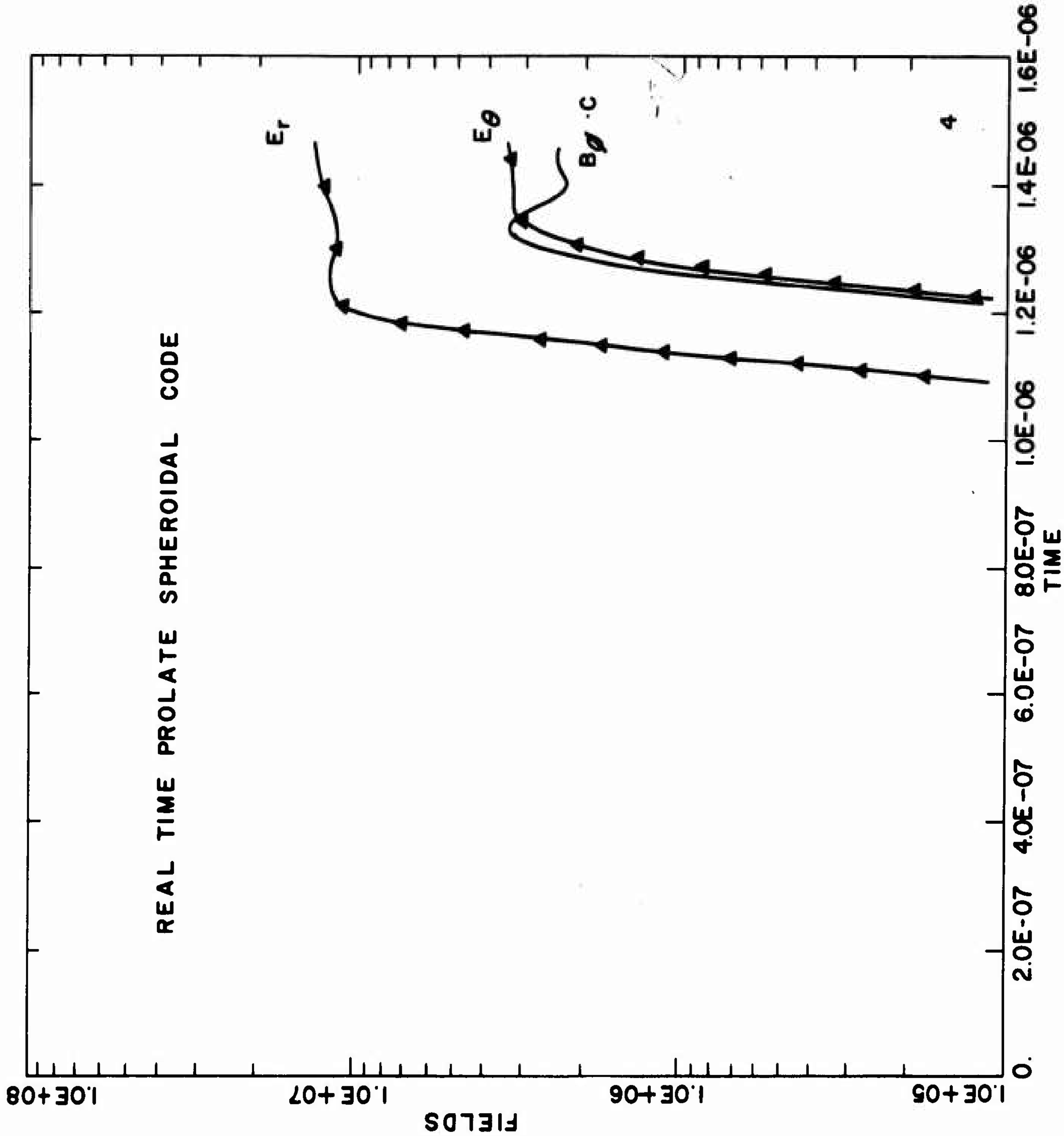
REAL TIME PROLATE SPHEROIDAL CODE
FIELDS
TIME
1.0E+05
1.0E+06
1.0E+07
1.0E+08
0.
2.0E-07
4.0E-07
6.0E-07
8.0E-07
1.0E-06
1.2E-06
1.4E-06
1.6E-06
E_r
E_θ
$B_\phi \cdot C$
4

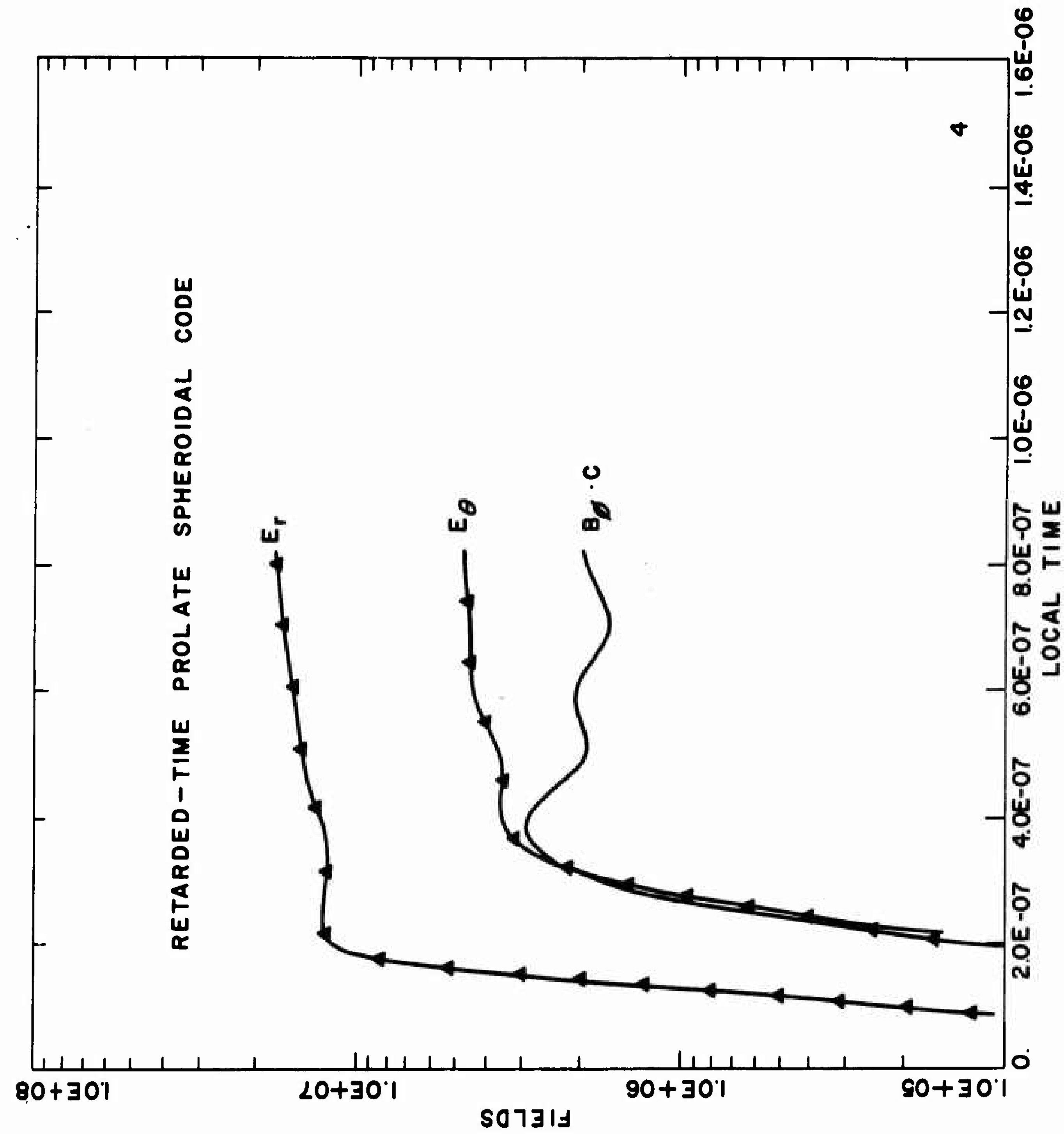
RETARDED-TIME PROLATE SPHEROIDAL CODE
4
E_r
E_θ
$B_\phi \cdot C$
LOCAL TIME
FIELDS
0.
2.0E-07
4.0E-07
6.0E-07
8.0E-07
1.0E-06
1.2E-06
1.4E-06
1.6E-06
1.0E+05
1.0E+06
1.0E+07
1.0E+08

APPENDIX II

CODE LISTING FOR INTEGRATION OF EXACT SOLUTION TO SPHERICALLY SYMMETRIC FIELDS

```
      PROGRAM EXSOL(OUTPUT)
C
C     TMAX - UPPER TIME LIMIT ON INTEGRATION
C     TR - RISE TIME
C     TP - LOCAL TIME FOR PEAK OF CURRENT PULSE
C     TSLAG - TIME LAG OF CONDUCTIVITY PEAK BEHIND CURRENT PEAK
C     JP - PEAK CURRENT AT GIVEN R
C     TPS - LOCAL TIME FOR PEAK OF CONDUCTIVITY PULSE
C     SP - PEAK CONDUCTIVITY AT GIVEN R
C
      REAL JZERO,JP,INT(1000)
      DATA R,TMAX,JZERO,RGAMMA,SZERO,RBETA,TR,TP,TSLAG,C,EPS/
     1240.,1.5E-6,6.1E8,300.,20.,200.,1.5E-7,1.666E-7,1.2E-8,3.E8, 8.85E
     2-12/
C
C     SET CONSTANTS
C
      REPS =-1./EPS
      TPS = TP + TSLAG
      TPSL = TPS + TP + 4.E-8
      R2 = R*R
      RC = R/C
C
C     SOLVE FOR PEAK CURRENT AND CONDUCTIVITY VALUES AT GIVEN R
C
      JP = JZERO/R2*EXP(-R/RGAMMA)
      SP = SZERO/R2*EXP(-R/RBETA)
C
C     ALFA-S AND BETA-S FOR SECOND AND THIRD FITS
C
      TEMP = ALOG(2.*JP)
      ALFAJ = TEMP/TR
      BETAJ = TEMP/TP
      TEMP = ALOG(2.*SP)
      ALFAS = TEMP/TR
      BETAS = TEMP/TPS
C
C     COEFFICIENTS FOR FIRST FIT TO CURRENT
C
      TEMP = EXP(2.*ALFAJ*(-TR))
      TJ = 1./(1.+TEMP)
      SS = (ALFAJ-ALFAJ*TEMP)/(1.+TEMP)**2
      A1 = SS/TJ
      B1 = ALOG(TJ)-(TP-TR)*A1
C
C     COEFFICIENTS FOR FOURTH FIT TO CURRENT
C
      TEMP1 = EXP(BETAJ*(TP+TR))
      TEMP = EXP(2.*BETAJ*TR)
      TF = TEMP1/(1.+TEMP)
      SF = TEMP1*(BETAJ-BETAJ*TEMP)/(1.+TEMP)**2
      TO = TP+TR
      A4 = SF*TO*TO/(TF*TF)
      B4 = 1./TF - A4/TO
C
C     COEFFICIENTS FOR FIRST FIT TO CONDUCTIVITY
```

```
C
      TEMP = EXP(2.*ALFAS*(-TR))
      TJ = 1./(1.+TEMP)
      SS = (ALFAS-ALFAS*TEMP)/(1.+TEMP)**2
      A1S = SS/TJ
      B1S = ALOG(TJ)-(TPS-TR)*A1S
C
C     COEFFICIENTS FOR FOURTH FIT TO CONDUCTIVITY
C
      TEMP1 = EXP(BETAS*TPSL)
      TEMP = EXP(2.*BETAS*(TPSL-TPS))
      TF = TEMP1/(1.+TEMP)
      SF = TEMP1*(BETAS-BETAS*TEMP)/(1.+TEMP)**2
      TO = TPSL
      A4S = SF*TO*TO/(TF*TF)
      B4S = 1./TF-A4S/TO
      DT = 5./(6.*C)
      T = RC + DT
      N = (TMAX-T)/DT + 1
      PRINT 35,R,C,EPS,TMAX,DT,JP,SP
      PRINT 30
C
C     FIND VALUES OF INTEGRANDS FOR TRAPEZOIDAL INTEGRATION
3
      DO 10 I = 1,N
      CALL CURRENT(T,TR,TP,ALFAJ,BETAJ,RC,FR,A1,B1,A4,B4)
      CALL CONDUCT(T,TR,TPS,TPSL,ALFAS,BETAS,RC,SIG,A1S,B1S,A4S,B4S)
      CALL TRAP(T,TR,TPS,TPSL,TMAX,ALFAS,BETAS,RC,SIGINT,A1S,B1S,A4S,B4S
     1)
      INT(I) = FR*EXP(REPS*SIGINT)
      PRINT 40,T,FR,SIG,INT(I),SIGINT
10    T = T+DT
C
C     DO INTEGRATION
C
      SUM = 0.
      NM1 = N-1
      DO 20 I = 2,NM1
20    SUM = SUM + INT(I)
      AREA = DT/2.*(INT(1)+INT(N)+2.*SUM)
      EFIELD = REPS*AREA
      PRINT 50, AREA,EFIELD
C
C     OUTPUT FORMAT STATEMENTS
C
30    FORMAT(1H0,11X,*TIME*,15X,*CURRENT*,10X,*CONDUCTIVITY*,9X,*INTEGRA
     1ND  INTEGRAL OF SIGMA BETWEEN T AND T MAX*)
35    FORMAT(1H1,*R =*F7.2/* C =*E12.5/* EPS =*E12.5/* TMAX =*E12.5/
     1* DT =*E12.5/* JP =*E12.5/* SP =*E12.5)
40    FORMAT(5E20.5)
50    FORMAT(1H0,*THE INTEGRAL WITH THE ABOVE SET OF INTEGRANDS, CALCULA
     1TED BY THE TRAPEZOID RULE IS *,E14.5/* THE E-FIELD WITH THIS INTEG
     2RATION IS*E14.5)
      END
```

```
      SUBROUTINE CURRENT(T,TR,TP,ALFAJ,BETAJ,RC,FR,A1,B1,A4,B4)
C
C     GIVEN REAL TIME AT PARTICULAR R, WILL SUPPLY CURRENT FROM ONE OF
C     FOUR FITS
C
      TU = T-RC
      IF(TU-TP+TR)60,60,51
51    IF(TU-TP)61,61,52
52    IF(TU-TP-TR)62,62,63
60    FR = EXP(A1*TU+B1)
      RETURN
61    TT = TU-TP+TR
      FR = EXP(ALFAJ*TT)/(1.+EXP(2.*ALFAJ*(TT-TR)))
      RETURN
62    FR=EXP(BETAJ*TU)/(1.+EXP(2.*BETAJ*(TU-TP)))
      RETURN
63    FR = TU/(A4+B4*TU)
      RETURN
      END
```

```
      SUBROUTINE CONDUCT(T,TR,TPS,TPSL,ALFAS,BETAS,RC,SIG,A1S,B1S,A4S,B4S)
     1S)
C
C     GIVEN REAL TIME AT PARTICULAR R, WILL SUPPLY CONDUCTIVITY FROM ONE
C     OF FIVE FITS
C
      TU = T-RC
      IF(TU-TPS+TR)60,60,51
51    IF(TU-TPS)61,61,52
52    IF(TU-TPSL)62,62,63
60    SIG = EXP(A1S*TU+B1S)
      RETURN
61    TT = TU-TPS+TR
      SIG = EXP(ALFAS*TT)/(1.+EXP(2.*ALFAS*(TT-TR)))
      RETURN
62    SIG = EXP(BETAS*TU)/(1.+EXP(2.*BETAS*(TU-TPS)))
      RETURN
63    IF(TU-1.E-5)141,141,144
141   SIG = TU/(A4S+B4S*TU)
      RETURN
144   SIG = SIG/2.
      RETURN
      END
```

```
      SUBROUTINE TRAP(T,TR,TPS,TPSL,TMAX,ALFAS,BETAS,RC,SIGINT,A1S,B1S,
     1A4S,B4S)
C
C     TRAPEZOIDAL INTEGRATION FOR CONDUCTIVITY
C
      DIMENSION SIG(50)
      TL = T
      TU = TMAX
      DT = (TU-TL)/49.
      DO 10 I = 1,50
      CALL CONDUCT(TL,TR,TPS,TPSL,ALFAS,BETAS,RC,SIGMA,A1S,B1S,A4S,B4S)
      SIG(I) = SIGMA
10    TL = TL + DT
      SUM = 0.
      DO 20 I = 2,49
20    SUM = SUM + SIG(I)
      SIGINT = DT/2.*(SIG(1)+SIG(50)+2.*SUM)
      RETURN
      END
```

```
//        EXEC      SETUCBQN
/&
13 NOV 68 10:57:45      39 BROWN       2065.5
```

APPENDIX III

EXAMPLES OF DIFFUSION EQUATION CALCULATIONS

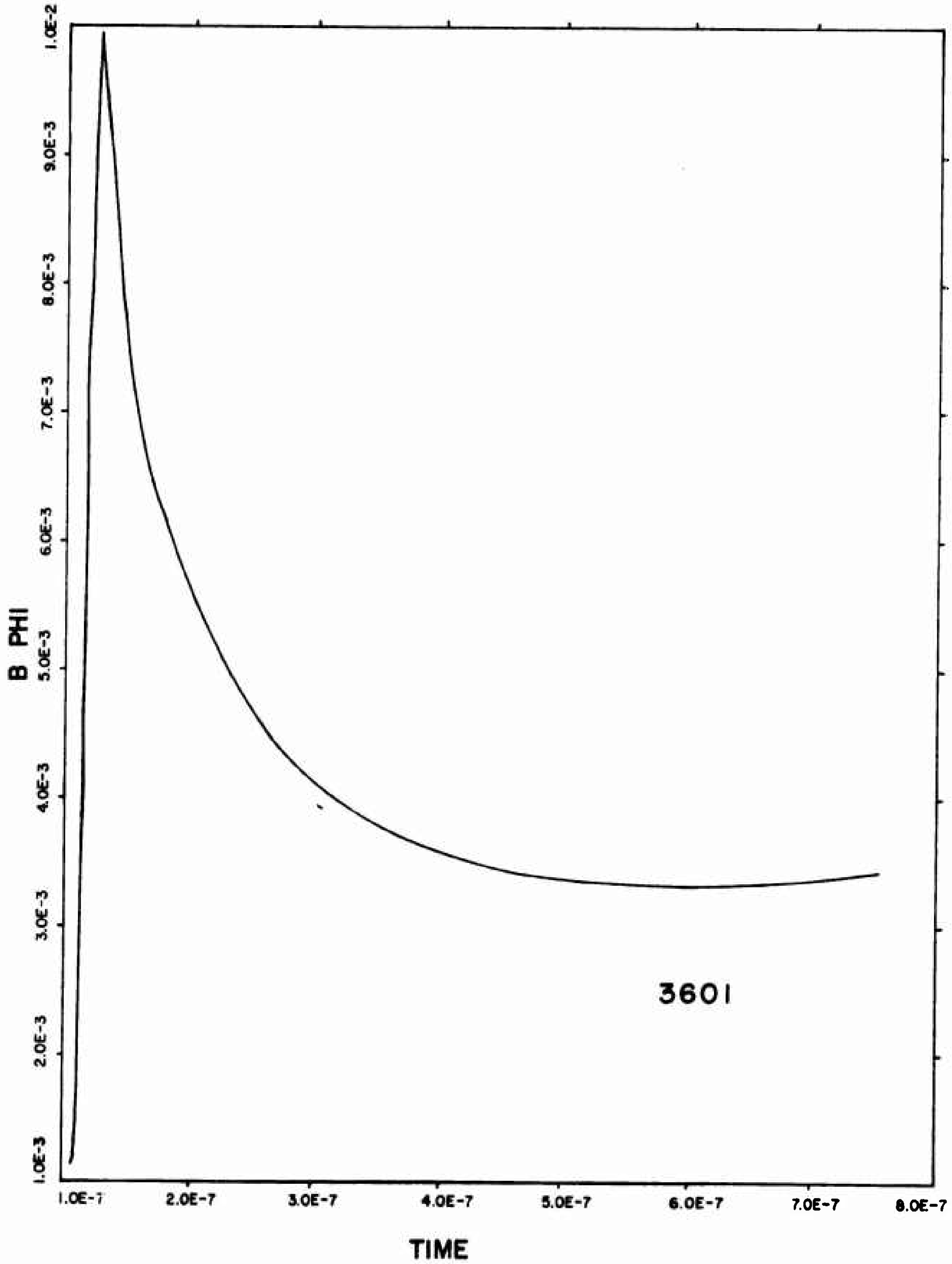
B PHI
1.0E-2
9.0E-3
8.0E-3
7.0E-3
6.0E-3
5.0E-3
4.0E-3
3.0E-3
2.0E-3
1.0E-3
1.0E-7
2.0E-7
3.0E-7
4.0E-7
5.0E-7
6.0E-7
7.0E-7
8.0E-7
TIME
3601

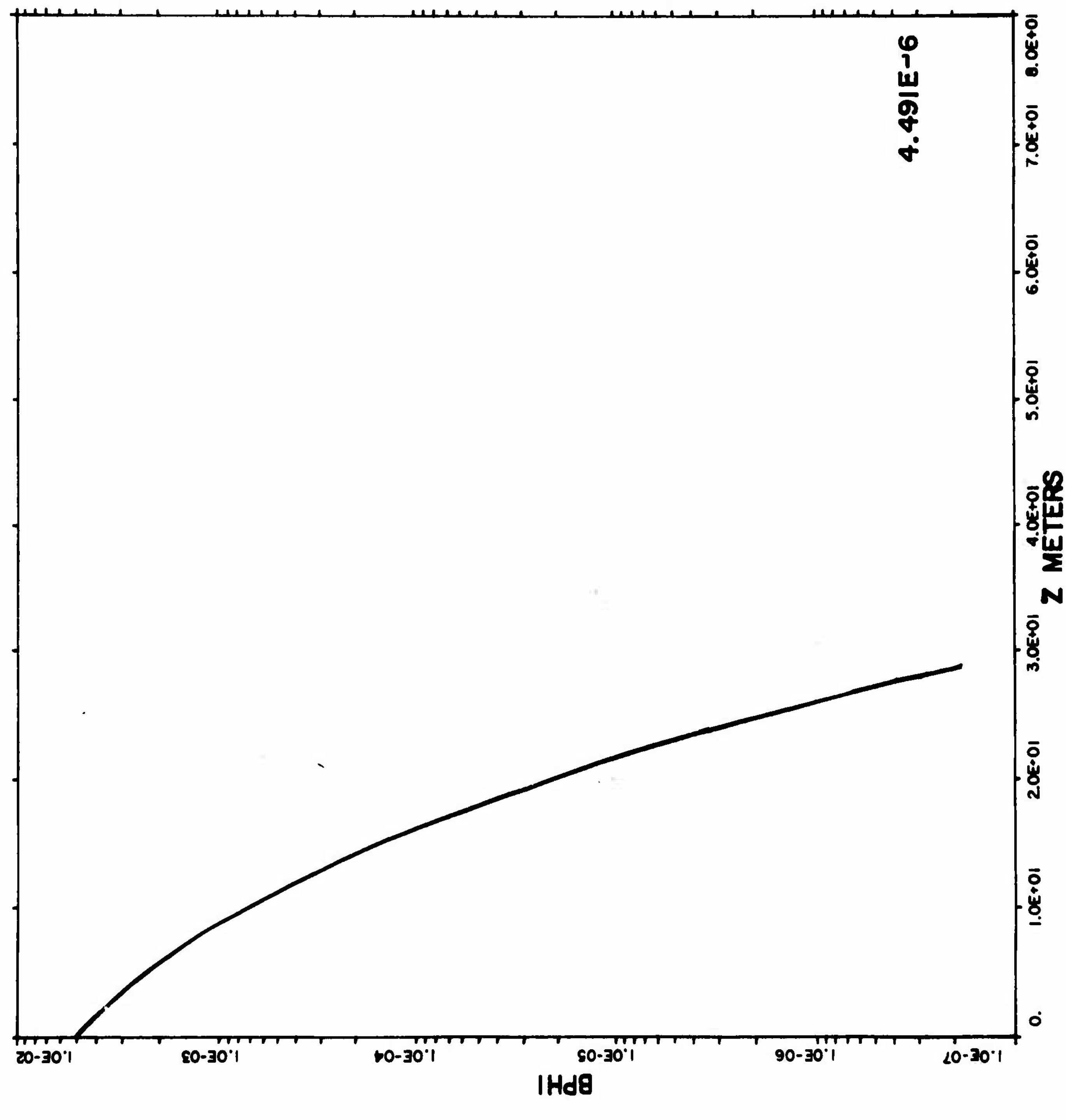
4.491E-6
Z METERS
0.
1.0E+01
2.0E+01
3.0E+01
4.0E+01
5.0E+01
6.0E+01
7.0E+01
8.0E+01
BPHI
1.0E-02
1.0E-03
1.0E-04
1.0E-05
1.0E-06
1.0E-07

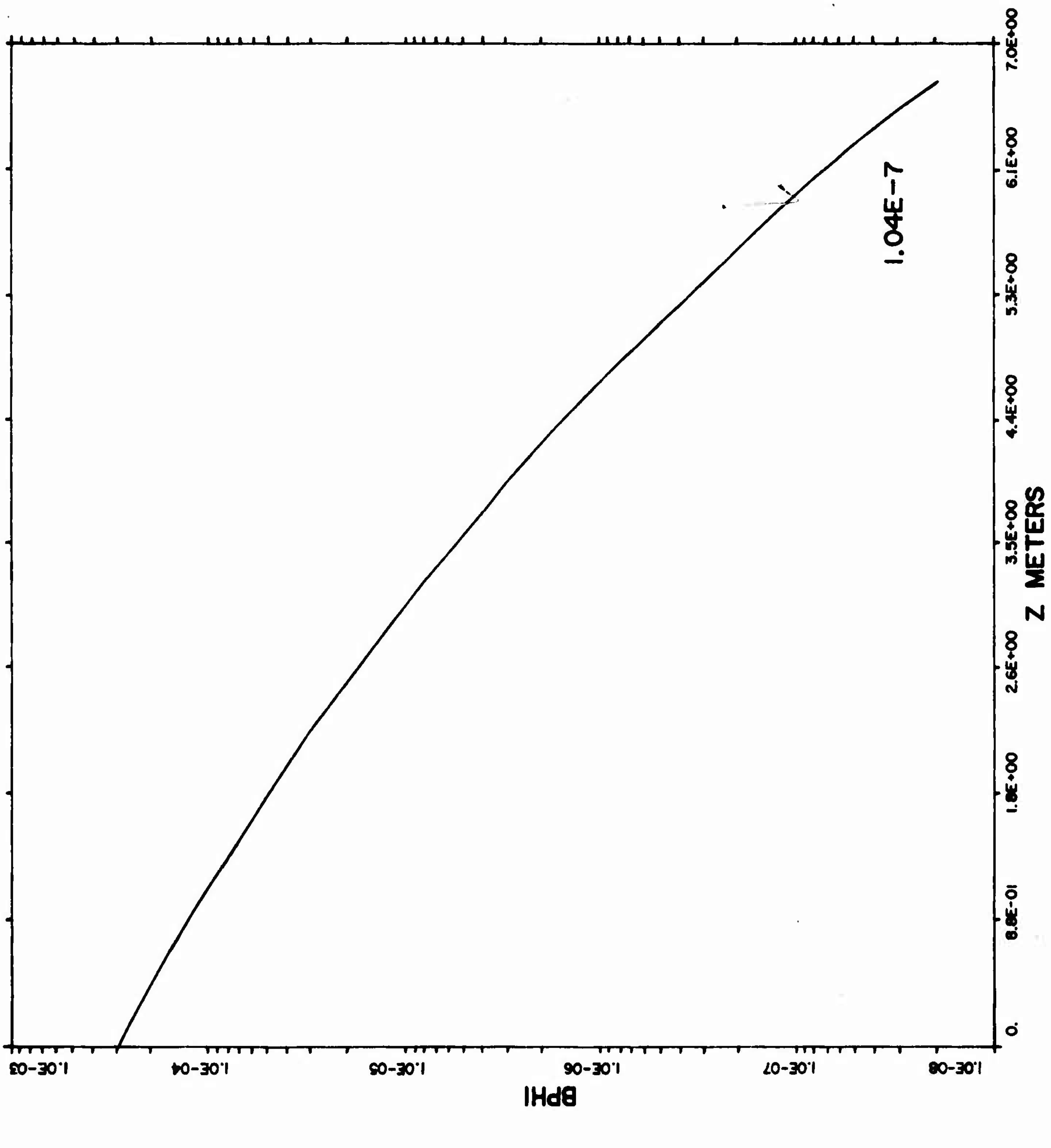
1.04E-7
Z METERS
BPHI
0.
8.8E-01
1.8E+00
2.6E+00
3.5E+00
4.4E+00
5.3E+00
6.1E+00
7.0E+00
1.0E-03
1.0E-04
1.0E-05
1.0E-06
1.0E-07
1.0E-08

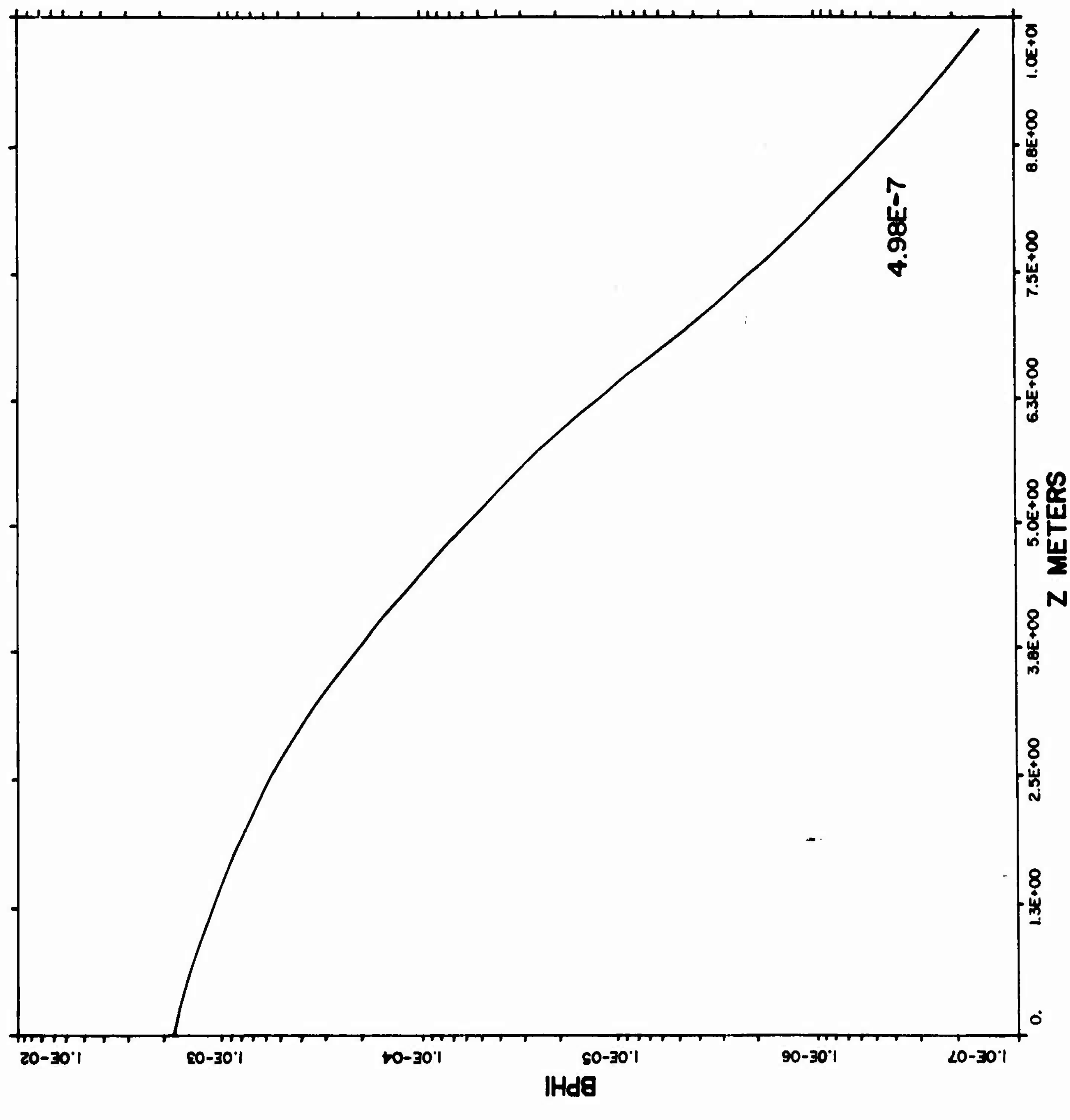
4.98E-7
Z METERS
0.
1.3E+00
2.5E+00
3.8E+00
5.0E+00
6.3E+00
7.5E+00
8.8E+00
1.0E+01
BPHI
1.0E-02
1.0E-03
1.0E-04
1.0E-05
1.0E-06
1.0E-07

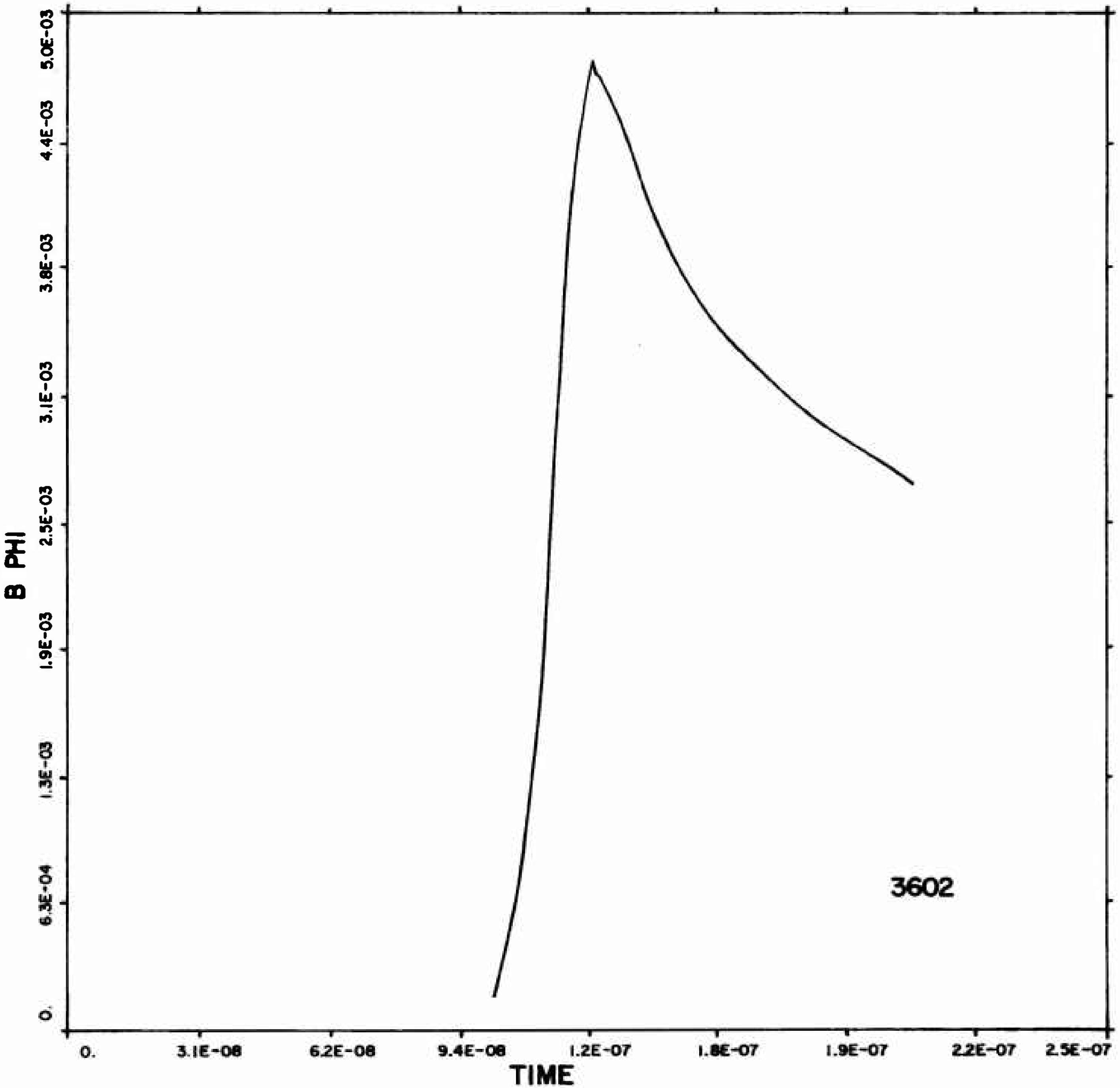
3602
B PHI
0.
6.3E-04
1.3E-03
1.9E-03
2.5E-03
3.1E-03
3.8E-03
4.4E-03
5.0E-03
TIME
0.
3.1E-08
6.2E-08
9.4E-08
1.2E-07
1.8E-07
1.9E-07
2.2E-07
2.5E-07

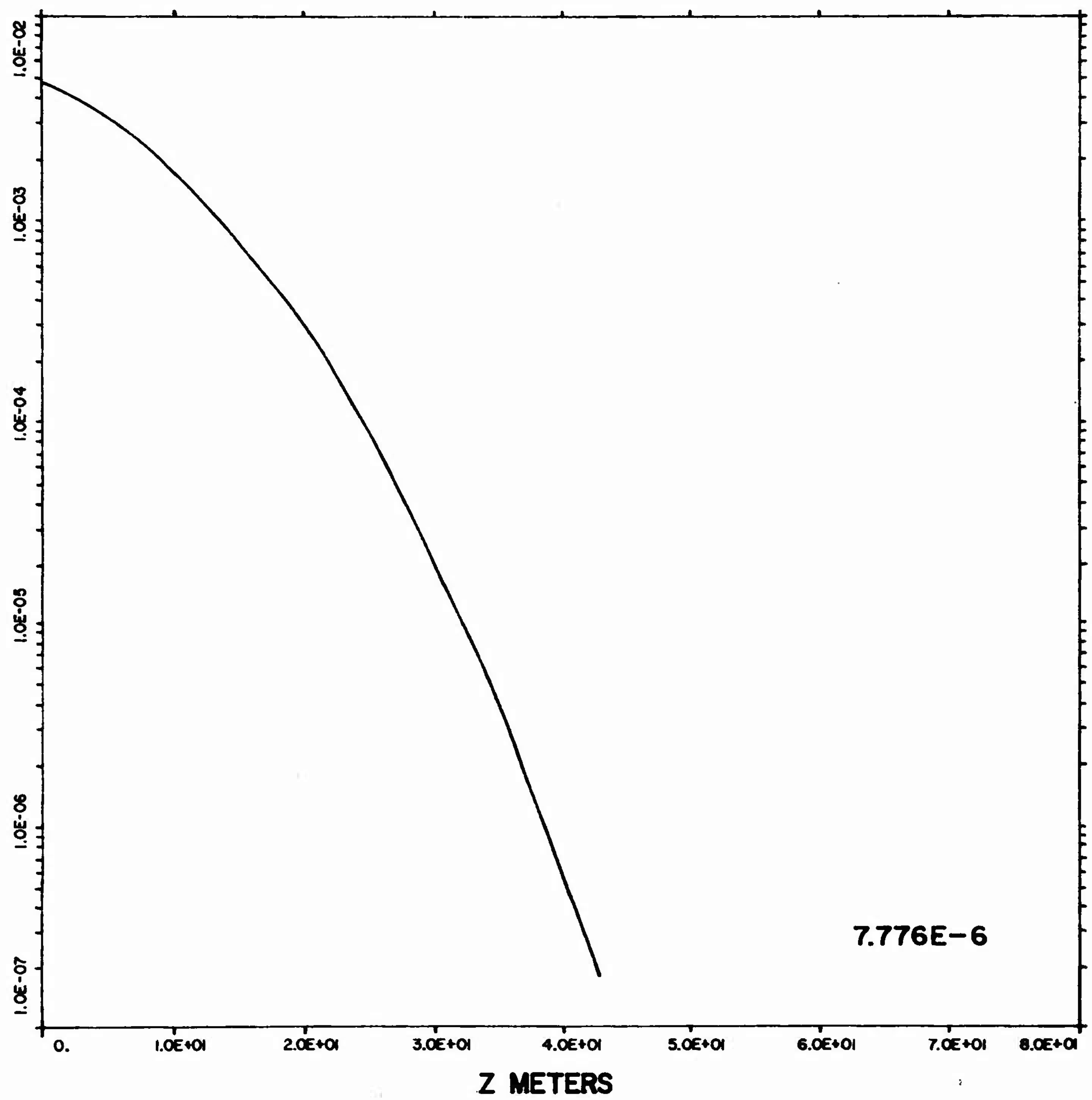
1.0E-02
1.0E-03
1.0E-04
1.0E-05
1.0E-06
1.0E-07
BPHI
7.776E-6
0.
1.0E+01
2.0E+01
3.0E+01
4.0E+01
5.0E+01
6.0E+01
7.0E+01
8.0E+01
Z METERS

UNCLASSIFIED

Security Classification

DOCUMENT CONTROL DATA - R & D

(Security classification of title, body of abstract and indexing annotation must be entered when the overall report is classified)

1. ORIGINATING ACTIVITY (Corporate author) The Dikewood Corporation Albuquerque, New Mexico 87106	2a. REPORT SECURITY CLASSIFICATION UNCLASSIFIED 2b. GROUP

3. REPORT TITLE

EMP ENVIRONMENTAL CODES FOR LOW-ALTITUDE BURSTS AND GROUND SOURCES

4. DESCRIPTIVE NOTES (Type of report and inclusive dates)

October 1967-October 1968

5. AUTHOR(S) (First name, middle initial, last name)

Richard L. Knight; Robert E. Budwine; Ralph T. Day

6. REPORT DATE	7a. TOTAL NO. OF PAGES	7b. NO. OF REFS
March 1969	110	7

8a. CONTRACT OR GRANT NO. F29601-68-C-0012 b. PROJECT NO. 5710 c. Subtask No. (DASA) 04.091 d. SAMSO Fund No. PD 68-9	9a. ORIGINATOR'S REPORT NUMBER(S) AFWL-TR-68-123 9b. OTHER REPORT NO(S) (Any other numbers that may be assigned this report) Contractor's report No. DC-FR-2064

10. DISTRIBUTION STATEMENT This document may be further distributed by any holder only with specific prior approval of AFWL (WLRP), Kirtland AFB, NM, 87117. Distribution is limited because of the technology discussed in the report.

11. SUPPLEMENTARY NOTES	12. SPONSORING MILITARY ACTIVITY
	AFWL (WLRP) Kirtland AFB, NM 87117

13. ABSTRACT

(Distribution Limitation Statement No. 5)

Progress accomplished under Air Force Contract No. F29601-68-C-0012 toward predicting the electromagnetic pulse produced by a nuclear weapon is reported herein. This work consists of the following: (1) a real-time finite difference code, using prolate spheroidal coordinates, which will predict the electromagnetic fields produced by certain current distributions with azimuthal symmetry, (2) a retarded time code which in other respects is similar to the one listed above, (3) a one-dimensional finite difference code for predicting the fields of a current distribution with spherical symmetry, (4) a computer code which numerically evaluates the exact solution of Maxwell's equations for the case of spherical symmetry, (5) a numerical solution of the diffusion approximation of Maxwell's equations in a region which includes an infinitely conducting earth, (6) work toward obtaining a Green's function for Maxwell's equations with some restrictions on the time dependence of the conductivity, and (7) a numerical integration code that combines the results of two previously existing Monte Carlo neutron and gamma ray transport codes in order to obtain currents produced by gamma ray sources in the ground.

DD FORM 1 NOV 65 1473

UNCLASSIFIED

Security Classification

14. KEY WORDS	LINK A		LINK B		LINK C	
	ROLE	WT	ROLE	WT	ROLE	WT
Electromagnetic pulse (EMP)						
Finite difference codes						
Diffusion equations						
Nuclear weapon ground sources						